

39. SEDIMENTOLOGY AND HISTORY OF THE NORTHEASTERN INDIAN OCEAN FROM LATE CRETACEOUS TO RECENT

Anthony C. Pimm, Scripps Institution of Oceanography, La Jolla, California

ABSTRACT

Eight sites were drilled on Leg 22 in the northeastern Indian Ocean. Three sites (214, 216, 217) on Ninetyeast Ridge penetrated a thick sequence of mostly Tertiary calcareous oozes passing down into shallow-water sediments with volcanogenic material in Sites 214 and 216. The age of the basal sequence increases northwards from Paleocene (214) through Maastrichtian (216) to Campanian (217). A nonmarine sequence of volcanoclastics and lignite overlies basalt at 214. Drilling terminated in a dolomite chert sequence at 217 before basalt was encountered. Two sites (213, 215), in deep water on either side of Ninetyeast Ridge, showed calcareous ooze of Paleocene to early Eocene age overlying basalt passing up into brown clay and finally siliceous ooze of late Miocene and younger age. A major hiatus centered in the Oligocene occurs at both these sites. One site (212), drilled in the deepest part of the Wharton Basin, penetrated a brown clay sequence interbedded with several thick calcareous units, each of a very short time duration. Evidence from sedimentary structures and calcareous microfossils indicate that these calcareous sediments deposited below the calcium carbonate compensation depth (CCD) have been reworked from shallower water. The age of basement at Site 212 is estimated at about 90 to 100 m.y. Site 211, situated in the northern part of the Wharton Basin, recovered Campanian calcareous ooze overlying basalt. An undated brown clay sequence lies between the calcareous ooze and a thick Pliocene section of terrigenous sediments, representing the distal portion of the Nicobar Fan. Siliceous ooze with some rhyolitic ash beds, presumably derived from the Indonesian volcanic arc, indicate cessation of terrigenous sedimentation here since the late Pliocene. Similar ash beds were also seen in Pleistocene sediments at Site 216. Site 218 was drilled in the central portion of the Bengal Fan, which here comprises a thick sequence of terrigenous sediments at least as old as middle Miocene. Variations in sand-silt-clay ratios coupled with the occurrence of interbeds of calcareous ooze in places indicate four major pulses of terrigenous sedimentation. Two thin beds of terrigenous sediments penetrated at Site 215 show that the distal portion of the Bengal Fan reached as far as 8°S in the late Miocene.

CONTENTS

Introduction	718	Clay Minerals	729
General	718	Detrital Minerals	731
Source of Data	718	Zeolites	733
Review of Main Results	718	Manganese	737
Site Summaries	718	Iron Oxides	737
Regional Patterns of Sedimentation	723	Glauconite	737
Distribution of Components and Structures	725	Sedimentary Structures	737
Calcareous Nannofossils	725	Major Sedimentary Facies	739
Foraminifera	726	Calcareous Ooze	739
Other Calcareous Fossils	729	Siliceous Oozes	742
Siliceous Fossils	729	Terrigenous Sediments	743

Pelagic Clays	743
Volcanogenic Clays	745
Regional Summary and Conclusions	763
Formation and Subsidence of Oceanic Crust	763
Deposition of Calcareous Sediments Below the CCD at Site 212	767
Acknowledgments	772
References	773
Appendices	774

INTRODUCTION

General

This paper is an attempt to provide a broad general summary and interpretation of all sedimentologic data collected on DSDP Leg 22. The *Glomar Challenger* sailed from Darwin, Australia on January 13, 1972. Three holes were drilled to the east of the Ninetyeast Ridge, three on the ridge itself, and two to the west of it (Figure 1). A total of 4663 meters was penetrated; of this total, 2543 meters were cored and 1380 meters (54%) recovered. The cruise terminated in Colombo, Ceylon on March 6, 1972.

Source of Data

The major source of data for this chapter was the visual core and smear slide descriptions prepared on board ship by the author in conjunction with R. Hekinian, R. W. Thompson, and J. Veevers. After the cruise, the author reexamined the smear slides and subsequently revised several of the shipboard descriptions based on this and additional thin section work. The DSDP laboratories provided grain-size and calcium carbonate analyses, and X-ray diffraction data. All age determinations and some of the observations on the state of fossil preservation were taken from the work of the shipboard paleontologists: S. Gartner (nannofossils), D. Johnson (Radiolaria), and B. McGowran (foraminifera). Estimates of relative abundances of fossil types and some notes on preservation were made by this author.

Bathymetric and magnetic data used as base maps and for paleogeographic reconstructions in this chapter are mainly taken from the work of Sclater and Fisher (in press), McKenzie and Sclater (1971), and the bathymetric chart of the eastern Indian Ocean from the new Russian Atlas (Udinster, pers. comm.).

The time scale used in this paper is essentially that of Berggren (1972) for the Cenozoic. The Tertiary/Cretaceous boundary is placed at 65 m.y. Following DSDP Leg 14 (Hayes, Pimm, et al., 1972), the boundary between Maastrichtian and Campanian is placed at 72 m.y. Data from Leg 22 and earlier sites drilled by DSDP indicate that the magnetic anomaly time scale of Heirtzler et al. (1968) is slightly inaccurate in the early Tertiary and Cretaceous. An informal revision of the ages assigned to magnetic anomalies

is given in Chapter 13, and a discussion of isotopic ages gathered on Leg 22 which forms the basis for some of these revisions is given in Chapter 12. For the purposes of this Chapter, the revised ages of magnetic anomalies used by this author are summarized in Table 1.

REVIEW OF MAIN RESULTS

Much of the sedimentologic data is summarized in a series of fence diagrams drawn roughly east to west across the Ninetyeast Ridge and Wharton Basin, north to south along the crest of the Ninetyeast Ridge, and westwards across the Bengal Fan. Figure 2 shows the distribution of cores in space and time and the approximate portions of the total sediment column that were recovered by the drilling operation. It can be seen that many of the holes drilled were continuously cored, particularly in the lower parts of the sedimentary record, and this in conjunction with good percentages of recovery enables the sedimentologist to be fairly confident that his samples are representative of the region. Stratigraphic logs of the Leg 22 sites are given in Figure 3.

Site Summaries

Site 211

Site 211 is situated in a flat topographic region on a gentle rise just south of the Java Trench in a water depth of 5535 meters. Early Campanian and Maastrichtian nannofossil clay to nannofossil ooze overlies weathered basaltic basement at a subbottom depth of 435 meters. Above this is a noncalcareous ferruginous brown clay, intruded near its base by a 12-meter-thick andesitic diabase sill. A 200-meter-thick unit of interbedded silts, sands, and siliceous oozes overlies the brown clay. The silts and sands are of Pliocene age and form an extension of the Nicobar Abyssal Fan into this area. The uppermost 100 meters of the hole yielded siliceous oozes of Pliocene and Quaternary age and some ash beds, which probably originate from island arc volcanism to the north.

Site 212

Site 212 was drilled in a water depth of 6243 meters in a small basin of partly ponded sediments in the deepest portion of the Wharton Basin. Sediment penetration was 516 meters. Five calcareous ooze to chalk units, from a few meters to 250 meters in thickness, dominate the stratigraphic section. These range in age from Pliocene to Late Cretaceous. Each calcareous unit has a narrow time range, the lower two units being of uniform age throughout, and contains residual and apparently current-sorted fossil assemblages. Three nonfossiliferous zeolitic brown clays, averaging 30 meters thick, separate the calcareous units. The lowermost brown clay lies directly over a metabasalt which is intercalated with recrystallized calcareous sediment. Observations suggest that the brown clays represent normal deep-basin oceanic sedimentation

TABLE 1
Revised Ages Assigned to
Magnetic Anomaly Time Scale

Age	Anom- aly No.	M.Y.
Campanian		

Maastrichtian	32	70
	31	
	30	
	29	
Paleocene	28	60
	27	
	26	
	25	
	24	
	23	
Eocene	22	50
	21	
	20	
	19	
	18	
	17	
Oligocene	16	40
	15	
	14	
	13	
	12	
	11	
Miocene	10	30
	9	
	8	
	7	
Pliocene	6	20
	5	
	4	
Pleistocene	3	10
	2	
	1	

below the CaCO₃ compensation level. The calcareous material, on the other hand, is postulated to be exotic to the area and to have been transported to the basin by

bottom current activity from areas above the CaCO₃ compensation level. The age of oldest datable sediment, 34 meters above basalt, is Late Cretaceous. Age of the recrystallized limestone in contact with the basalt is unknown; however, the extrapolated age of sediment immediately above basalt ranges between 90-100 m.y. depending upon the sedimentation rate chosen for the brown clay.

Site 213

This site was situated in a water depth of 5611 meters south of a 500-meter-high ridge which prevented the distal Nicobar Fan sediments on the eastern side of Ninetyeast Ridge from extending farther south. The stratigraphic column at Site 213 is 154 meters in thickness and contains four stratigraphic units with gradational contacts. These units comprise an uppermost radiolarian-diatom ooze of Quaternary to middle Miocene age, a nonfossiliferous zeolitic brown clay, a nannofossil ooze of early Eocene to late Paleocene age, and a basal iron-manganese oxide sediment overlying weathered pillow basalt. A 12 meter thickness of the brown clay corresponds to a 30 m.y. time period. Stratigraphic evidence is consistent with a gradual deepening of the oceanic crustal plate from above the CCD at its formation to below it in the middle Tertiary. By late Tertiary the site had migrated into an area of high siliceous plankton productivity. The oldest sediment age of 57-58 m.y. places an upper limit on the age of magnetic anomaly 26 in this area.

Site 214

Site 214 is situated on the crest of Ninetyeast Ridge, in a water depth of 1655 meters. The 490-meter-thick stratigraphic column comprises several distinct stratigraphic units ranging from pelagic to shallow water, to nonmarine and subaerial. Uppermost of these is a thick pelagic foraminiferal and nannofossil ooze, glauconitic at its base, which ranges in age from late Pleistocene to early Eocene/Pliocene. This grades down into a glauconitic shelly carbonate silt and sand (with some reworked volcanic material) of Paleocene age, which is underlain by lignitic and volcanoclastic sediments interbedded with differentiated flows. A coarse amygdalar basalt occurs below these sediments and volcanics at a depth of 490 meters, possibly representing basement of Ninetyeast Ridge. The sequence is in accord with a progressive subsidence of the ridge, at least during the Paleocene.

Site 215

Site 215 was drilled west of Ninetyeast Ridge in 5309 meters of water. The stratigraphic column in the area is 155.5 meters in thickness and is divided into four units. These include an upper radiolarian-diatom ooze of Quaternary/late Pliocene to late Miocene age; two thin terrigenous silty layers (distal portion of Bengal Fan sediments) of late Miocene age; a four-meter-thick brown clay, corresponding with a 40 m.y. time period; a nannofossil ooze with some chert ranging from early Eocene to mid-Paleocene in age; and a basal iron oxide-rich mid-Paleocene nannofossil ooze. The lithology and

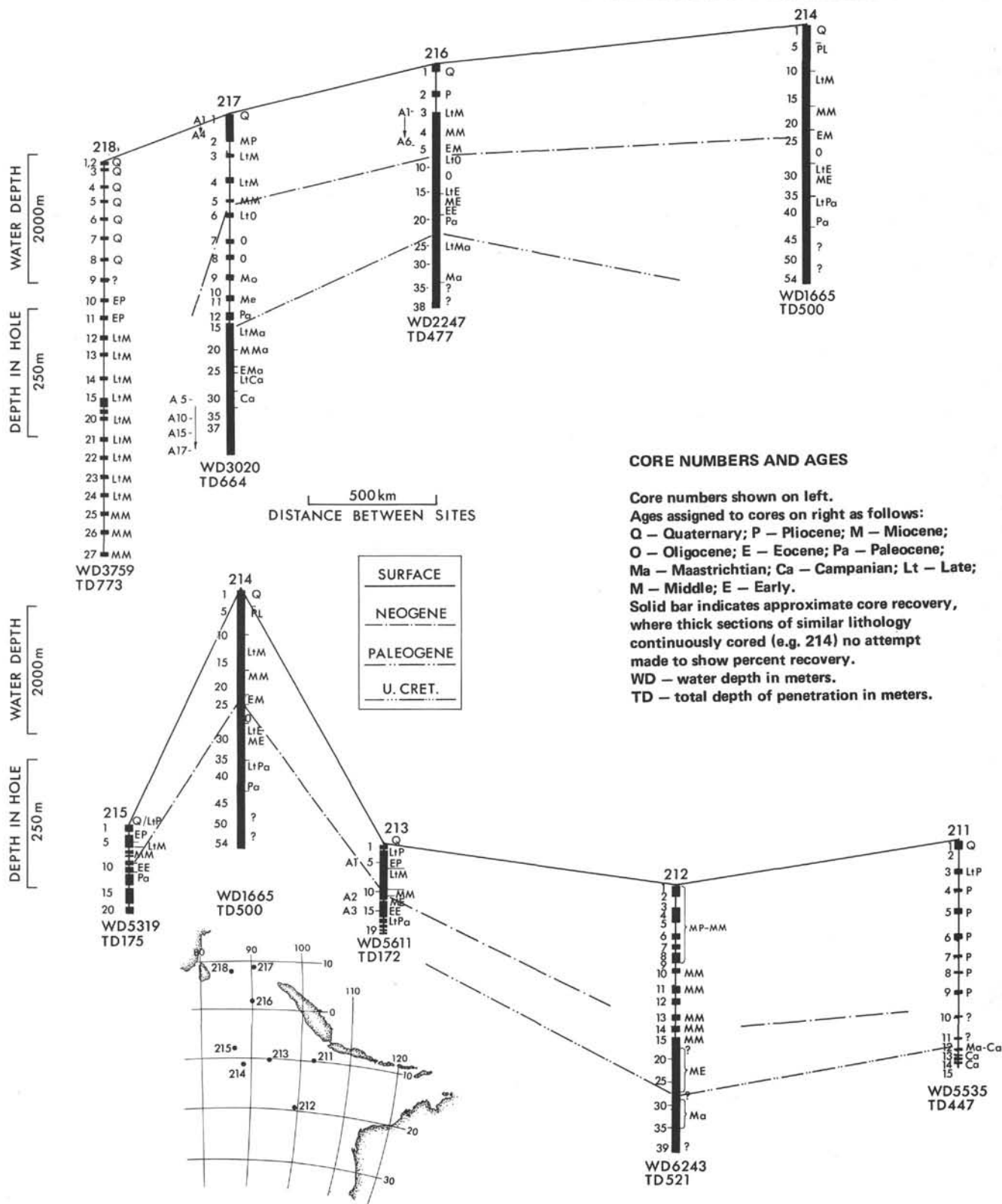


Figure 2. Distribution of cores recovered on Leg 22.

biostratigraphy of Site 215 for most of its history closely resembles Site 213, which is on the opposite side of Ninetyeast Ridge, suggesting that the Indian and Australian plates have behaved in a similar manner at least since late Paleocene/early Eocene times. Evidence exists for the synchronous subsidence of both areas since this time, and

the subsidence can be correlated with that established for the crest of Ninetyeast Ridge at Site 214.

Site 216, 216A

Site 216 was drilled on the crest of Ninetyeast Ridge near the equator, in a water depth of 2237 meters. The

intensely bioturbated. This is underlain by scoriaceous and amygdalar chloritized basalt containing rare veinlets of native copper. This stratigraphy resembles that of Site 214, 1300 km to the south along the crest of Ninetyeast Ridge. Chronologic and lithologic evidence at both sites combine to suggest progressive downwarping of the Ridge from north to south during Late Cretaceous and Tertiary times. sediment thickness at this site is 457 meters. The upper part consists of an uppermost Pleistocene to upper Maastrichtian nannofossil ooze to chalk which is glauconitic at the base and contains a few chert stringers. This is underlain by an upper Maastrichtian shallow-water unit comprising shelly and glauconitic micarb chalk and limestone (micrites) intermixed with volcanic clay and discrete ash beds, in part

Site 217, 217A

Site 217 is situated in 3010 meters of water on the eastern flank of the northernmost portion of Ninetyeast Ridge. The stratigraphic column at this site comprises three units. Uppermost is a clay-rich nannofossil ooze unit, 145 meters thick, of Quaternary to middle Miocene age. Between 145 and 600 meters is a unit with shallow-water affinities, composed of nannofossil ooze and chalk above and carbonate siltstone partly shelly and silicified below, which ranges in age from late Miocene to late Campanian. The lowermost unit of Campanian age, from 600 to 664 meters, is an interbedded sequence of dolarenite, chert, claystone, and some shelly carbonate siltstone (biomicrite). The occurrence of clays within the upper nannofossil ooze unit since middle Miocene times may correlate with the onset of nearby Bengal Fan sedimentation, which in turn may represent a major Himalayan orogenic phase in the Miocene. A combination of biostratigraphic and lithologic observations indicates that the Ninetyeast Ridge in the vicinity of Site 217 subsided from about sea level to oceanic depths during Late Cretaceous times. These observations also suggest that the Ridge at Site 217 has been attached to the Indian crustal plate, that it moved north (relative to Australia) with the plate during the Maastrichtian, and that the Indian and Australian plates behaved as one from early Tertiary to the present.

Site 218

Situated in the Central Bengal Fan in 3749 meters of water, Site 218 was drilled to 773 meters in a turbidite sedimentary sequence. The stratigraphic column, which was only partly penetrated, comprises several sedimentary units which include silts, sandy silts, and clayey silts, interbedded with some nannofossil ooze layers. The sediments range in age from Quaternary down to middle Miocene at the bottom of the hole. On the basis of dominant grain sizes of the terrigenous sediments and the distribution of pelagic material, four distinct "pulses" of turbidity current activity, resulting in coarse sediments, are tentatively recognized. One of these occurs in the middle Miocene, two in the late Miocene-early Pliocene, and one in the Pleistocene. The youngest "pulse" is overlain by several meters of pelagic ooze, suggesting postglacial cessation of turbidity current activity in the area of the site.

Regional Patterns of Sedimentation

Dominant, and some significant minor, components from the smear slide analyses were plotted on the fence

diagrams (Figure 4) and provide a ready guide to the regional patterns of sedimentation in the eastern Indian Ocean. Sediment accumulation rates are plotted in Figure 5.

The following dominant components were recognized: calcareous ooze, siliceous ooze, brown clay, terrigenous material, and volcanoclastics.

Ninetyeast Ridge is covered by a Tertiary (Site 214) and Tertiary to Upper Cretaceous (Sites 216, 217) pelagic carbonate sequence. This sequence passes down into carbonates with a distinctly shallow water aspect containing molluscs and glauconite. The transition takes place in progressively older sediments to the north: at Site 214, in the late Paleocene; at Site 216, in the late Maastrichtian, and at Site 217 in the middle Maastrichtian. Below this shallow-water sequence at Sites 214 and 216, volcanoclastic and reworked volcanogenic sediments (with interbedded lignites at Site 214) are present. In Site 217, abundant chert and dolarenites toward the base of the thicker carbonate sequence prevented penetration to the volcanic sequence which is presumed to exist at greater depth. A few thin chert stringers were also seen in the Paleocene carbonate sequence at Site 216.

A thick sequence of Miocene to Quaternary terrigenous sediments with a few thin pelagic carbonate interbeds make up the central part of the Bengal Fan in the area of Site 218. In late Miocene times, the distal portion of this fan reached as far south as Site 215, where two thin beds of terrigenous sediment were penetrated. These same terrigenous sediments, carried into the Indian Ocean by the Ganges and Bramaputra rivers, also spilled over through the gap between Ninetyeast Ridge and the Indonesian arc (building the topographic feature known as the Nicobar Fan) and reached as far south as the southern Sumatra-Java region (Site 211) in Pliocene times. The considerable thickness and relatively coarse grain size of these Pliocene terrigenous sediments at Site 211 and the remarkable distance they travelled from their source attest to the tremendous energy of their transporting medium. The Neogene carbonates on the northern end of Ninetyeast Ridge, at Site 217, also contain a considerable admixture of clay-sized terrigenous material, which probably was also derived from the same source as the Bengal Fan sediments, but in this case, from the lower energy part of the transporting agency.

In the deep water (>5300 meters) sites (211, 213, 215) on either side of Ninetyeast Ridge between 8° and 11°S, the Neogene is dominated by siliceous oozes deposited beneath the high productivity zone just south of the Equator in the Indian Ocean. A few andesitic-rhyolitic ash beds occur in this diatom-radiolarian ooze sequence at Site 211 as this is close enough to be under the influence of subaerial volcanic eruptions from the Indonesian arc system. Below this siliceous ooze sequence are typical deep-sea pelagic brown clays, zeolitic in part, with only sparse siliceous fossils. Presumably then, these sites were not under the influence of the high productivity subequatorial system in Miocene and earlier times.

In early Eocene-late Paleocene times, Sites 213 and 215 were located in water shallow enough for pelagic carbonate oozes to be preserved while in Site 211 similar sediments are only preserved in the Upper Cretaceous.

The sediment blanket in the Wharton Basin is usually thin (≈100 meters), but at the location of Site 212, ponded

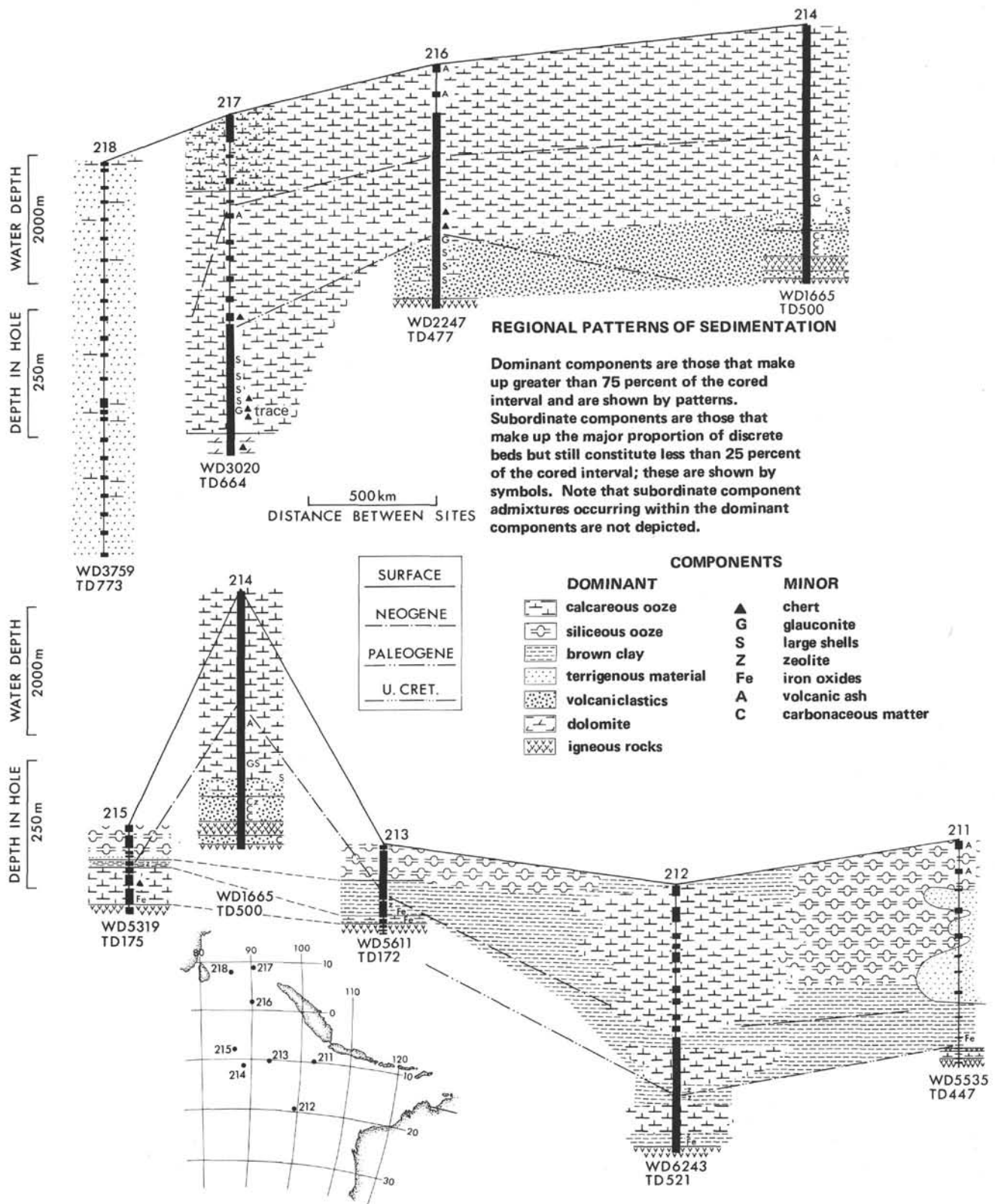


Figure 4. Regional patterns of sedimentation.

sediments in the deepest part of the basin are more than 500 meters thick. The recovered sediments included three units of zeolitic brown clays, each about 30 meters thick, and these are probably typical in nature and total thickness

of sediments over the whole basin. However, the anomalous thickness of sediments at Site 212 is due to several units of carbonate ooze which have been reworked from an unknown source that must have been shallower than the

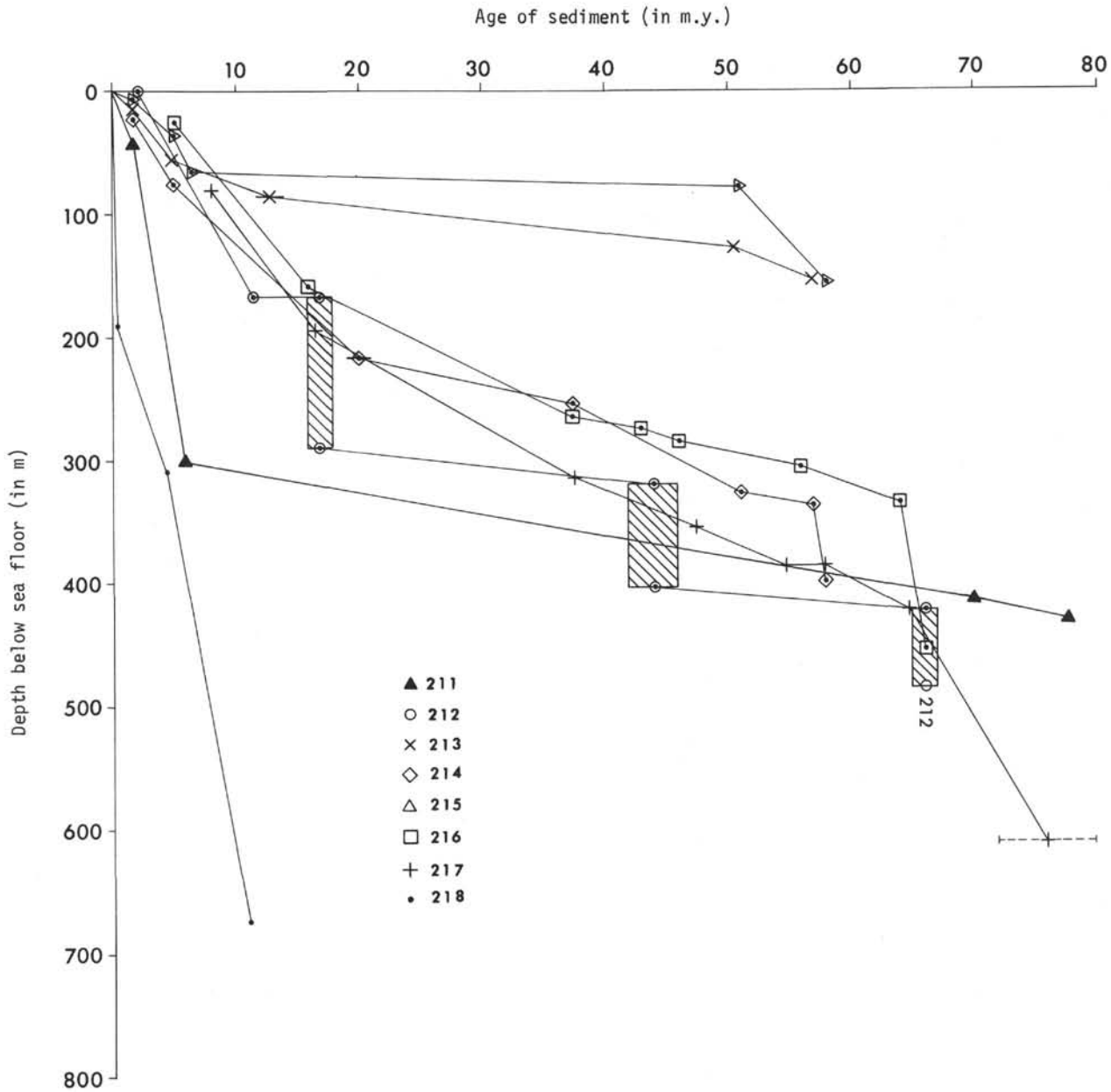


Figure 5. Sediment accumulation rates for Leg 22 sites.

carbonate compensation depth. Sedimentary structures and paleontology provide good evidence to support the view that the carbonates penetrated at Site 212 are exotic.

An iron oxide-rich facies, mostly in clays but also occurring in carbonate, occurs in the lower parts of the sediment column at all of the sites formed on typical deep-water oceanic crust generated from a spreading center (Sites 211, 212, 213, 215), but this facies was not seen in any of the sediments occurring on Ninetyeast Ridge where the basaltic rocks, as seen at the base of Sites 214 and 216, were probably extruded subaerially.

DISTRIBUTION OF COMPONENTS AND STRUCTURES

Calcareous Nannofossils

The abundance and preservation of calcareous nannofossils is summarized in Figure 6.

Fairly thick, and mostly continuous, sequences of nannofossil ooze were penetrated at the three sites (214,

216, 217) drilled on Ninetyeast Ridge. At Site 214, accumulation rates of this ooze were 11 m/m.y. for the Quaternary, 21 m/m.y. for the Pliocene, and 8 m/m.y. for the Miocene. The relative proportions of nannoplankton to foraminifera are about the same in Quaternary and Pliocene sediments; so the accumulation rate for nannoplankton ooze in the Pliocene is almost double that of the Quaternary and follows the observation of Bramlette (1958), Berger (1972), and scientists on other DSDP legs. The lower accumulation rate of the Miocene (versus Pliocene) nannoplankton ooze is most probably a dissolution artifact causing a considerable reduction in the foraminifera content (see below).

At Site 217, the accumulation rate for Quaternary and Pliocene sediments is about the same (12 m/m.y.) and only slightly lower (9 m/m.y.) in the Miocene.

Because of discontinuous coring at Site 216, direct comparisons of Quaternary and Pliocene accumulation rates cannot be made. However, it is apparent that the Miocene accumulation rate of nannoplankton ooze is only about half that of the Pliocene and Quaternary—~7 versus ~14 m/m.y.

The preservation of the nannoplankton floras at all three Ninetyeast Ridge sites is good in Pliocene and younger sediments but deteriorates downhole so that in Miocene and older sediments it is mostly fair to poor (Figure 6). Towards the base of each hole, hardly any carbonate fragments of silt-size are recognizable as nannoplankton. This occurs at approximately 330 meters in Sites 214 and 216, i.e., Paleocene and late Maastrichtian, respectively; and 480 meters in Site 217, i.e., mid-Maastrichtian.

A few thin interbeds of Quaternary to Miocene age contain nannoplankton in the predominantly terrigenous section recovered at Site 218. With the exception of the surface core, the preservation of the flora is only fair.

Mostly fair to poorly preserved nannoplankton floras were recovered in the basal sections at 211 (Cretaceous), 213, and 215 (early Eocene to Paleocene).

Site 212 contains several distinct units of nannoplankton ooze or chalk, all of which have been reworked from shallower depths. The lower two chalk units of Eocene and Cretaceous age contain a flora which has been subjected to extensive dissolution (see Chapter 3). The preservation of the younger Neogene floras is generally good.

Foraminifera

The abundance of foraminifera and state of their preservation is summarized in Figure 7. Owing to their size and uneven distribution when mounted on smear slides, it is hard to estimate foraminifera percentages. However in some places, grain-size data (Appendix A) is available, and the percent of the coarse fraction ($>62\mu$) in calcareous oozes can be used to supplement smear slide data as this is almost solely made up of planktonic foraminiferal tests.

The only site containing a complete sequence of Cenozoic calcareous oozes, which was continuously cored and for which complete grain-size data is available, is 214. Triangle plots of the grain-size data are given in Figure 8. It can be seen from these plots that the abundance of foraminifera (i.e., sand fraction) falls into three major groupings according to age. Foraminifera are very abundant

in Quaternary to early Pliocene with a progressive decrease from about 52 to 25 percent (Appendix A). From earliest Pliocene to near the base of the middle Miocene, there is a marked drop in foraminifera abundance with all but two (22% each) values ranging from 3 to 16 percent. Again, below this there is a further marked decrease in the foraminifera content to usually about 1 percent or less near the base of the Miocene. Owing to the inherent difficulties of estimating foraminifera percentages from smear slides, the only marked change seen in these slides was the lower reduction of foraminifera occurring in the middle Miocene.

Although there is less data available from Site 216, the same trend seen in Site 214 of foraminifera reduction with increasing age is apparent here as Pliocene and younger sediments contain a much higher percentage of foraminifera than Miocene sediments. Also, in Site 217, foraminifera are rare in the pre-Pliocene, but common in younger sediments.

To find out whether this variation in foraminifera content is a primary result of productivity or a secondary effect imposed on the fauna by partial dissolution of the assemblage, an examination of the foraminifera species abundance charts given by Berggren et al. (Chapter 30) was made. From the work of Parker and Berger (1971), a solution ranking of planktonic foraminifera has been established. Using this information, the various species of *Globigerinoides* present in the assemblages at Sites 214, 216, and 217 can be used to determine how much of the assemblage has been lost to dissolution.

At Site 214, *G. ruber*, the species least resistant to dissolution, is most abundant in Pleistocene and late Pliocene sediments (N.22-N.20; Cores 3, 4, 5). Other species that are slightly more resistant to dissolution—*G. trilobus*, *G. sacculifer*, *G. fistulosus* and *G. conglobatus*—are common, but they make up a smaller proportion of the total assemblage than *G. ruber*. In the Pliocene (N.19; Cores 6-10), *G. ruber* disappears below Core 6, and *G. trilobus* and *G. sacculifer* are most abundant. In the late Miocene, *G. conglobatus* has mostly disappeared. By middle Miocene times (N.14), *G. sacculifer* disappears, and in the early Miocene (N.4) *G. trilobus* has gone. At Site 216, *G. ruber* is moderately common in the Pleistocene (N.22-23; Core 1) and disappears in the early Pliocene (N.20-19; Core 2). *G. conglobatus* is very common in the Pleistocene but shows a marked reduction in the early Pliocene. Similarly, at Site 217, *G. ruber* disappears in the Pliocene. Most abundant in the Pleistocene are *G. sacculifera* and *G. conglobatus*. The former shows a marked reduction in the early Pliocene (N.20-19) and the latter disappears.

Therefore, at Sites 214, 216, and 217, the foraminifera species least resistant to dissolution are the first to disappear downhole.

Another observation is that Quaternary and Pliocene calcareous oozes at Site 214, situated at 11°20'S, contain a much higher proportion of foraminifera to calcareous nannoplankton than at the latitudes of Sites 216 and 217, between the Equator and 10°N. Two possible explanations can be advanced to explain this reduction of foraminifera to the north: (a) dissolution of foraminifera due to the greater water depth at Sites 216 (2247 m) and 217 (3020 m) than at Site 214 (1665 m) and/or (b) lower productivity of planktonic foraminifera from waters to the

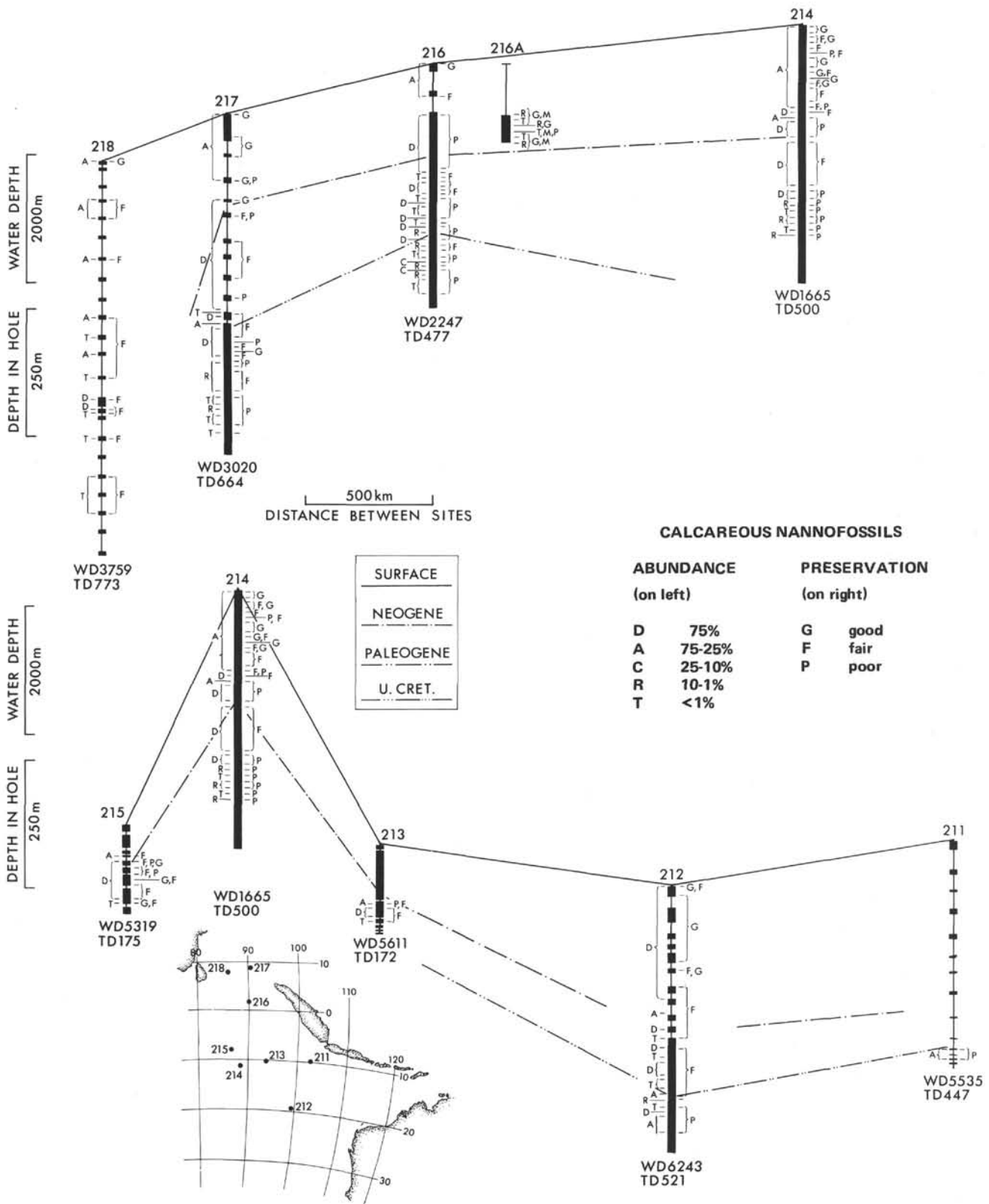


Figure 6. Abundance and preservation of calcareous nannofossils.

north of the subequatorial zone of high productivity in the Indian Ocean. Evidence from the species lists of Berggren (Chapter 30) again indicate that the former explanation is

more acceptable. At Site 214, *G. ruber* is the most abundant species in the Pleistocene, but at Sites 216 and 217, this delicate species is far less common in the total

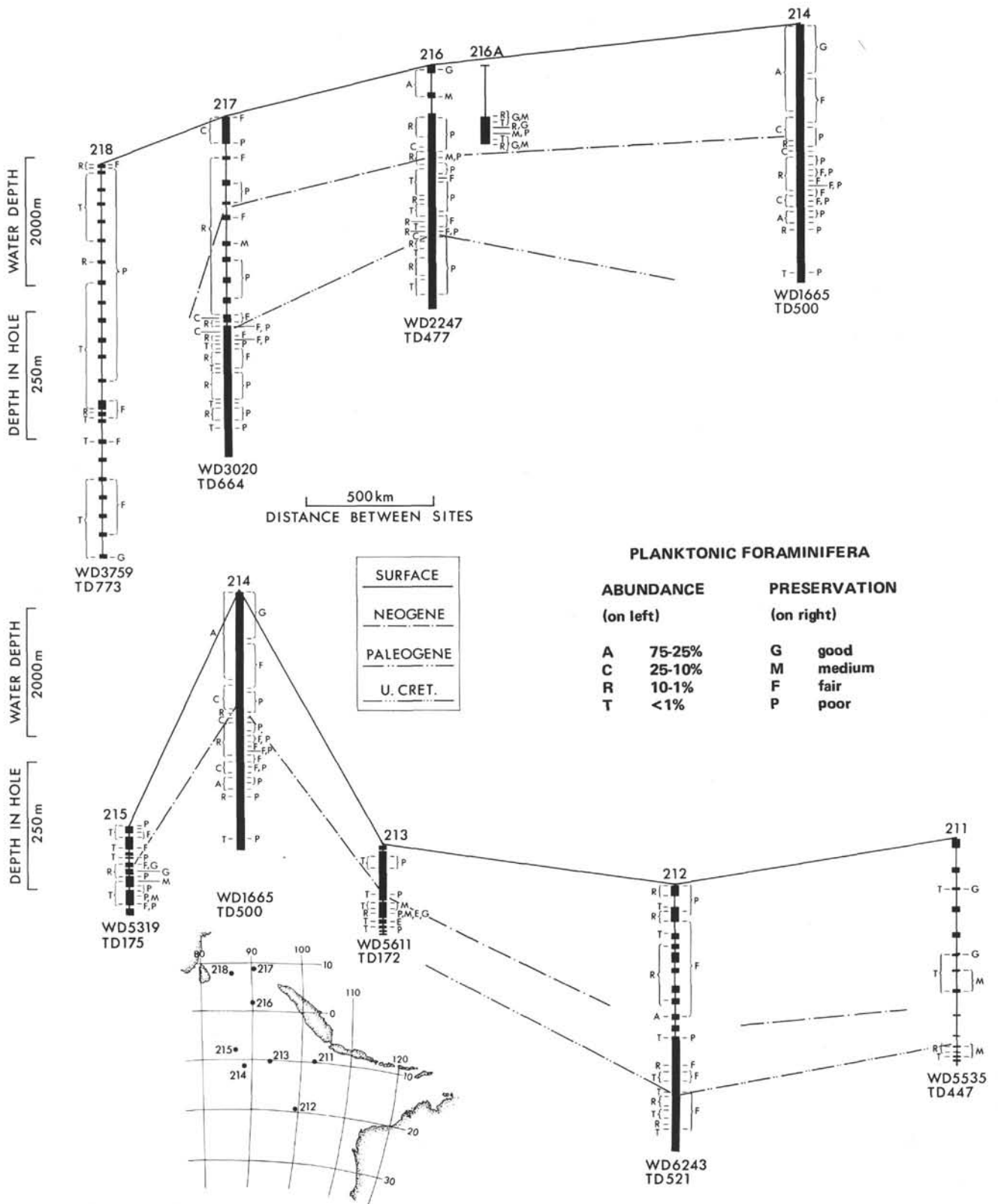


Figure 7. Abundance and preservation of foraminifera.

assemblage and the more resistant forms such as *G. conglobatus* and *G. sacculifer* are more abundant.

Returning to Site 214, for which the most data is available, a rough estimate of the proportion of the total

foraminiferal assemblage lost to dissolution can be made using the solution rankings of *Globigerinoides* as described above. Quaternary to late Pliocene assemblages have probably suffered only small loss (<25%) due to dissolution

GRAIN SIZE FOR SITE 214

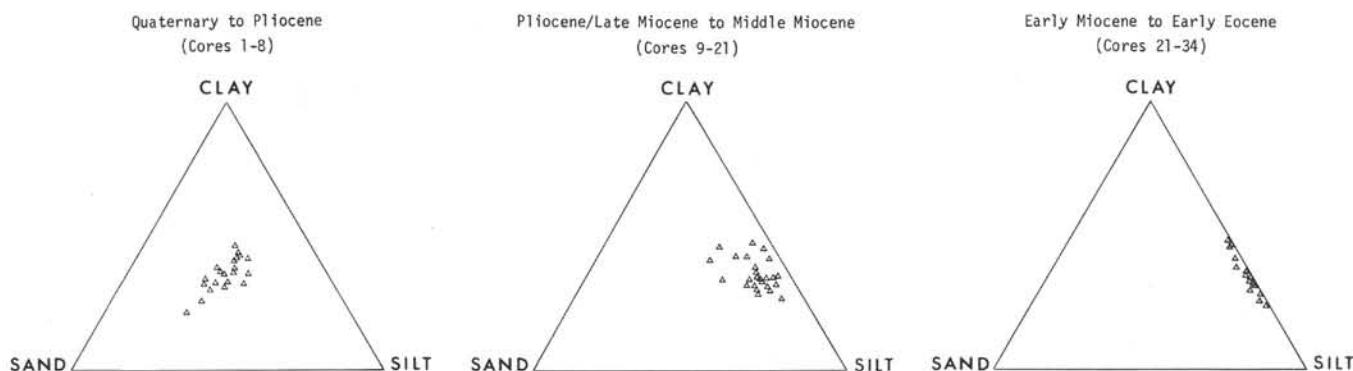


Figure 8. Grain-size analyses of calcareous sediments at Site 214.

of delicate species. Early Pliocene to middle Miocene assemblages have suffered a moderate loss (<50%), but by early Miocene times perhaps as much as 80 to 90 percent of the total original foraminiferal assemblage has been lost because of dissolution.

The abundance of foraminifera in Pliocene and Quaternary sediments is matched by their better state of preservation (Figure 7) at both Sites 214 and 216. Elsewhere in calcareous oozes from Ninetyeast Ridge, the preservation is mostly fair to poor in Cenozoic and Mesozoic faunas.

The only other site which contains foraminifera in abundance is 212 where a few zones in the calcareous units contain 40-50 percent (250-265 m, 288 m) and the others, a maximum of 30 percent (479-482 m). These foraminifera-rich zones are laminated, have a gross textural grading, and often contain a few coarse-silt- to sand-size grains other than foraminifera. The concentration of foraminifera here is due to current action (the foraminifera are reworked from elsewhere—see discussion of Site 212) and not productivity of overlying waters.

Elsewhere in Leg 22 sites, foraminifera are present in rare to trace amounts, and their preservation is usually moderate to poor (for details see Figure 7 and Appendix B).

Other Calcareous Fossils

Basal sediments from the three Ninetyeast Ridge sites (214, 216, 217) contain numerous large thick-shelled calcareous fossils indicative of shallow-water conditions (Figure 4). Pelecypods are most numerous, especially large thick-shelled *Inoceramus* and oysters, but gastropods, molluscs, and brachiopods are also present. The age of sediments containing these fossils is late Paleocene in 214, late Maastrichtian in 216, and late Maastrichtian to late Campanian in 217.

Siliceous Fossils

Siliceous fossils, mostly diatoms and Radiolaria with some silicoflagellates and sponge spicules, were the dominant component in Quaternary to upper Miocene sediments deposited below the CCD and within the subequatorial zone of high productivity as at Sites 211,

213, 215 (Figure 9). In these sites, diatoms are usually far more numerous than Radiolaria, often by as much as 2 or 3 to 1; preservation is usually good. Note that Site 212 contains only traces of siliceous fossils in the Neogene. This may be partly due to dissolution because of the great depth here, but more important, the site is situated south of the subequatorial zone of high productivity.

Site 214, situated on Ninetyeast Ridge and at a similar latitude to 211, 213, and 215, contains well-preserved Radiolaria back to the late Miocene, but these and other siliceous fossils here are greatly diluted by calcareous fossils. Despite this dilution, the siliceous fossils make up about 5 percent of the sediment, and of this amount, diatoms are more numerous than Radiolaria and silicoflagellates about as common. In middle Miocene, the preservation is only moderate, and below this all siliceous fossils disappear until the Paleocene (see later).

Sites 216 and 217, situated progressively farther north on Ninetyeast Ridge, contain rare to trace amounts of siliceous fossils with moderate to good preservation of Radiolaria through much of the Eocene. At the base of the middle Eocene in 216 and in the uppermost Paleocene in 217, siliceous fossils disappear coincident with the appearance of chert stringers. Extensive chertification occurs in Campanian sediments at 217.

At Site 216, diatoms and Radiolaria are present in about equal amounts in Quaternary calcareous oozes, but in Site 217, the former are no longer present at all. Although the data is very limited, the reduction to the north (from 214 through 216 to 217) of the diatom content among the Quaternary siliceous fossils may also be linked to the weakening of the high productivity zone in the same way as a low foraminifera-nannoplankton ratio among calcareous fossils indicates low productivity.

Note in the lower part of the sections cored at 214 (Paleocene) and 216 (Maastrichtian), sponge spicules and diatoms are most common, and silicoflagellates are also present in these shallow-water sediments.

Clay Minerals

Where samples were taken for X-ray diffraction analysis, the distribution of various clay minerals is shown in Figure 10. Five main clay minerals were detected: the continental

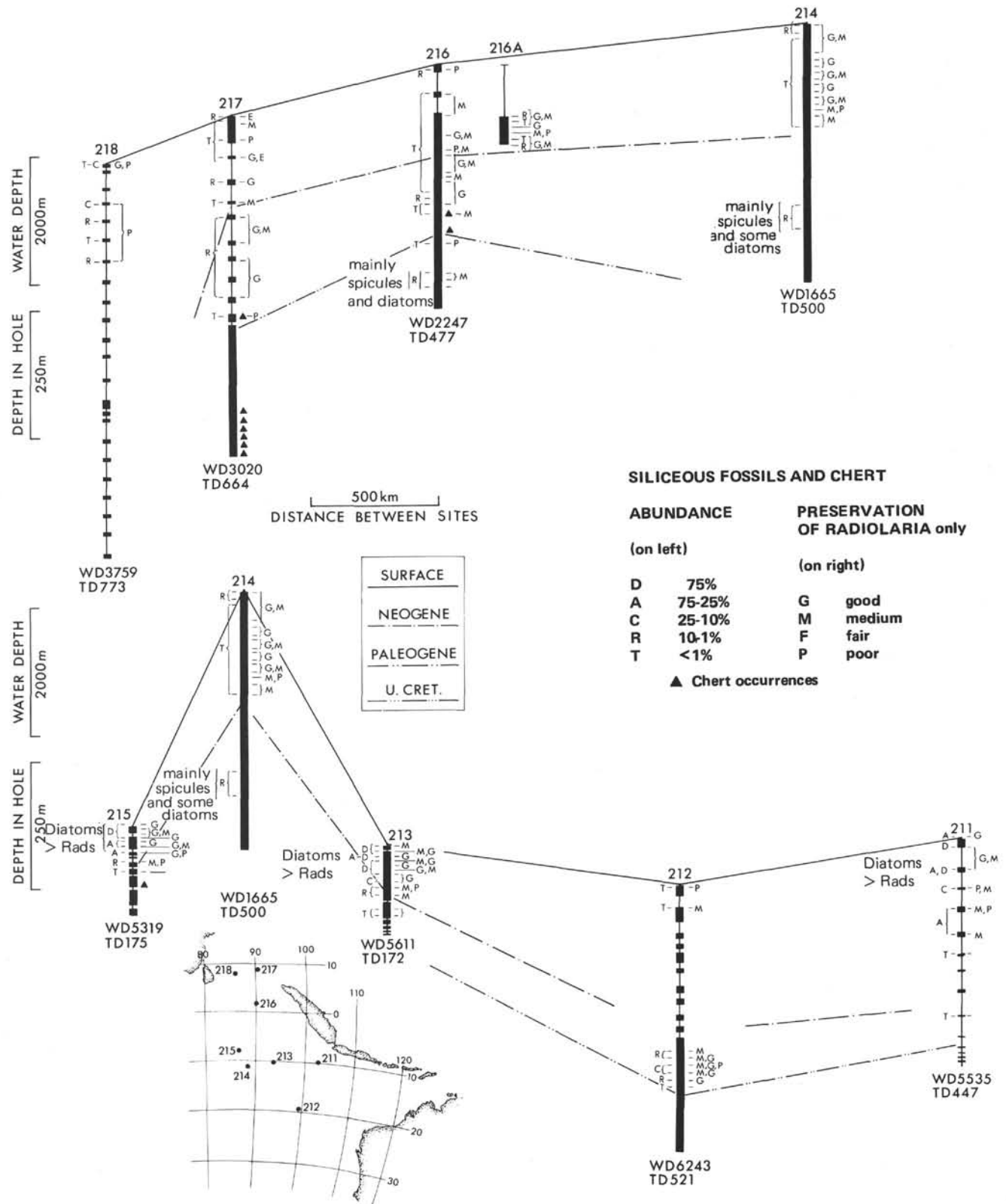


Figure 9. Distribution of siliceous fossils and chert.

detrital minerals kaolinite, mica-illite, and chlorite; montmorillonite, derived from volcanic material; and palygorskite, a mostly authigenic phase in these Leg 22 sediments. Detrital quartz of clay size is ubiquitous but is

treated separately under a different section as it is not a true clay mineral. Also present in a few places, is clay-sized zeolite of authigenic origin, but this is also described elsewhere.

Detrital Clay Minerals

Mica-illite is the most common detrital clay mineral and is abundant in the Miocene to Quaternary sediments of the Bengal Fan (Site 218). It is also common to abundant in Neogene pelagic clays and siliceous oozes deposited in deep water (below the CCD) at Sites 211, 213, and 215.

Kaolinite is common in most sediments from the eastern Indian Ocean (Sites 211, 212, 213) and appears to show some age dependence. The X-ray data (Chapter 37) shows that in Site 212, kaolinite is common (10-20%) in Tertiary sediments, but in the lowermost clay unit below Upper Cretaceous chalk, it is rare or absent. In Sites 213 and 215, Miocene and younger brown clays contain kaolinite, but in both sites it is absent in Eocene sediments. In Site 211, only the brown clay of Core 10 (undated but probably of lower Tertiary age) contains kaolinite in common amounts, but below this, none of the cores contains kaolinite. As kaolinite is largely produced in areas of tropical weathering, this would indicate potential source areas for the material in these sites from Indonesia and North Australia. Some kaolinite is also present in Neogene sediments from Site 215, but elsewhere in Leg 22 material, it is mostly lacking or rare.

Detrital chlorite is comparatively rare in Leg 22 sites, and the only site where small amounts are consistently present is 218.

Volcanogenic Clay Minerals

Montmorillonite is particularly abundant, (frequently as the sole clay mineral) in the volcanoclastic sediments from the lower portions of sites on the Ninetyeast Ridge (Paleocene age in Site 214 and Maastrichtian age in Site 216).

A variety of montmorillonite known as beidellite, where aluminum replaces silicon in the montmorillonite lattice, is present in considerable amounts, together with montmorillonite, in the volcanoclastic sediments which are interbedded with lignites in the lower section of Site 214.

In pelagic clays of all ages and Neogene siliceous oozes from Sites 211, 212, 213, and 215, montmorillonite is common to abundant and occurs in amounts comparable to mica-illite or kaolinite. No assessment can be made as to the relative proportions of montmorillonite formed in situ from the breakdown of basic volcanic rocks or that reworked from continental volcanic sources. Chloritized volcanic rock and glassy lava fragments are common in the volcanogenic material from Sites 214 and 216 (see section later).

Palygorskite

Palygorskite occurs in abundance in Paleogene and Cretaceous sediments at the base of the sedimentary section in Sites 211, 212, and 213 (Figures 10, 11). It is present in both calcareous oozes and brown clays, but more abundant in the latter, and shows a marked increase in abundance in sediments closest to the basalt. In all three sites, the palygorskite occurs in association with other major constituents clearly indicative of a volcanic source as follows: in Site 211 (409-428 meters), K-feldspar and montmorillonite; in 212 (484-508 meters), clinoptilolite, quartz, K-feldspar, and montmorillonite; and in 213

(100-150 meters), montmorillonite, phillipsite, and K-feldspar. Therefore, the origin of this basal palygorskite-rich section above basalt is most probably related to a hydrothermal alteration of sediments primarily formed from the breakdown of volcanic material.

In Site 215, palygorskite is very abundant in brown clay 75 meters above basalt. The palygorskite-rich interval (74-77 meters) in this site is associated with other major constituents indicative of a volcanic source—phillipsite and montmorillonite. Thus, a hydrothermal origin for the palygorskite is again most likely. Between the palygorskite interval in the brown clay and basalt is a calcareous ooze sequence. One sample X-rayed from this ooze close to the basalt did not show significant palygorskite despite a predominance of montmorillonite in the $<2\mu$ calcite-free fraction. An iron oxide facies in the calcareous sediments closest to the basalt would appear to indicate some hydrothermal activity here (Pimm, Chapter 20).

Elsewhere in Leg 22 sediments, palygorskite was rare or absent. Even on a calcite-free basis, the only other sites which showed palygorskite were in sporadic occurrences well above basalt in Sites 212 and 216 (Figure 11). The occurrences in Site 212 are in brown clay at 289 and 319 meters. In the former sample, the mineral association is mixed and not clearly distinctive as to its origin. However, in the lower sample, clinoptilolite is very abundant in the bulk sample and may indicate an altered volcanic ash bed.

In Site 216, the palygorskite occurs in calcareous sediments. Between 292 and 345 meters, the palygorskite is associated with montmorillonite and some clinoptilolite. However, in marked contrast, the occurrence at 121 meters shows an association with continentally derived kaolinite and illite and, therefore, is probably reworked from a land area rather than an alteration product of volcanic material as in all other Leg 22 samples.

Detrital Minerals

Figure 12 shows the distribution of the three major detrital minerals in the 2-20 μ range (calcite-free basis) as determined by X-ray diffraction. All numbers discussed below refer only to this fraction.

Although only a small number of samples from the recovered sediments were submitted for X-ray, certain trends are still very apparent. By comparing Figure 4 with Figure 12, it can be seen that most X-ray samples were taken from the noncalcareous portion of the sedimentary columns penetrated. However, in a few calcareous samples, the calcite-free 2-20 μ fraction appears to follow the same trends as the noncalcareous sediments X-rayed (e.g., Sites 211, 212, and 213).

At Site 211, there is a very pronounced contrast in the type of feldspar occurring in Quaternary to Pliocene sediments and that occurring in the lower Tertiary (?) to Cretaceous. The younger sediments have a preponderance of plagioclase (16-22%) over K-feldspar (5-8%), but in the older sediments K-feldspar is very abundant (43-60%), and plagioclase is lacking. The quartz content is variable, but always common to abundant, yet shows no significant age trends. Illite (mica) shows a gradual decrease downhole

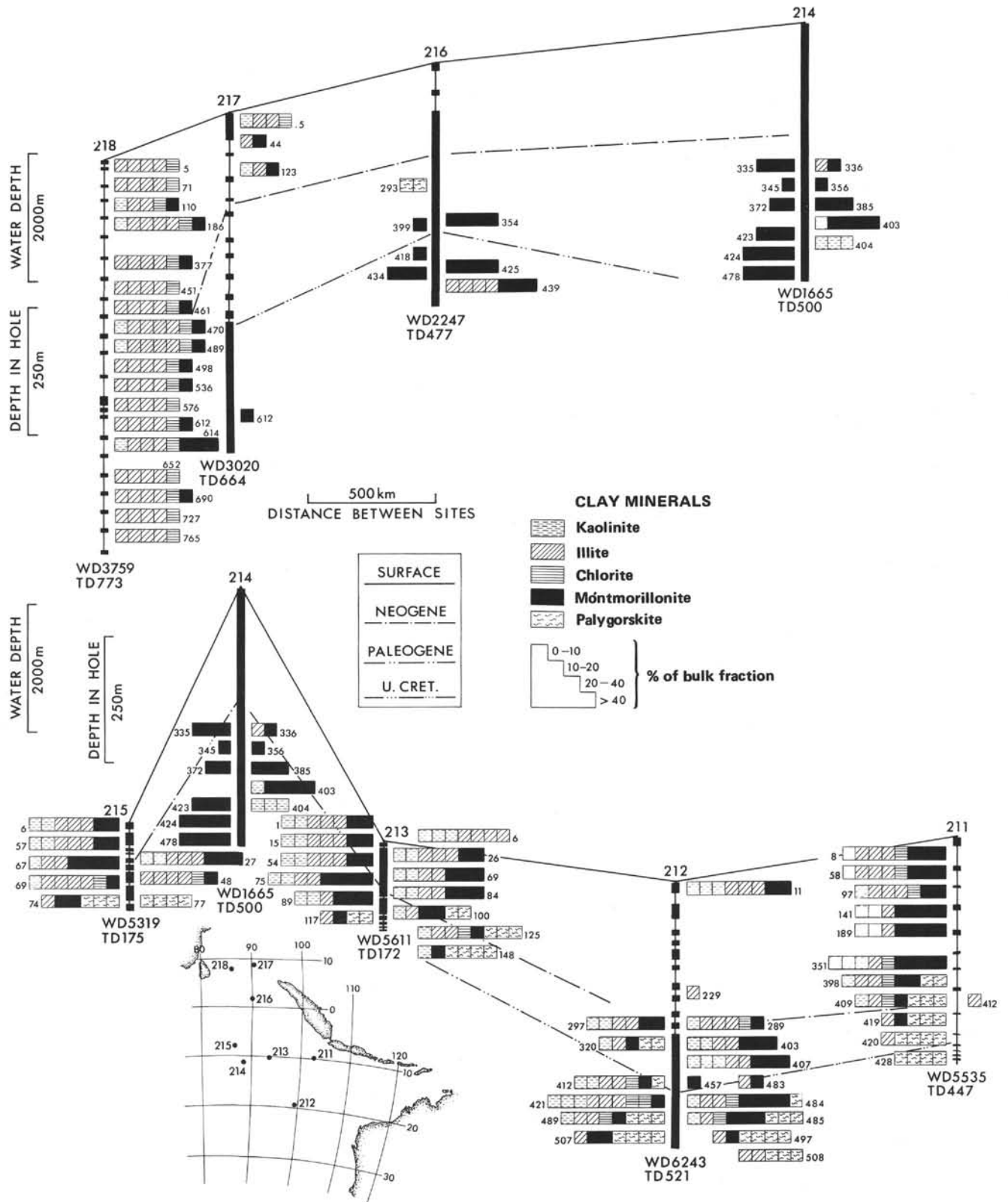


Figure 10. Distribution of clay minerals, sample depths are written at the end of the bars.

(>20% to <5%) but with no dramatic variation like the feldspars.

Most samples (Paleogene and older) X-rayed from Site 212 showed somewhat constant quartz, K-feldspar,

plagioclase, and illite contents downhole (very approximate ratios 2:1:1:1). The lowermost sample from Site 212 was taken in zeolitic iron oxide-rich claystone 8 m above basalt and the X-ray results showed 50 percent K-feldspar, no

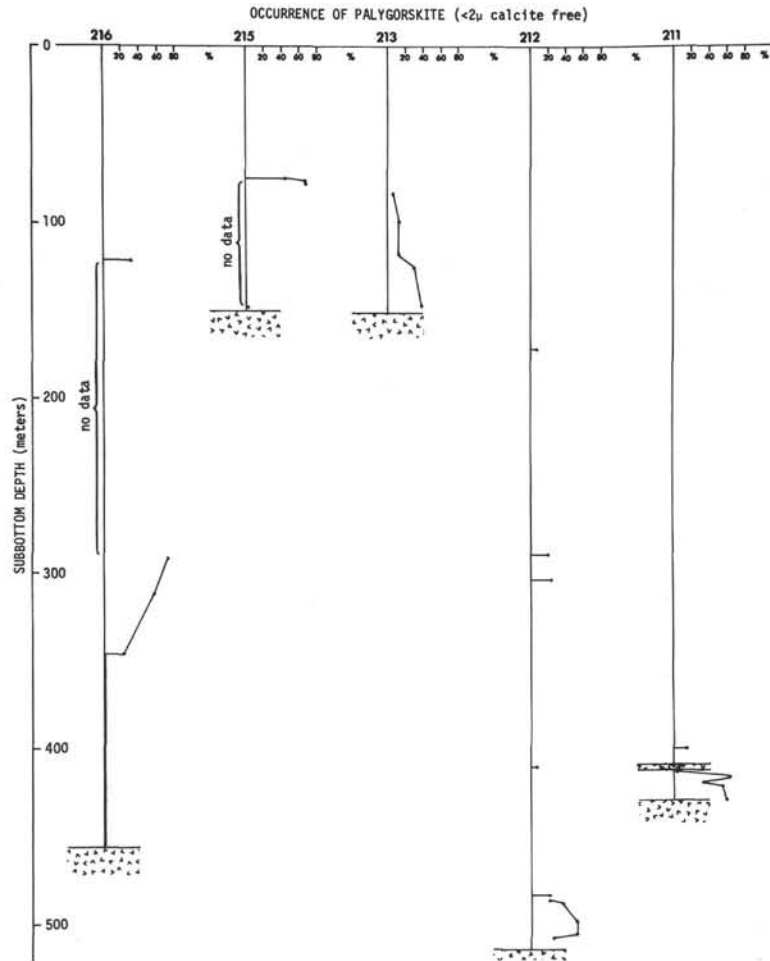


Figure 11. Occurrence of palygorskite.

plagioclase, and quartz and illite contents similar to those above.

At Site 213, plagioclase is almost totally lacking in all samples X-rayed (older pre-mid-Miocene to early Eocene), but K-feldspar is low in pre-early Eocene sediments and markedly more abundant in lower Eocene sediments (Cores 14, 16) so that it is generally as abundant as, or more abundant than, quartz.

Insufficient data is available from Site 215, where comparable older sediments to those rich in K-feldspar at Site 213 were not X-rayed. There is at this site, however, a moderate increase of K-feldspar and a slight decrease of plagioclase with depth. Quartz is far more abundant than either feldspar type. A high content of illite (49%) is seen in the sediments of Core 8 (69.20 m), which are interpreted as being the distal portion of the Bengal Fan (compare with Site 218).

Paleocene sediments from Site 214 show a marked change in the type of feldspar present at a depth of 390 meters. Above this depth, plagioclase ranges from 22 to 75 percent with no K-feldspar present and below 390 meters, plagioclase is almost totally absent and K-feldspar ranges from 24 to 83 percent. This change coincides with a significant lithologic boundary between glauconitic shallow-water carbonate sediments above, and volcanic clay and volcanoclastic sediments interbedded with lignite below.

The thick sequence of Neogene detrital sediments penetrated at Site 218 in the Bengal Fan shows a very uniform detrital mineral assemblage with abundant illite and quartz, the former usually dominant over the latter, and much smaller amounts of feldspar, with plagioclase predominating over K-feldspar.

The abundance of K-feldspar over plagioclase feldspar in the lower portions of the stratigraphic column at all sites sampled (211, 212, 213, 214) suggests that at least some of the K-feldspar could be of authigenic origin.

Zeolites

The distribution of zeolites is shown in Figure 13. Zeolites were comparatively rare in Leg 22 sediments, mostly being restricted to brown clays of early Miocene to Paleogene age in Sites 212, 213, and 215 and to volcanoclastic sediments of Paleogene age in Site 214 and Cretaceous age in 216.

Throughout the brown clays of Site 212, zeolite was seen in all smear slides but only detected in three intervals by X-ray diffraction. This is due to the highly variable degree of crystallization, and in places (Cores 36, 37) where as much as 50-70 percent zeolite was estimated from smear slides, none was reported from the X-ray data. Rarely well crystallized laths, 12-15 μ in length, were seen. In the X-ray

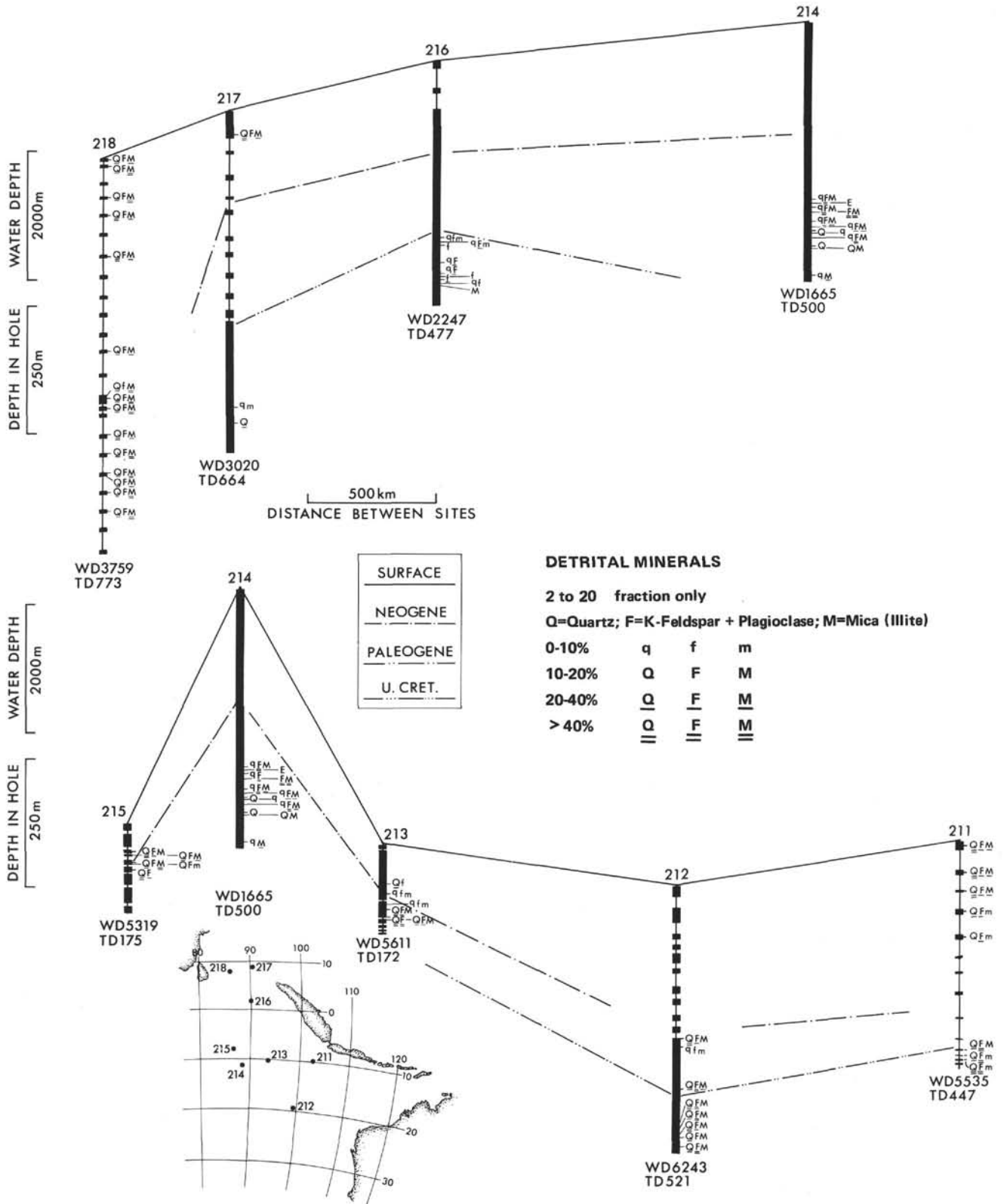


Figure 12. Distribution of detrital minerals.

samples of early Eocene and older age, the zeolite was identified as clinoptilolite, although one sample (Core 18) also contained a very minor amount of phillipsite.

In contrast to Site 212, phillipsite was the only zeolite detected in Site 213. It occurs in upper Miocene to post-early Eocene brown clays. Only a thin section of

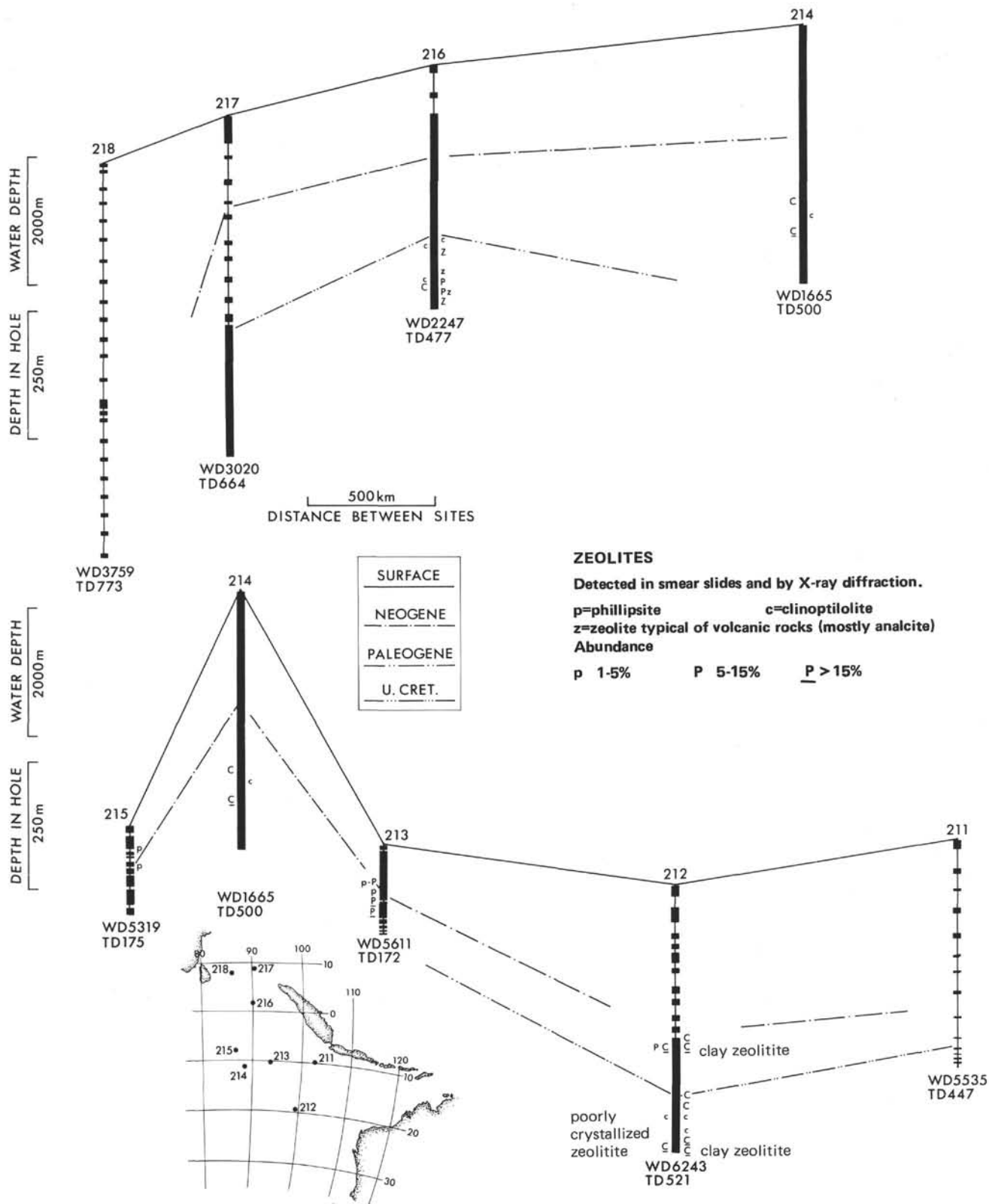


Figure 13. Distribution of zeolites.

post-early Eocene brown clay was penetrated in Site 215, but again phillipsite was the only zeolite detected. In the volcanogenic sediments of Site 216, clinoptilolite and

phillipsite were detected and, in addition, a third zeolite analcite was also present. This latter mineral is typical of volcanic rocks.

In Site 214, clinoptilolite occurs in the nonmarine sequence in rare restricted horizons except at 391 meters, where two samples X-rayed consisted almost entirely of clinoptilolite. The sediment here is brown in color, strongly lignitic, and contains abundant white flecks.

On the limited data available from Leg 22, clinoptilolite appears to be the dominant zeolite in Eocene and older sediments, but phillipsite is more common in younger sediments, and clinoptilolite is lacking.

Manganese

No manganese nodules were recovered from any Leg 22 sites, probably, because the sedimentation rates are too high even in areas below the CCD where siliceous oozes were recovered from the sites. Nowhere in any of the Leg 22 sites are true pelagic brown clays at the surface. The manganese seen in Quaternary and Pliocene sediments at Sites 213 and 215 (Figure 14) occurs as ubiquitous black specks or concentrated into dark bands. Minor amounts of Mn were also seen in brown clays occurring at depth in Sites 212, 213, and 215.

Elemental analyses showing the distribution of Mn in Sites 211, 212, and 213 are given elsewhere in this volume (Chapter 20).

Iron Oxides

Small amounts of iron oxides (mostly goethite) are ubiquitous in sediments within an oxidizing environment. The iron oxides occur as small yellow-brown granules of varying shape and are most common in the brown clays in Sites 211, 212, 213, and 215. Trace amounts of iron oxide also occur in the mostly oxidized calcareous oozes of Site 212. The distribution of iron oxides is summarized in Figure 14.

A basal iron oxide-rich facies is developed in calcareous and clay sediments at Sites 211, 212, 213, and 215. The iron oxide here is very abundant, particularly in close proximity to the basalt, and is mostly goethite with some hematite. Much of the iron is amorphous and not detectable by X-ray diffraction. Elemental Fe analyses and a discussion of this facies are given by Pimm (Chapter 20).

Glauconite

Glauconite, occurring as dark to pale green and pale brown sand-size grains, was detected in four sites (Figure 14). In Sites 214 and 216 on Ninetyeast Ridge, glauconite is fairly common in shallow-water carbonate sediments. Trace amounts of glauconite were also seen in calcareous oozes from Sites 212 and 217.

At Site 214, glauconite is present throughout 65 meters of Paleocene to early Eocene carbonate silty sands. The Paleocene sediments (Cores 37-41) contain up to 5 percent of mostly green glauconite, and up to 10 percent (~70 percent of the sand fraction) of green and brown glauconite core found in early Eocene sediments (Cores 35-36). The glauconite is mostly in the form of homogeneous

rounded-subrounded grains; only rarely were glauconitized foraminiferal casts seen. The dominantly green Paleocene glauconite often contains pyrite and is associated with reduced pyrite-rich sediments. The occurrence of brown glauconite grains in the upper part of this glauconite sequence indicates micro-oxidizing environments or reworking from elsewhere. At 335 meters depth and about 12 meters below the top of the glauconitic sequence, there is a hiatus of about 4 m.y. between late Paleocene (foraminiferal Zone P.4) and early Eocene (P.7) sediments.

Approximately 56 meters of Maastrichtian (Cores 23-29) nannofossil chalk and volcanic clay shelly micarb chalk at Site 216 contain significant amounts of glauconite. Throughout this interval, the glauconite usually makes up 5 to 10 percent of the sediment. The form of the glauconite is rather variable and only in a few places (Cores 28, 29) do subrounded grains similar to those at Site 214 occur. In Cores 25-29, the glauconite is all green, and forms most subangular small grains. In Core 24, it occurs as irregular green aggregates often intimately associated with foraminiferal tests, a few of the latter containing brown glauconite(?) in their test chambers. Also in Core 24, there is a 7-cm-thick laminated bed consisting of about 50 percent green glauconite. Traces of glauconite also occur above and below this thick section of glauconite-rich sediments.

In Site 217, the interval 570 to 625 meters contains trace amounts of glauconite in upper Campanian to lower Maastrichtian limestone.

The middle Eocene chalk unit in Site 212 also contains trace amounts of glauconite in a few cores between 326 and 402 meters.

Sedimentary Structures

No attempt is made here to systematically describe all the variety of sedimentary structures encountered in the sediments recovered on Leg 22. Figure 15 summarizes the main types and distribution of sedimentary structures in each site. For details, the reader should see the core descriptions in each site report.

However, in a few instances the type of sedimentary structures are particularly important in interpreting the sedimentary history of certain units; these are discussed below.

At Site 212, several units of calcareous ooze occur within a sequence of pelagic brown clays deposited below the CCD.

In Core 2 calcareous oozes are interbedded with brown clay beds. One clay bed is 4.4 meters thick but the other five are only 10-40 cm thick. Contacts between these lithologies are usually sharp except for two calcareous oozes which show a very sharp base but a transitional top—the ooze gradually giving way to clay (Plate 1a). Faint laminations 2-3 mm thick reflect variations in content of foraminifera in Core 5. Core 13 is strongly laminated and even cross laminated in zones 5-50 mm thick which contain as much as 40-50 percent foraminifera (Plate 1b, c). In Core

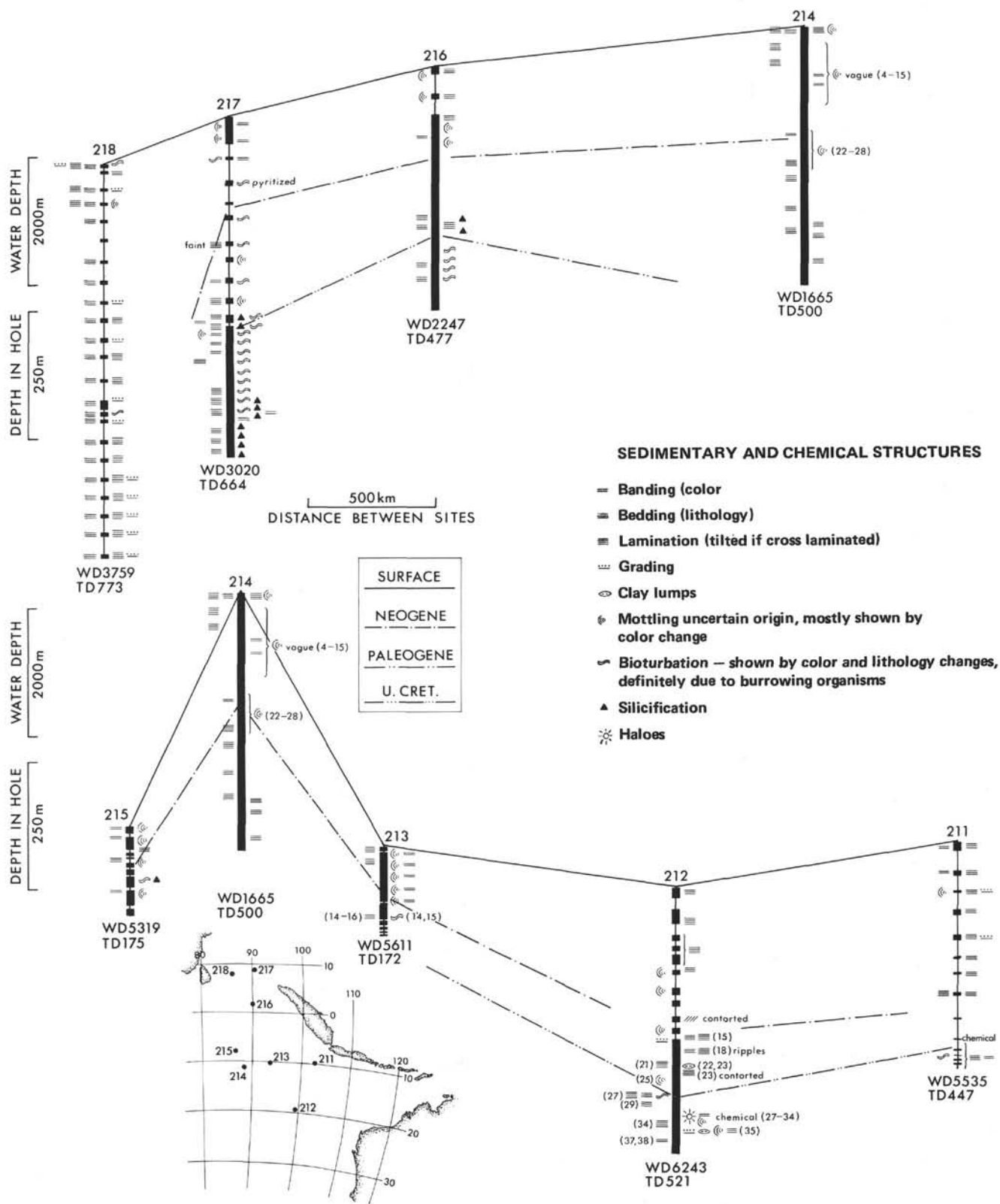


Figure 15. Sedimentary structures.

15, the base of the chalk unit is also well laminated and graded in the lower part due to an increase in foraminifera content and also to fragments of the underlying greenish clay. The actual contact with underlying clay is sharp but irregular. A 1-cm-thick reduced zone of grayish-blue-green

claystone lies on top of brown clay immediately beneath the contact.

A 20-cm-thick grayish-olive-green interbed of clay occurs within the chalk of Core 23. The lower contact of the clay is gradational, but the upper one is sharp. The white chalk

just below this has pale yellowish-brown laminations 1-10 mm thick which range from regular, to wavy, to contorted as recumbent folds (Figure 4, Plate 1). Some green claystone fragments are present in the darker laminations. The contact of this chalk unit with clay is sharp (Core 27 and the chalk immediately above is bluish white in color, not light gray or pinkish gray as higher up). A 23 cm thick reduced dark greenish gray to bluish gray occurs in the brown clay 42 cm below the contact. In Cores 27 and 28, several thin bleached olive zones are surrounded by dark reddish-brown hematite(?) haloes (Figure 5, Plate 1). The bleached zones appear to contain volcanic ash and more zeolite than the surrounding clay. The contact between clay and the next chalk unit below was lost between Cores 29 and 30. The base of the lowermost (Cretaceous) chalk unit was cored in Core 35. Above the contact, the chalk is color banded in 1-cm greenish-gray and olive-gray bands and shows an increasing content of foraminifera downwards, and in the lowermost 70 cm, green claystone fragments similar to the 40-cm-thick zone of grayish-green reduced clay below the contact and lying on top of the lowermost brown clay sequence.

The interpretation of these calcareous ooze/chalk units in deep-sea brown clay at Site 212 is presented in the regional conclusions section. However, the lamination, cross lamination, grading, sharp basalt contacts, and transitional upper zones into clay, and the inclusion of underlying clays in the lowermost sections of calcareous units, all point to significant sorting, winnowing, and erosion by submarine currents of varying intensity.

Some general observations on sedimentary structures in the predominantly terrigenous sequence at Site 218 in the Bengal Fan were given in the site report. Enlargements of some of the core photographs are given in Plates 2, 3, and 4 to illustrate the most important features of this succession. In the regional summary and conclusions section at the end of this chapter, downhole variations in sand:silt:clay ratios have been used to show the existence of four major pulses of deposition of coarser terrigenous material. In the brief description of the sedimentary structures given here, the pulse numbers (1 through 4) refer to those shown in Figure 40 at the end of this chapter.

In the upper part of Hole 218 (down to Core 12), the silty sand and sandy silt beds of Pulses 1 and 2 are thicker than below (up to 50 cm). They are poorly sorted and show clear grading (Figures 1-3, Plate 2). In some places, some of the graded beds have both a sharp lower and upper contact (Figure 4, Plate 2) suggesting some erosion prior to, or during, deposition of the younger beds. A few sandy silt and clayey silt laminations were seen (Figures 4, 5, Plate 2), and they are more common in the interval of finer grained sedimentation between Pulses 1 and 2 (Core 8; Figure 5, Plate 2).

In the middle section of Hole 218 (Cores 13-19) between Pulses 2 and 3, the sandy beds are thinner and commonly are only about 5 cm thick (Core 16, Figure 1, Plate 3). Within this section, some sandy silt laminae, less than 1 cm thick, and a few well-sorted thin silt laminae appear with some regularity. (As these cores were photographed soon after splitting, these features do not show up clearly because the core surface was too wet). The most distinctive feature of this section is the presence of

several nannoplankton chalk beds which show abundant burrows, mottles, worm tubes, and fecal pellets (Cores 16, 13, 18, 19; Plates 3a-d). Also present are structures of a nonorganic origin such as lamination and minor folding (Figures 3, 4, Plate 3).

The lower section (Cores 20-27) includes Pulses 3 and 4 with an intervening period of quieter conditions. These lower two pulses are much finer grained than the two above. This whole lower interval is characterized by well-developed cyclicity of sedimentary features. The graded sandy silt beds reach a maximum of 20-25 cm in thickness (Figures 3, 4, Plate 4), but are usually thinner. Laminae of clean silt occur both singly and as multiples a few cm thick (Figures 1, 3, 4, Plate 4). In the interval between Pulses 3 and 4, some beds of bioturbated nannoplankton chalk occur once again (Figures 2, 4, Plate 4). The most unique sedimentary feature of this lower portion of Hole 218 is the occurrence of darker laminae (<1 mm thick) of more clay-rich extremely fine grained silt at regular intervals with an average spacing of about 2 cm (Figures 1, 3, 6, Plate 3). This pattern is superimposed on all other gross sedimentary features—even graded sandy silt beds (Figure 4, Plate 4)—with the exception of the pelagic bioturbated intervals. The origin of these laminae is uncertain, but presumably they represent the finest fraction of periodic depositional events such as times of exceptionally heavy discharge of sediment-laden flood waters from the Ganges-Brahmaputra river system. Using the limited paleontological data available for the Miocene section here (see later), a 2-cm spacing would indicate an approximate 400 year frequency when each event affected Site 218.

MAJOR SEDIMENTARY FACIES

Calcareous Ooze

General Discussion

Table 2 summarizes the composition of a representative selection of calcareous oozes recovered on Leg 22. The calcium carbonate analyses are plotted in Figure 16, and a complete listing is given as Appendix C.

The calcareous oozes at the two southerly sites (214, 216) on Ninetyeast Ridge are extremely pure. In Site 214, Pleistocene to lower Eocene oozes contain a very narrow range of CaCO_3 between 92 and 97 percent, gradually increasing with depth. Pleistocene to Paleocene oozes from Site 216 also have a narrow range of CaCO_3 (83% to 97% with most values over 90%). In Site 217, a much greater admixture of noncalcareous material is present, particularly down to the late Miocene where CaCO_3 ranges from 52 to 71 percent (see discussion of 217A below). Lower Miocene to lower Maastrichtian oozes in Site 217 mostly have CaCO_3 values greater than 80 percent, but the range is much greater than in the other two sites on Ninetyeast Ridge—about 30 versus 5 in 214 and 15 in 216. The only variation among the calcareous components in these oozes is the relative proportions of nannoplankton to foraminifera; the latter only becoming common in the Pliocene and Quaternary sediments. This variation in foraminifera content is believed to be mainly a secondary feature due to dissolution effects (see foraminifera section earlier).

TABLE 2
Analysis of Calcareous Ooze/Chalks

Site-Core:	212-12	212-32	214-3	214-37	216-4	216-21	216-32	217-4	217-34	217-37	211-12	213-16	215-16	218-6
Subbottom (m):	228.90	457.40	19.30	345.20	121.10	311.20	418.00	122.60	582.50	611.80	411.90	144.60	147.80	109.70
Age:	E. Mid-Miocene	Late Cretaceous	Pleist.	Paleo.	Mid. Mio.	Paleo.	Lt. Maas.	Lt. Mio.	E. Maas. - Lt. Camp.	E. Maas. - Lt. Camp.	Maas.	Lt. Paleo.	Paleo.	Pleist.
Quartz ^a	9	5	19	—	18	8	—	11	1	6	15			17
Feldspar ^a	7	6	8	17	—	—	7	3			17		10	3
Mica-illite ^a	10	5	30	—	20	—	—	23		4	30			26
Chlorite ^a	—	—	—	—	9	—	—	4			2			7
Kaolinite ^a	16	1	25	—	22	—	—	11					6	7
Heavy Minerals ^b														
Iron oxides ^b	1										4			
Pyrite ^a			—	5	—		12		2	3				
Glauconite ^b				5					Tr					
Montmorillonite ^a	58	82	7	78	—	34	81	48	92	81	33		84	40
Palygorskite ^a	—	—	—	—	31	56								
Zeolite ^a	Tr (S,S)	2	—	—	—	2			2	5				
Barite ^b	—								3					
Siliceous fossils ^b			Tr	2	Tr	—	5	8						
Volcanic glass ^b	—		Tr	1	Tr		5-10		Tr					
Calcite ^c	98	97	100	88	100	99	87	86	85	12	81	100	100	50
Dolomite ^b										80	1			
												All U-2 ^d		

^aX-ray of <2 μ calcite free.

^bSmear Slide.

^cBulk X-ray.

^dSee Chapter 37.

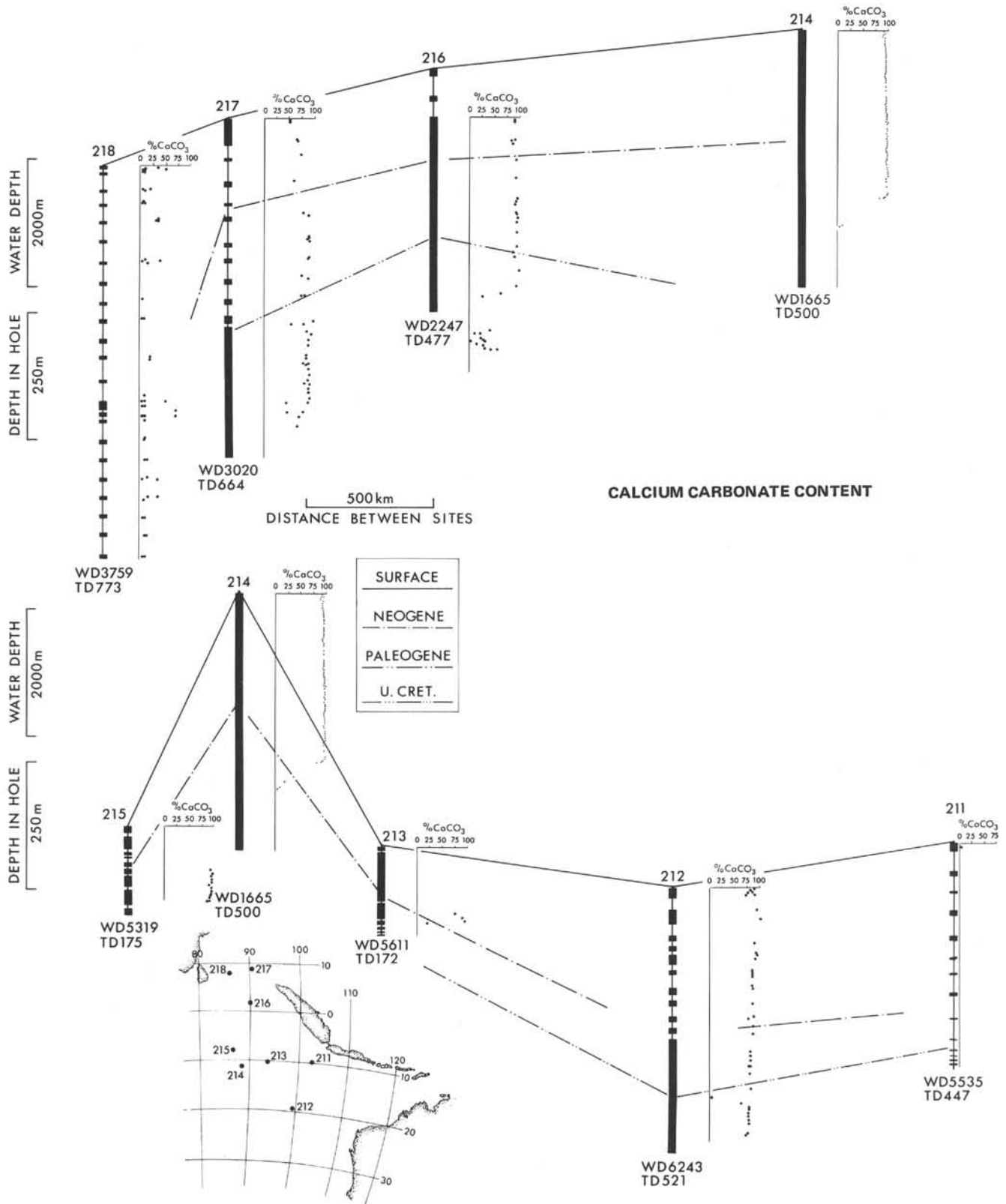


Figure 16. Calcium carbonate content.

Abundant porosity data (measured on the GRAPE) is available from Site 214, which was continuously cored. Limited data is also available from Sites 216 and 217. A summary of this data is given below:

Site	Age	Depth (m)	Range of Porosity (%)
214	Quaternary to Pliocene	0-85	71-64
	Miocene	85-219	63-54
	earliest Miocene to Eocene	219-230	50-44
216	Quaternary to Pliocene	0-50	68-63
	Miocene	80-177	60-56
	Oligocene	187-260	59-53
217	Quaternary to Pliocene	0-50	75-64
	Miocene	70-190	69-59
	Oligocene	230-310	58-50
	Eocene to Paleocene	340-420	58-43 (few values only)

In conclusion, the porosity reduction with depth is a fairly constant linear decrease for calcareous oozes at all three sites. From the surface down to about 50 meters, the porosity decreases from >70 to 65 percent; from 50-200 meters, porosity decreases from 65 to 55 percent; and below 200 meters, the porosity is usually less than 55 percent.

Among the noncalcareous components, minor variations are apparent from the X-ray diffraction data on the 2μ calcite-free analysis (Table 2). In Miocene and younger sediments from Ninetyeast Ridge, the clay fraction mostly comprises material of continental origin: quartz, illite, and kaolinite. In Paleocene and Cretaceous oozes analysed, montmorillonite (or in one case palygorskite) is very abundant, but the continental contribution is almost totally lacking.

In Sites 211, 213, and 215, calcareous oozes only occur in the older Tertiary or Cretaceous. In Site 211, continentally derived clay minerals are more abundant than montmorillonite, but in 213 and 215, continental components are lacking. Several CaCO_3 analyses are only available from Site 215 and show a consistently high content (89%-97%) in early Eocene and Paleocene sediments.

The calcareous oozes in Site 212 have all been redeposited during several relatively short time periods (see later). The variation in CaCO_3 content is fairly small, but there is a trend toward lower values in the older units. Range of values (percent CaCO_3) for each unit are as follows: middle Pliocene 75-89; middle to late Miocene 83-93; early middle Miocene 75-86; middle Eocene 77-82; Late Cretaceous 72-77. The only variation in the noncalcareous fraction of the two units sampled is very minor—almost absence of kaolinite and a higher proportion of montmorillonite in the Cretaceous (Table 2).

Discussion of 217A Surface Cores

Because of the variation in carbonate content and the pronounced alternation of light and dark layers seen in late Miocene and younger sediments in Hole 217 and the wide spacing of cores in the upper section here (only 4 cores in top 125 m), it was decided to drill Hole 217A and continuously core the upper section back into the Pliocene.

Many authors (Arrhenius, 1952; Hays, et al, 1969; Kaneps, 1973) have reported cyclic carbonate sedimentation and some have suggested correlation of the intervals richer in CaCO_3 , relative to clay content, with glacial stages.

Unfortunately, of the four cores taken in Hole 217A, none had a complete recovery, and it is not possible at this time to speculate whether a portion of the cored interval was lost or the drilling actually compressed the sediment recovered into a shorter length than the interval cored.

Closely spaced samples were analyzed for CaCO_3 content and the results are plotted in Figure 17. The range of CaCO_3 is from 45 to 72 percent with pronounced cyclical variations. Two age datums were recognized on the basis of nannoplankton floras (S. Gartner, personal communication): the top of the *P. lacunosa* Zone (NN19) ~350,000 years B.P. between 2.65 and 2.90 meters, and the top of the *D. brouweri* Zone (NN18) (Pleistocene/Pliocene boundary ~1.83 m.y.B.P.) between 22.30 and 22.50 meters. The fact that these datums can be tied down accurately (nannoplankton samples were only taken at 25 cm intervals) suggest that not too much vertical contamination was caused by the drilling process despite the rather disturbed appearance of the color bands.

The absence of paleomagnetic reversal data and the presence of gaps (due to coring artifacts) in the carbonate curves prevent an accurate comparison with the carbonate fluctuations of other workers. Even over intervals close to the two fixed time datums, the curve from 217A does not match the curves from the Equatorial Pacific. The two other sites (216 and 214) drilled on the Ninetyeast Ridge closer to the high productivity region of the Indian Ocean did not show the same marked color banding in the surface cores nor did the carbonate analyses indicate any fluctuations in CaCO_3 content; in fact the analytical results were extremely uniform.

The variations in carbonate content at Site 217 are most likely related to a fluctuating supply of terrigenous clay brought into the head of the Bay of Bengal by the Ganges and Brahmaputra rivers. This may of course be related to glacial stages as sea level lowering at such times would cause a lowering of the base level and a subsequent increase in erosion. However, it should be noted that in Hole 217, clay is abundant in calcareous oozes down to a depth of 145 meters i.e., late Miocene.

Siliceous Oozes

Siliceous oozes were only recovered from three sites (211, 213, 215). They range in age from late Miocene to Quaternary. The predominant components are diatoms and Radiolaria, and evidence was presented earlier to show

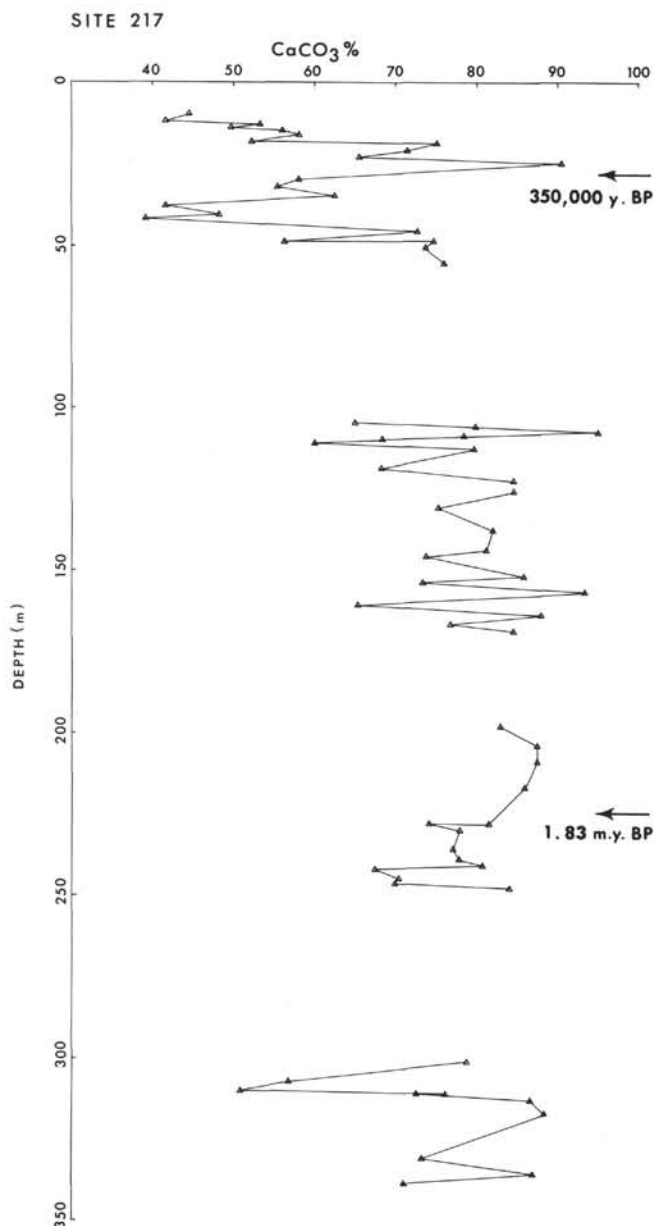


Figure 17. Fluctuations in calcium carbonate content in Hole 217A.

these oozes were deposited beneath the zone of high productivity situated just south of the Equator in the Indian Ocean. In Sites 213 and 215, it could be estimated that the oozes accumulated at about 12 m/m.y.

Among the nonbiogenic constituents, all three sites show a very uniform composition (Table 3). Terrigenous minerals predominate with quartz and illite being more abundant than kaolinite and feldspar. Montmorillonite is also fairly common.

Terrigenous Sediments

Two sites (218, 211) penetrated thick sequences of terrigenous sediments. At Site 218, a middle Miocene to

Quaternary sequence is 773 meters thick, and at Site 211, a Pliocene sequence is 200 meters thick. Using the limited paleontologic data available (Chapter 9), accumulation rates can be estimated as follows:

- 1) Site 218 (maximum rates): Quaternary 110 m/m.y.; Pliocene 35 m/m.y.; Miocene 50 m/m.y.
- 2) Site 211 (minimum rate): Pliocene 65 m/m.y.

X-ray diffraction data of representative samples of terrigenous sediments is given in Table 4. The dominance of illite with less abundant quartz is clearly apparent in Sites 218 and 211. Two thin beds of much finer grained terrigenous sediments of Miocene age were penetrated in Site 215. Their affinity to coarser grained sediments at Site 218 is clearly seen from the X-ray data (Table 4). The noncalcareous <2 micron fraction in Pleistocene sediments at Site 217 also gave a typical X-ray analysis for terrigenous sediments.

A heavy mineral analysis of the terrigenous sediments at Site 218 is presented in Chapter 38. The results of this study indicate a predominance of an acid igneous and high rank metamorphic suite of heavy minerals in the Quaternary and Pliocene but a transition to a more predominantly low rank metamorphic and altered suite of heavy minerals in the Miocene.

Grain-size analyses of terrigenous sediments at Sites 218 and 211 are given in Figure 18 and downhole variations in sand-silt-clay ratios are discussed in the regional conclusions section at the end of this chapter.

Pelagic Clays

The only site which penetrated a fairly thick sequence of pelagic brown clays was 212, where a total thickness of 97 meters was recovered. The clays here are interbedded with redeposited carbonate units so some age control is available despite the barren nature of the clays themselves. Dating of carbonate immediately adjacent to the clay suggests an average accumulation rate of 1 m/m.y. with a range of from 0.7 to 1.6 m/m.y. in different clay units. However, this assumes no sedimentary discontinuities in the clays, which, in the light of the major discontinuities (Oligocene) discovered in the clay at the deep-water Sites 213 and 215 (see later), may be unjustified.

The bulk X-ray diffraction data (representative samples listed in Table 5) indicate that continentally derived constituents such as quartz, kaolinite, and illite predominate in the Tertiary clays at Site 212. Even among the clay-sized fraction ($<2\mu$) volcanically derived constituents, either montmorillonite or palygorskite, are only dominant in Cretaceous sediments (see X-ray results in Chapter 37). Limited data from Sites 211, 213, and 215 show that volcanic constituents are more abundant (up to 50% of bulk sample) in Tertiary sediments than they are in these sediments at Site 212.

The significance and or genesis of palygorskite, zeolite types, and kaolinite were discussed in the distribution of components section earlier as they also occur in other lithologies despite their being most abundant in clays.

TABLE 3
Analysis of Siliceous Oozes

Site-Core:	211-3	213-1	213-3	213-6	215-1	215-4	215-7
Subbottom (m):	57.90	0.70	26.10	53.70	6.40	27.00	57.10
Age:	Plio.	Quat.	Lt. Plio.	Lt. Mio.	Quat.	E. Plio.	Lt. Mio.
Quartz ^a	24	31	26	26	24	27	28
K-Feldspar ^a	4	—	—	3	—	—	—
Plag-Feldspar ^a	11	14	8	11	9	6	8
Mica-illite ^a	27	25	30	25	35	24	28
Chlorite ^a	3	—	—	—	—	—	—
Kaolinite ^a	5	19	19	18	17	19	16
Fe-oxides ^b		1	2	7	3	—	—
Montmorillonite ^a	26	11	17	16	15	24	20
Siliceous fossils ^b		84-95	74	78	92	80?	72

^aBulk X-ray.^bSmear Slide.

TABLE 4
Analysis of Terrigenous Sediments

Site-Core:	211-4	215-6	217-1 ^c	218-2	218-8	218-15	218-26
Subbottom (m):	97.20	47.80	0.40	8.20	186.10	451.00	690.00
Age:	Plio.	Lt. Mio.	Pleist.	Pleist.	Pleist.	Lt. Mio.	M. Mio.
Quartz ^a	26	20	19	19	22	21	22
Plag-Feldspar ^a	10	4	3	6	4	3	4
K-Feldspar ^a	5	2	2	3	—	—	3
Mica-illite ^a	38	61	38	65	53	63	54
Chlorite ^a	2	6	7	6	6	7	8
Kaolinite ^a	3		4	—	3	—	—
Heavy minerals ^b				5	10	2-7	—
Fe-oxides ^b				—	—	8	—
Montmorillonite ^a	16	7	26	—	5	—	—
Calcite ^a				—	7	4	7

^aBulk X-ray.^bSmear Slide.^c<2 μ calcite free fraction.

TABLE 5
Analysis of Pelagic Clays

Site-Core:	211-10	212-2	212-16	212-28	212-37	213-10	213-14	215-9
Subbottom (m):	351.00	10.70	297.50	411.70	497.30	88.70	125.20	74.40
Age:	Mid. or E. Tertiary?	Mid. Plio. or younger	Oligo.?	Eoc?	Cret.	Mid. Mio.	E. Eoc.	E. Tertiary
Quartz ^a	16	35	29	14	24	14	13	10
Plag.-Feldspar ^a	2	7	5	5	8	9	—	—
K-Feldspar ^a	8	5	12	14	16	—	25	8
Mica-illite ^a	8	21	17	19	13	9	13	6
Chlorite ^a	1	—	—	10	2	—	2	—
Kaolinite ^a	21	21	18	20	3	14	1	—
Fe-oxides ^b	15	2-10	15	9	—	5	18	10
Montmorillonite ^a	42	11	18	8	9	37	10	13
Palygorskite ^a	—	—	—	9	26	—	35	36
Zeolite ^b	—	1	40	4	—	3	1	10
Siliceous fossils ^b	Tr	—	—	—	—	4	1	—

^aBulk X-ray.^bSmear Slide.

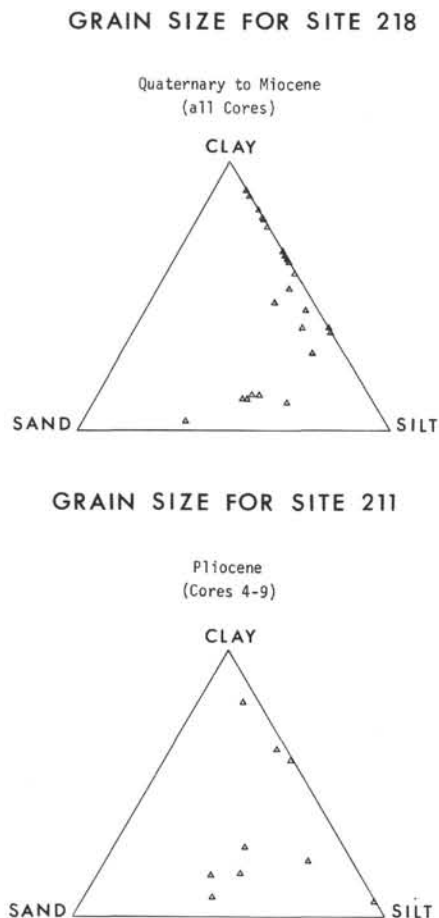


Figure 18. Grain-size analyses of terrigenous sediments.

Volcanogenic Sediments

The distribution of volcanogenic sediments/components in all Leg 22 sites is shown in Figure 19.

Sites 214 and 216, drilled on Ninetyeast Ridge, penetrated fairly thick sequences of volcanogenic sediments resting directly on basalts in the lower part of each hole. In Site 214, this sequence occurs in the interval 390 to 490 meters and is interbedded with lignites (see Chapter 22) and intermediate differentiated rocks (see Chapter 17). Terrestrial palynomorphs are abundant in the lignites (see Chapter 24). The volcanogenic material at Site 214 is almost totally pyroclastic, with the exception of three thin intervals of volcanic conglomerate, and does not contain any marine fossils. Some volcanogenic material, mostly

volcanic clay (identified by X-ray analysis as feldspar and montmorillonite) but with some basaltic volcanic glass still visible, is reworked into the shallow-water marine calcareous sediments some 20 to 30 meters above the top of the nonmarine volcanoclastic section. Site 216, by contrast, contains mostly epiclastic material mixed with calcareous sediments containing shallow-water marine fossils throughout the interval of 396 to 457 meters. Although much of the volcanogenic material at Site 216 is reworked, some discrete basaltic ash beds were penetrated. Table 6 gives a representative selection of X-ray diffraction analyses of these volcanogenic sediments from Sites 214 and 216. More detailed descriptions of these sequences at each site are given below.

Elsewhere in Leg 22 sites, volcanogenic material is sparsely distributed (Figure 19), and even where present makes up only a very small proportion of the recovered core material. Sites 211 and 216, situated closest to the Indonesian island arc system, contain a few rhyolitic ash beds, up to 15 cm thick, in late Pliocene to Quaternary and Pleistocene sediments, respectively. Similar ash pockets and laminae were also sparsely present in Sites 212 and 213. Campanian sediments near the base of Site 211 contain a few thin (≤ 4 mm) ash beds, which consist mostly of altered basaltic glass with some incipient plagioclase and palagonite and common iron oxide aggregates.

TABLE 6
Analysis of Volcanogenic Sediments

Site-Core:	214-41	214-46	214-52	216-26	216-33
Subbottom (m):	384.50	423.30	477.80	360.20	425.50
Age:	Paleo.	Paleo.?	Paleo.?	Lt. Maas.	Lt. Maas.
Quartz ^a	<1	10	3	<1	
K-Feldspar ^a		53	23		
Plag.-Feldspar	39				4
Augite ^a					11
Pyrite ^a	27	2			<1
Montmorillonite ^a	21	34	63	57	49
Beidellite ^a	—	Pres.	Pres.		
Zeolite ^a					18
Analcite ^a				15	
Chabazite ^a				Pres.	
Calcite ^a	12	—	6	27	15
Siderite ^a			5		
Glauconite ^b	2	—	—	10-15	—

^aBulk X-ray.

^bSmear Slide.

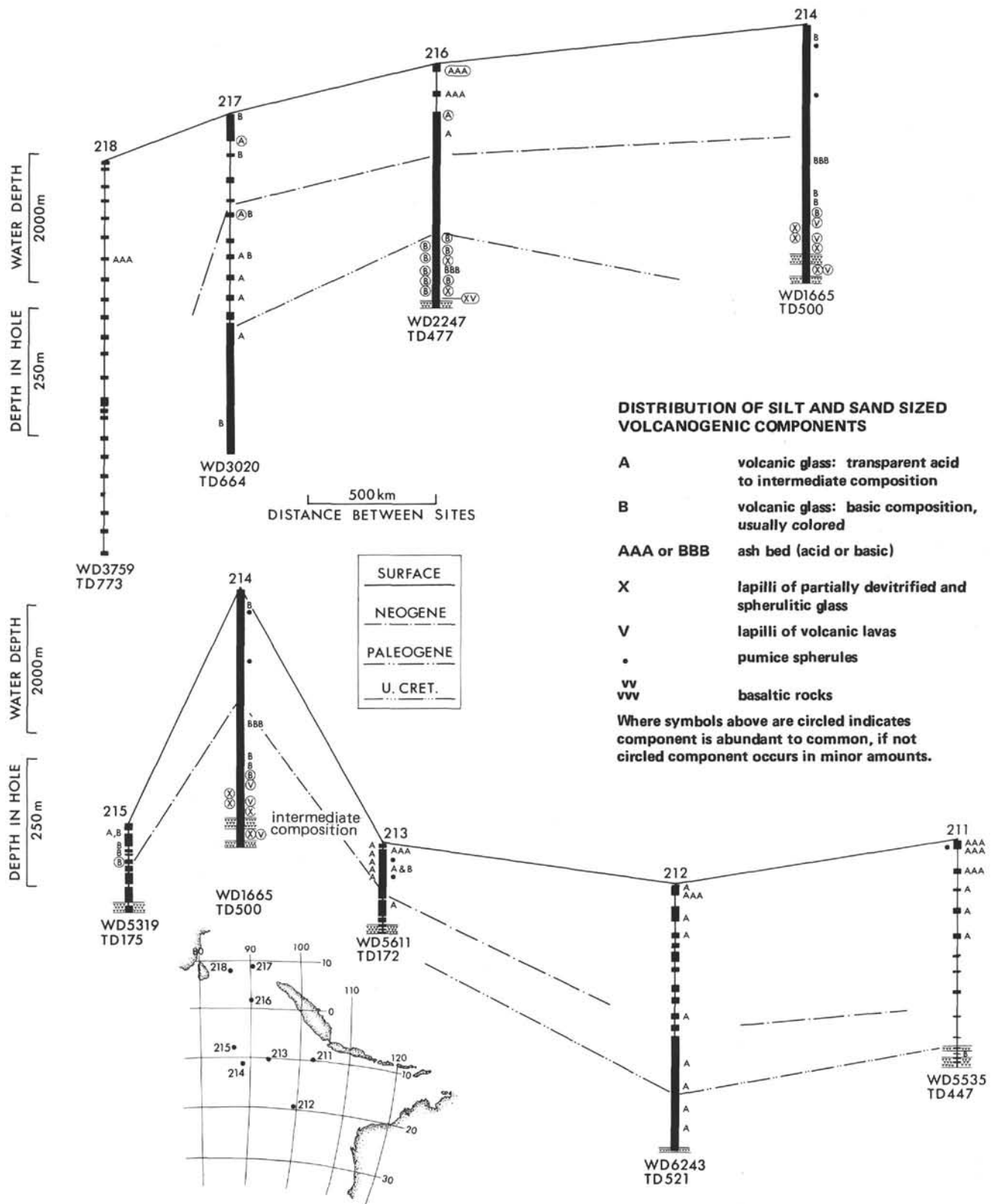


Figure 19. Distribution of volcanogenic sediments.

SITE 214

Figures 20 through 29 which follow show core photos and thin section photomicrographs of representative samples showing transition from basal shallow-water sediments through nonmarine volcanoclastic lignite sequence into volcanic rocks at Site 214.

Tuffaceous biomicrite-glaucinitic, with gastropods and bivalves. Thin sections (Sample 40, CC) show scattered forams, many filled with pyrite, fairly fresh angular to subangular plagioclase, pale brown irregular fragments of volcanic glass with vesicles and inclusions, chloritized and rounded volcanic rock fragments, and pyrite in a fine-grained microcrystalline calcite matrix. An X-ray analysis at 108 cm gave the following composition: calcite 26%, aragonite 12%, plagioclase 40%, montmorillonite 15%, pyrite 6%, and quartz 1%.

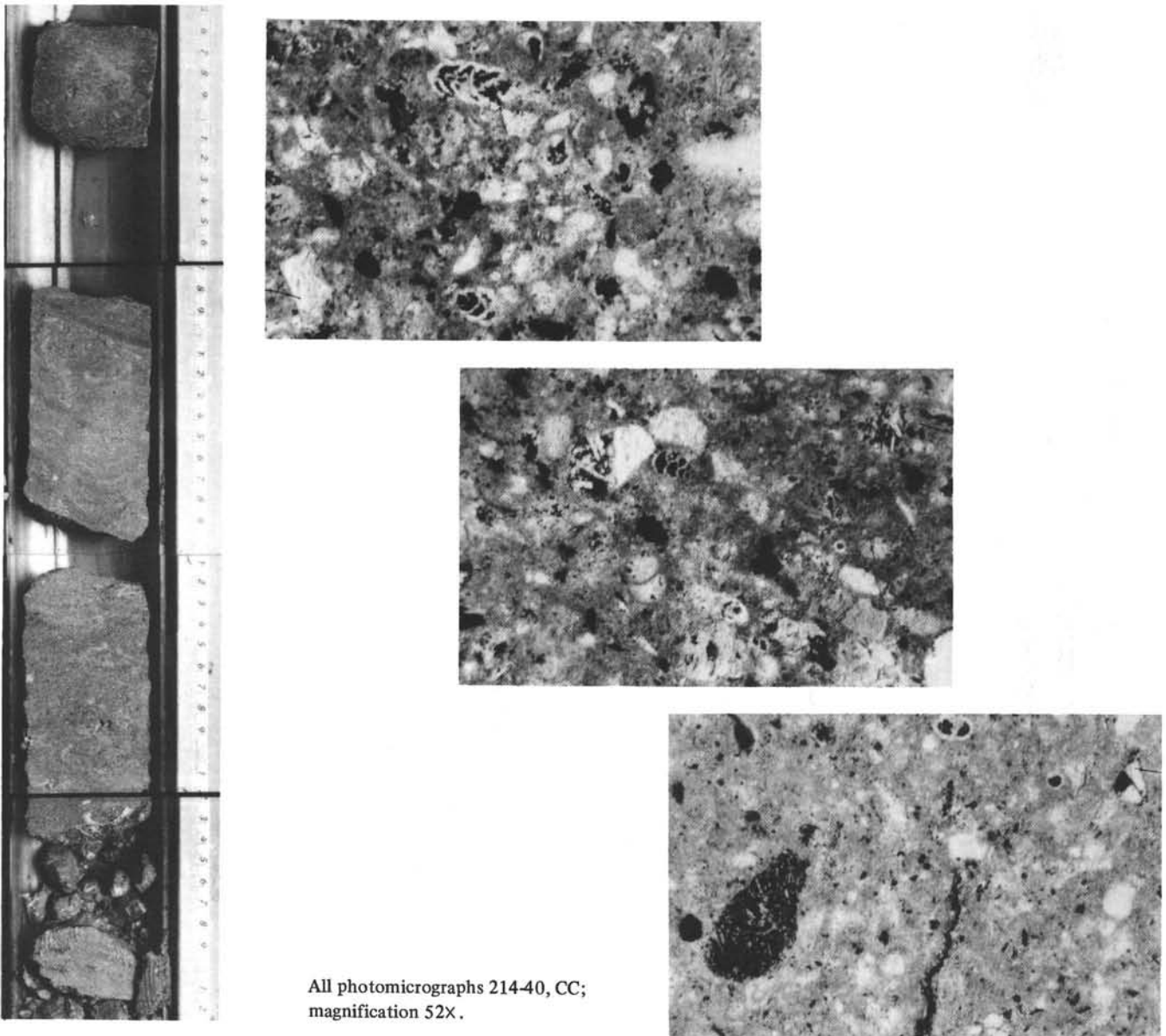
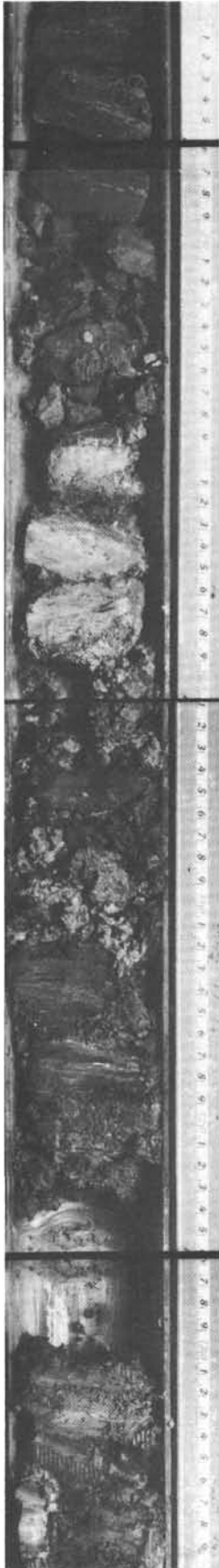


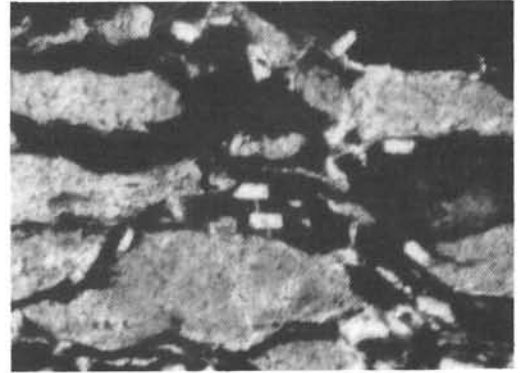
Figure 20. Sample 214-40-1, 65-105 cm.



Lignite and volcanic clay. Thin sections show aggregates of clayey material (lignitic?) in a matrix of brown glass which contains, in places, abundant small laths of a silicate mineral (probably feldspar). In places, the glass shows fluidal textural features. X-ray analyses at 93 and 108 cm showed that clinoptilolite and beidellite are major constituents of the clays.



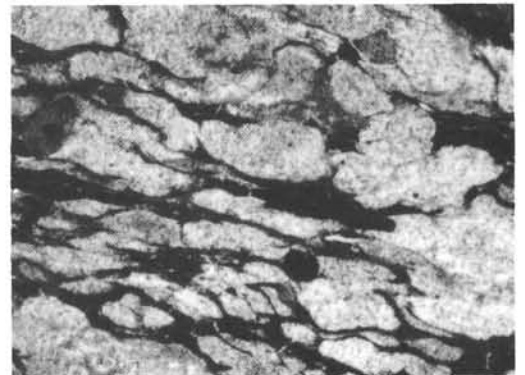
214-42-1, 74 cm; magnification 52X.



214-42-1, 74 cm; magnification 130X.



214-42-1, 90 cm; magnification 52X.



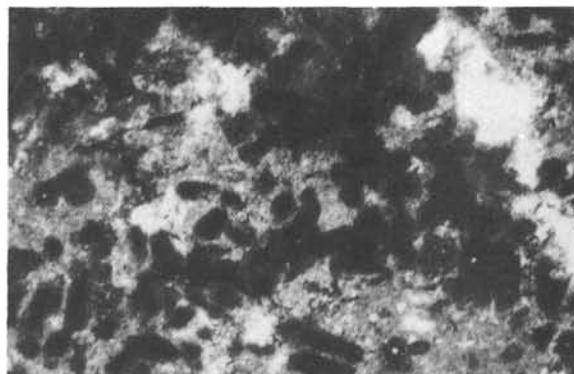
214-42-1, 74 cm; magnification 52X.

Figure 21. Sample 214-42-1, 68-140 cm.

Volcanic clay with some lignitic fragments in places and indurated volcanic conglomerate between 12 and 38 cm. The volcanic conglomerate consists of rounded fragments of extrusive intermediate volcanic rocks in a calcitic cement. The extrusive fragments are made up of sodic plagioclase and iron oxide minerals and show a trachytic texture. Some fragments show feldspar laths completely replaced by calcite. A few large plagioclase grains occur and are partially replaced by calcite. Some size sorting is apparent between 12 and 38 cm. The calcite forms sparite rims (28 cm) around some of the rock fragments and also makes up the bulk of the fine-grained matrix showing undulatory extinction (28 cm) or, more rarely, as interlocking anhedral grains. The clayey material (e.g., 75 cm) is mostly devitrified glass. Some areas contain abundant small opaque iron-rich shapes (both circular and lath-shaped) which sometimes have hematite rims. Patches of fibrous radiating zeolite are rare. Flowage structures are also still visible in a few areas.



214-44-1, 75 cm; magnification 52X



214-44-1, 75 cm; magnification 52X



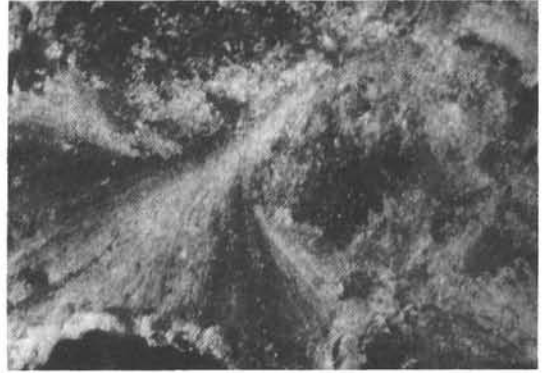
214-44-1, 28 cm; magnification 52X



Figure 22. Sample 214-44-1, 0-75 cm.



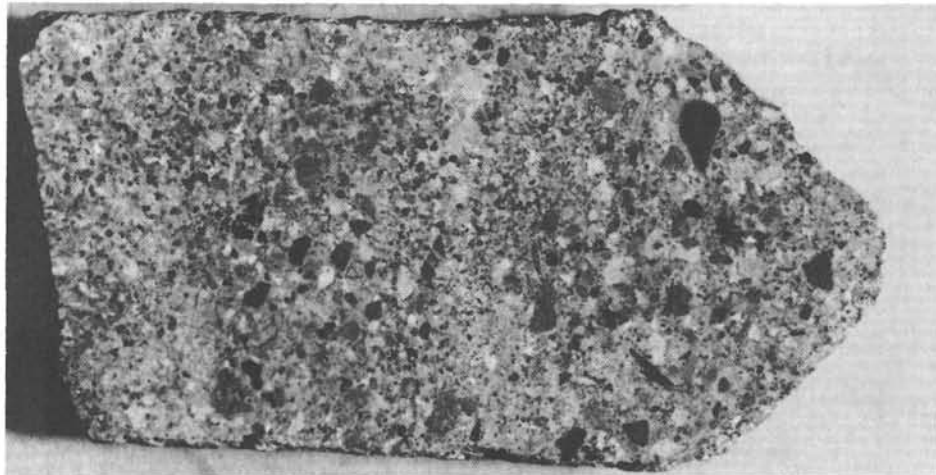
214-44-1, 28 cm; magnification 52X



214-44-1, 28 cm; magnification 52X



214-44-1, 12-25 cm



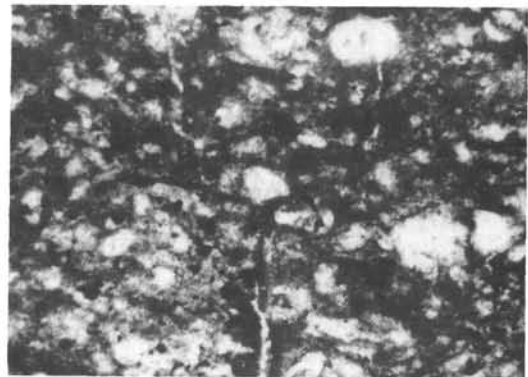
214-44-1, 26-38 cm

Figure 22. (Continued).

Volcanic clay with some lignite-rich laminae and indurated volcanic conglomerate (125-147 cm). The clay at 95 cm is mostly devitrified glass with some layering due to varying proportions of brown glass and pyrite; a few altered feldspar crystals are also present. An X-ray analysis here gave the following composition: K-feldspar 17%, montmorillonite 56%, plagioclase 5%, kaolinite 4%, pyrite 14%, gibbsite 4%, and abundant beidellite. At 110 cm, the dark lignitic clay showed 60% K-feldspar on X-ray analysis, with 21% kaolinite, 13% quartz, 7% pyrite, abundant beidellite, and no montmorillonite. Enlargements to natural size are shown of the volcanic conglomerate between 136 and 148 cm. This interval consists of well-rounded to subrounded fragments of extrusive rocks with partially altered sodic plagioclase laths. These extrusive rocks show a wide variety of textures ranging from highly glassy with few feldspar microlites, vesicular and amygdalar glass, to trachytic. Some fragments are enriched in chlorite and serpentine, and others have been mostly replaced by calcite. A few angular grains of feldspar are also scattered throughout the fragments. Some of the extrusive fragments have feldspar phenocrysts. Many of the large extrusive fragments have sparite rims which are thickest along the long axis of the core, the sparite being orientated in this direction. Obviously then, some pore space existed after water transport and deposition of the extrusives, but some constraint was imposed upon the neck as the sparite grew around the pebbles because of its consistent orientation. Some areas show two stages of growth — an irregular area of crystals between the pebbles is filled with aragonite(?) and then later the pore spaces still available were filled with the oriented sparite around the pebbles themselves. Most of the matrix in the rock consists of completely recrystallized calcite.



214-44-1, 139 cm; magnification 52X.



214-44-1, 95 cm; magnification 52X.



214-44-1, 136 to 148 cm.

Figure 23. Sample 214-44-1, 76-150 cm.



214-44-1, 139 cm; magnification 52X.



214-44-1, 139 cm; magnification 52X.



214-44-1, 139 cm; magnification 52X.



214-44-1, 139 cm; magnification 52X.

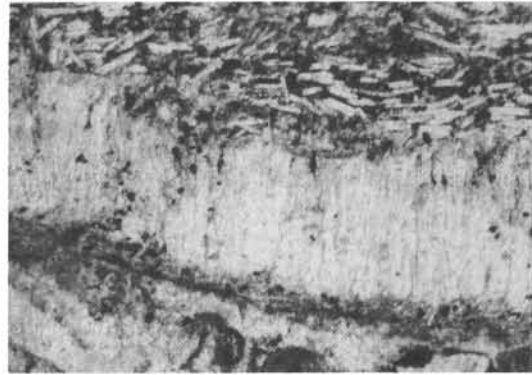


214-44-1, 139 cm; magnification 52X.

Figure 23. (Continued).



214-44-1, 139 cm; magnification 52X.



214-44-1, 139 cm; magnification 52X.



214-44-1, 139 cm; magnification 52X.



214-44-1, 139 cm; magnification 52X.

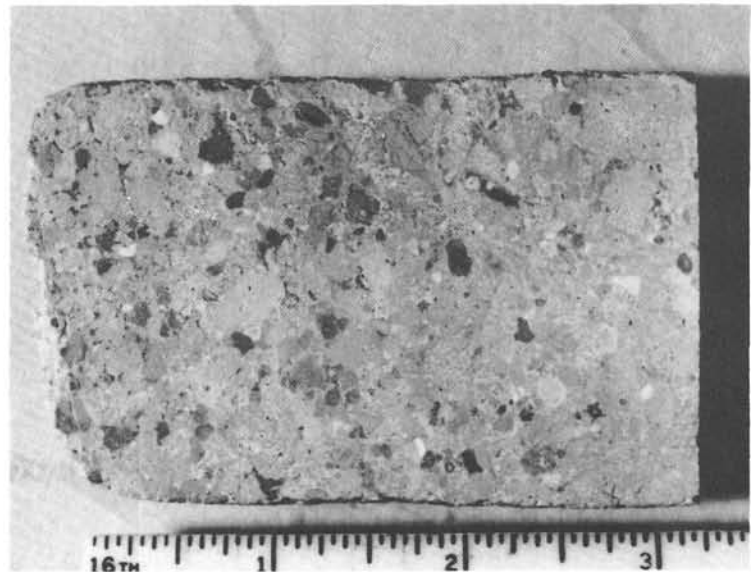


214-44-1, 136-148 cm.

Figure 23. (Continued).

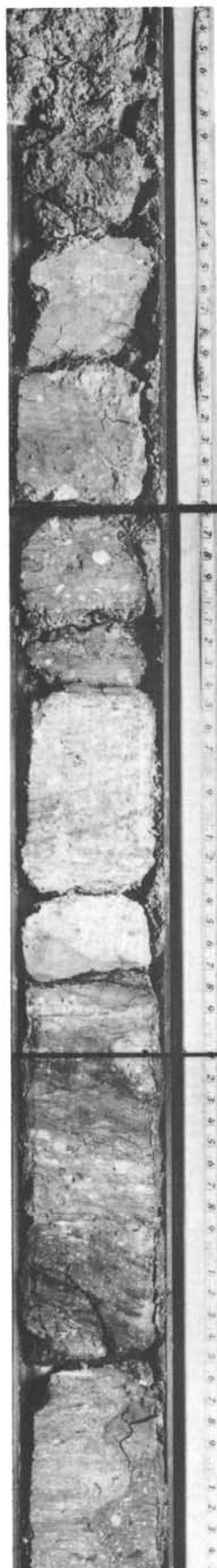


Volcanic clay with some lignite and indurated volcanic limestone between 131 and 150 cm. The limestone contains subrounded to subangular extrusive rock fragments which are almost entirely made up of feldspar laths. Some extrusives show secondary patches and veinlets of calcite alteration and a few have abundant opaques. Only a few subhedral feldspar crystals are present. Some light colored glass of probably acidic composition is also present. Seventy percent of the rock is made up of radiating calcite with undulatory extinction. In a few places the matrix has the appearance of partly devitrified glass(?), iron rich in part, but has an overprint of calcite obscuring the original texture.



214-45-1, 141-150 cm.

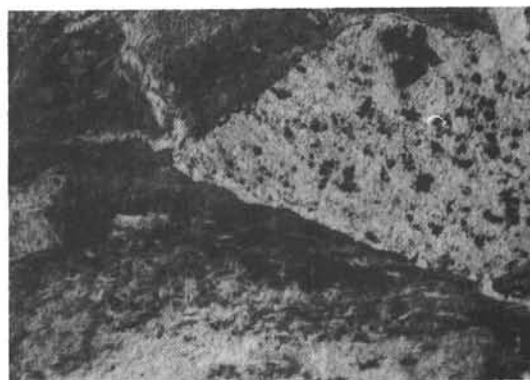
Figure 24. Sample 214-45-1, 76-150 cm.



Volcanic clay and lapilli tuff. Many of larger pale colored lapilli are chloritized pumice fragments. No size grading visible. Note erosional feature in clay between 66 and 76 cm. Thin section at 44 cm shows mostly extrusive lava fragments of varying texture: mostly feldspar laths, laths with abundant pyrite, very dark glassy iron rich with fine feldspar microlites, and occasionally chloritized vesicular fragments. Some euhedral feldspar crystals are present. The matrix is mostly clay with very small fragments of extrusives. An X-ray analysis at 27 cm in green clay showed the following composition: K-feldspar 54%, montmorillonite 34%, quartz 10%, pyrite 2%; beidellite is also present.



214-46-2, 44 cm; magnification 52X.



214-46-2, 44 cm; magnification 52X.

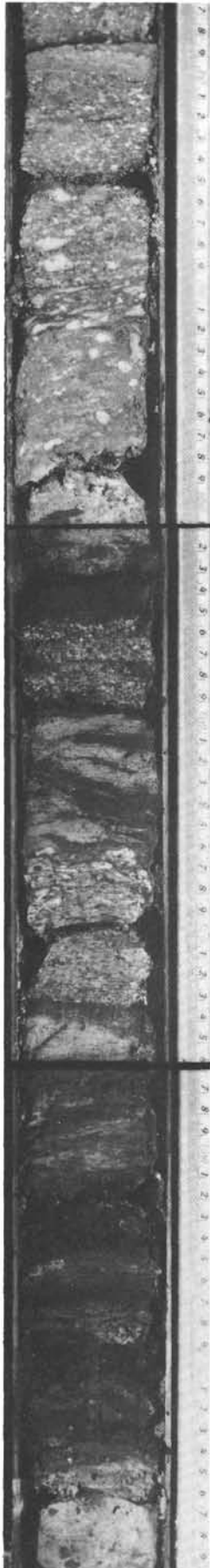


214-46-2, 44 cm; magnification 52X.

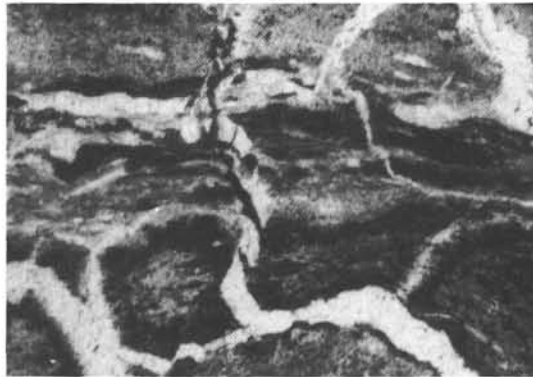


214-46-2, 44 cm; magnification 52X.

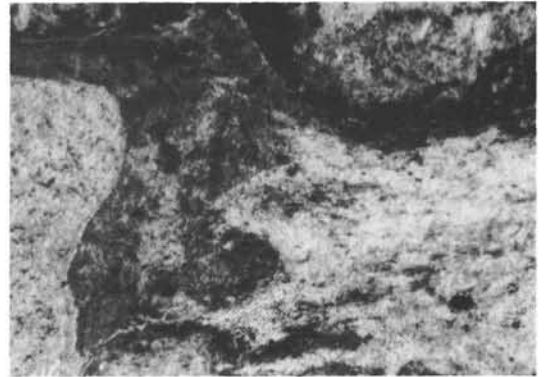
Figure 25. Sample 214-46-2, 3-76 cm.



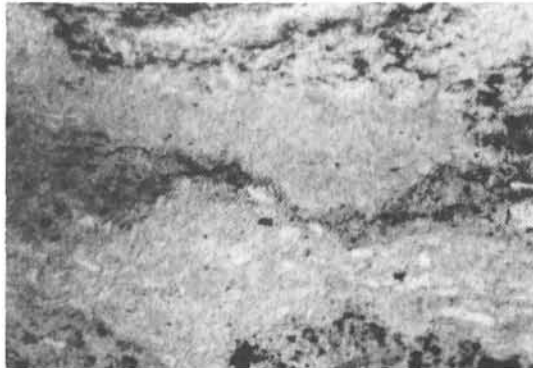
Lapilli tuff, volcanic clay, and lignite are interbedded throughout this section (see color frontispiece to this volume). The tuff is clearly welded between 87 and 92 cm and 116 and 123 cm. Thin sections also demonstrate this welding of glassy extrusive lavas between one another. The extrusive fragments vary from glassy fragments with perlitic structures to feldspar laths with varying amounts of opaques. A few subhedral feldspar crystals also occur. The extrusives with well-developed laths are not usually so welded as the glass-rich varieties. The matrix is mostly dark brown altered glass (now clay) with a few microlites. Some brown glass shows flowage and occasionally unusual dark chain-like shapes extend through the glass. An X-ray analysis at 143 cm gave a composition of montmorillonite 65%, K-feldspar 16%, pyrite 16%, and quartz 4%, with beidellite also present.



214-46-2, 84 cm; magnification 52X.



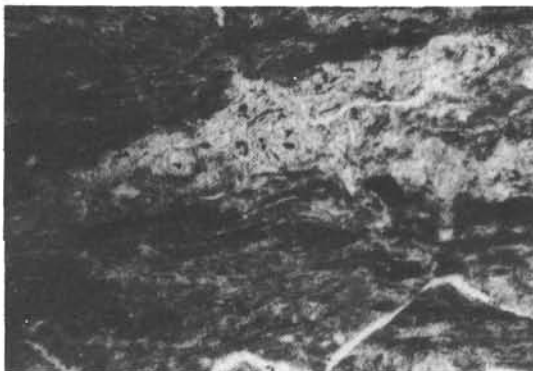
214-46-2, 84 cm; magnification 52X.



214-46-2, 84 cm; magnification 52X.



214-46-2, 84 cm; magnification 52X.

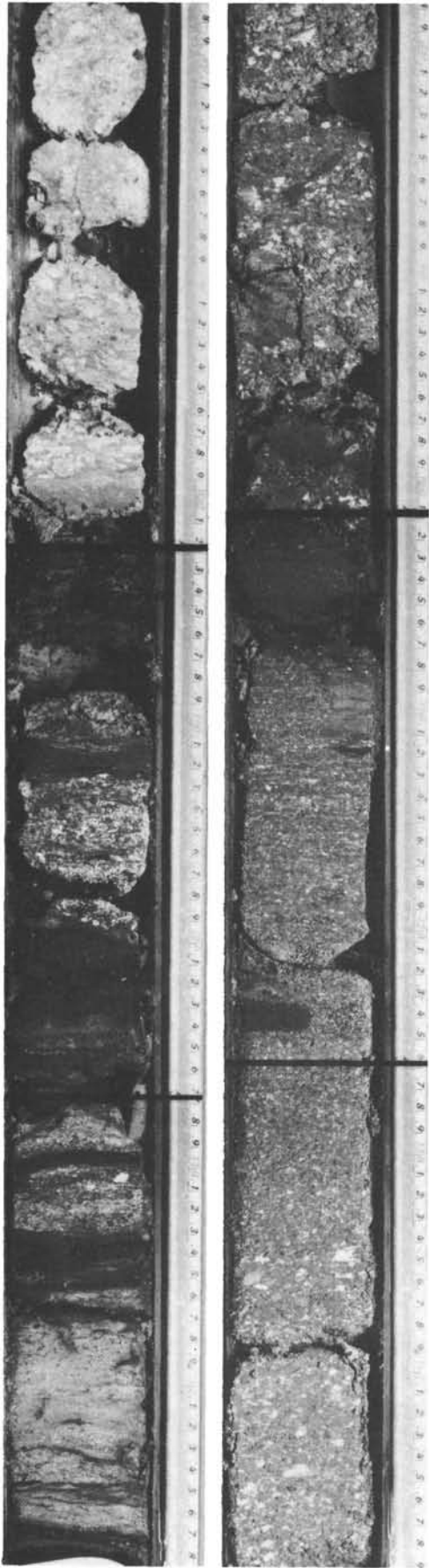


214-46-2, 119 cm; magnification 52X.



214-46-2, 84 cm; magnification 52X.

Figure 26. Sample 214-46-2, 76-150 cm.



Lapilli tuff, volcanic clay, and lignite similar to 46-2. In thin sections, very dark brown glass is well banded and some dark brown glass shards are still visible.

Lapilli tuff with interbed and fragments of lignite. Some of the pale green and white fragments are strongly weathered devitrified glassy and partly chloritized extrusives. A few still show feldspar laths. The matrix is almost totally altered dark brown glass with some scattered feldspar crystals. A few zeolite filled amygdales were also seen.



214-46-3, 138 cm; magnification 52X.



214-46-3, 138 cm; magnification 325X.

Figure 27. Samples 214-46-3, 77-150 cm and 214-47-1, 78-150 cm.

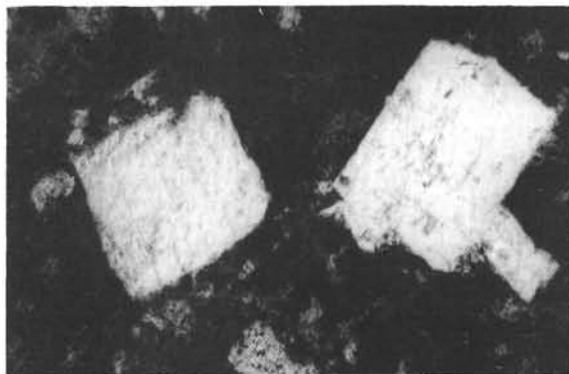


Cores 48 to 51 recovered almost completely uniform medium dark gray fine-grained intermediate (“andesitic”) differentiated rock. The rock has a trachytic texture with plagioclase laths in a matrix of pyroxene granules, iron ore, and fresh light brown glass. Where it is in contact with glassy tuff below, the igneous rock shows a chilled margin (Core 51, 115 cm).

Fragments of lignite, volcanic clay (originally glassy tuff), and lapilli tuff. Thin sections show a few extrusive rock fragments, glass shards, feldspar phenocrysts, and opaques set in a glassy matrix. Some of the glass is partially altered to palagonite. Some extrusive fragments are fine-grained, made up mostly of plagioclase laths showing a fluidal texture. Other coarser grained extrusive fragments have an intersertal texture.

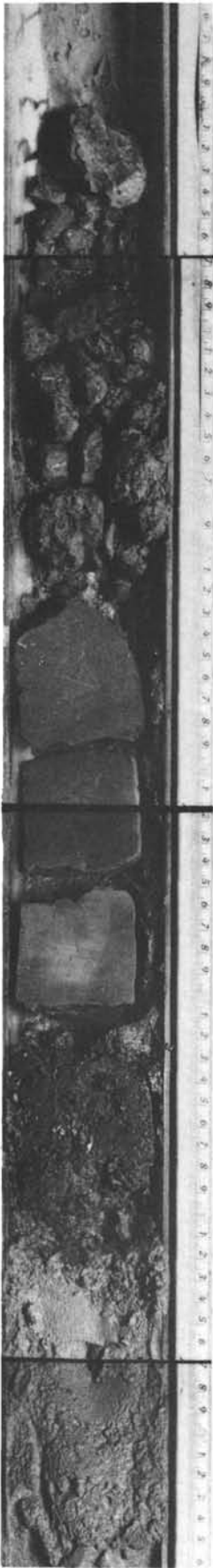


214-52-1, 120 cm; magnification 52X.



214-52-1, 120 cm; magnification 52X.

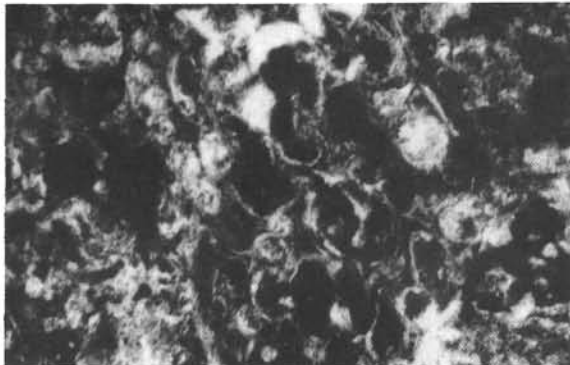
Figure 28. *Samples 214-51-1, 75-150 cm and 214-52-1, 103-150 cm.*



Fragments of aphanitic basalt in which occurs an approximately 20 cm (40-60 cm) thick vitric tuff horizon. Basalt was recovered from 53-1 above, and from Core 54 below. Thin sections of the tuff show glass with abundant vesicles in places. The vesicles are most commonly filled with yellowish-green vermiculite-chlorite radiating fibers showing strong pleochroism. Rarely, feldspar and zeolite occurs in the vesicles. Volcanic shards are visible in places and are altered into chlorite and palagonite. A few small extrusive rock fragments were also seen.



214-43-2, 50 cm; magnification 52X.



214-43-2, 50 cm; magnification 52X.



214-43-2, 50 cm; magnification 52X.

Figure 29. Sample 214-53-2, 20-80 cm.

Petrographic descriptions of the volcanogenic material at this site are given in Figures 30 through 32.

(a) Chloritized green pumice fragments from an altered vitric tuff interbedded with glauconitic volcanic claystone. Where the glass is unaltered it is brown in color. Elsewhere in the thin section, a few glass shards still remain. Also present are dark brown glassy lava fragments containing feldspar phenocrysts, isolated feldspar fragments, less common clinopyroxene crystals, and a few foraminifera. 216-29, CC; magnification 52X. (b) Dark brown altered glass fragments with foraminifera. Elsewhere, a few extrusive fragments comprising feldspar laths and pyroxene grains, feldspar phenocrysts, and pyroxene grains were seen in the devitrified green-brown glass matrix. An X-ray analysis here gave the following composition: montmorillonite 49%, phillipsite 18%, augite 11%, calcite 15%, plagioclase 4%, clinoptilolite 3%, and pyrite 1%. 216-33-1, 100 cm; magnification 52X. (c) Fragments of vesicular glass in a matrix of calcite and devitrified glass. 216-34-4, 57 cm; magnification 52X. (d) Spherulitic glass fragments from a basaltic vitric tuff. The spherules are mostly filled with chlorite and to a lesser extent calcite, though analcite is occasionally present. Elsewhere, elongate feldspar crystals are also present. 216-34-4, 79 cm; crossed nicols; magnification 52X. (e) Calcite replacing and filling cavities between chloritized glass shard with brown glass rims. 216-34-4, 79 cm; crossed nicols; magnification 52X. (f) Vitric Tuff – spherulitic glass in which spherules filled with calcite and glass. Some euhedral feldspar crystals present. 216-34-4, 79 cm; magnification 130X.

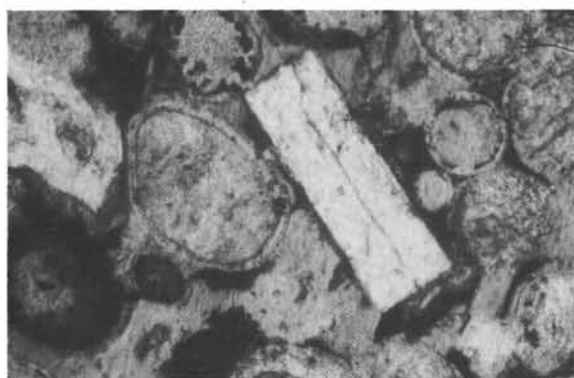
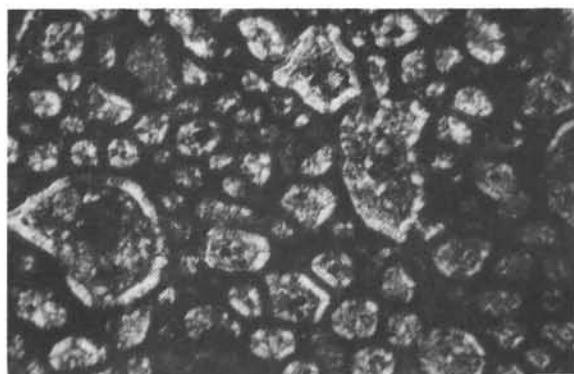
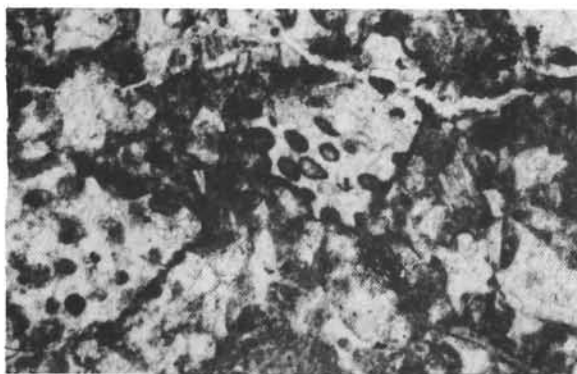
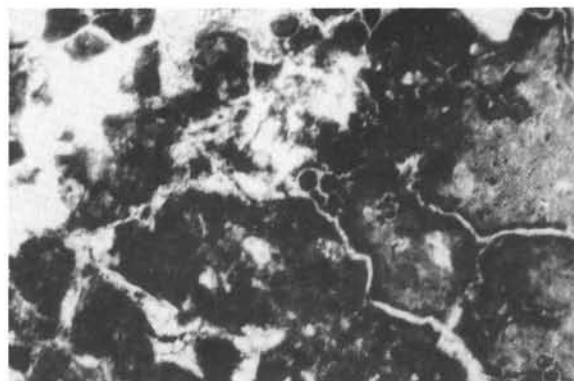
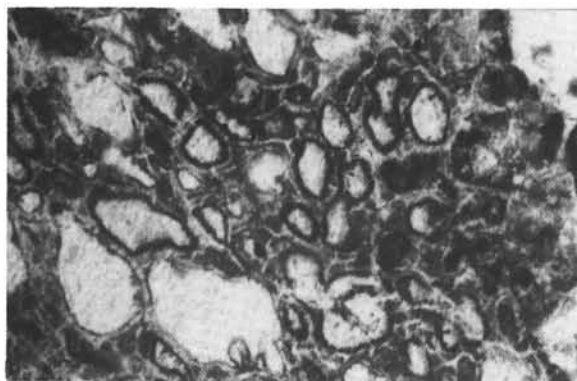


Figure 30. *Volcanogenic sediments from Site 216.*

(a, b) Vitric Tuff – chloritized glass shards sometimes with brown glassy rims. Some of the shards and much of the matrix replaced by calcite and rarely analcite. 216-34-4, 79 cm; magnification 52X. (c, d) Extrusive glassy lava fragments with some feldspar laths in a partly calcitized clayey (altered glass?) matrix. 216-35-3, 18 cm; magnification 52X. (e, f) Spherulitic glassy extrusive fragments. The spherules are filled with chlorite and calcite. Most of the glass is also altered into either chlorite or calcite. A few elongate feldspar crystals are present. 216-35-3, 18 cm; magnification 52X.

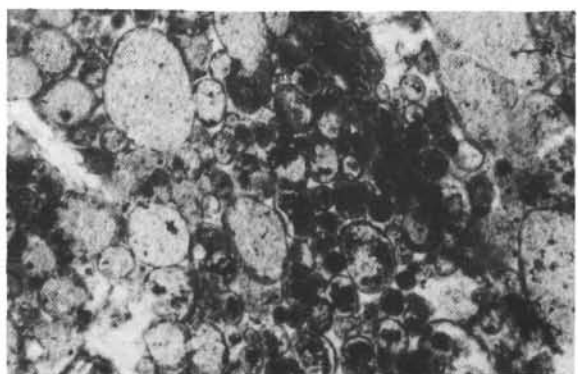
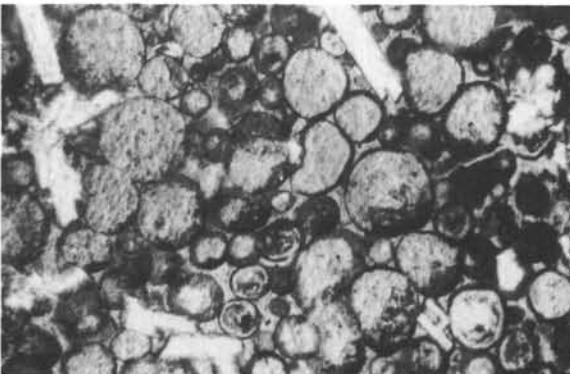
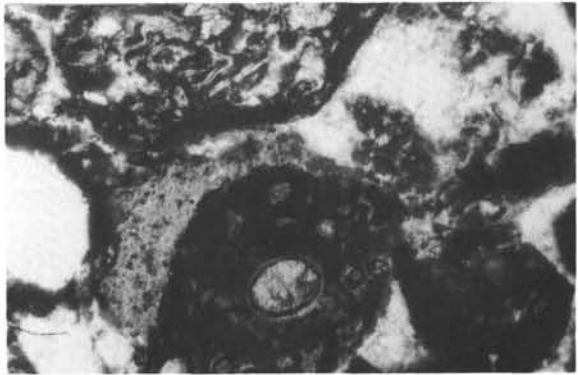
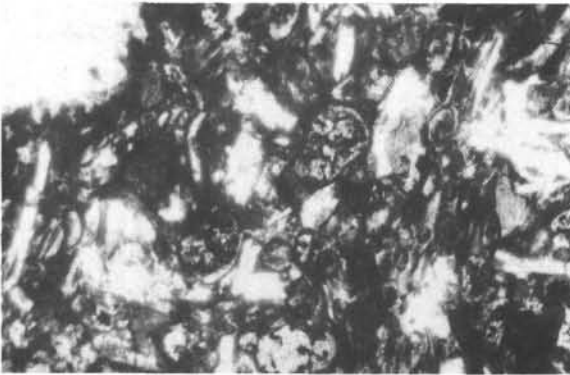
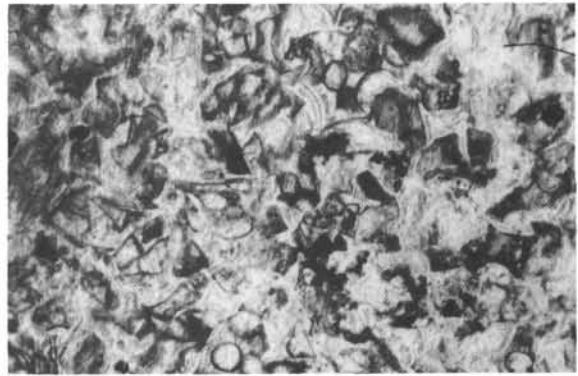
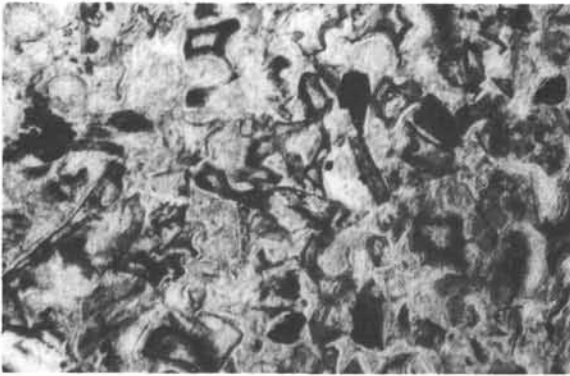


Figure 31. *Volcanogenic sediments from Site 216 (cont'd).*

(a, b) Tuffaceous limestone – glass shards, feldspar, and extrusive rock fragments in a matrix of calcite and fine-grained carbonate with foraminifera and altered glass and palagonite. 216-36-3, 47 cm; magnification 52X. (c, d) Basaltic tuff immediately above basalt flows. Dark glassy fragments with plagioclase laths some of which show a sheaf-like texture. Radiating fibers of yellowish-green vermiculite-chlorite fill cavities in the matrix and replace feldspar in some places. The matrix consists of altered green volcanic glass with dark streaks of sphene(?). Analcite occurs as radiating fibers in a few cavities and some epidote was also seen. 216-36-4, 70 cm; magnification 52X.

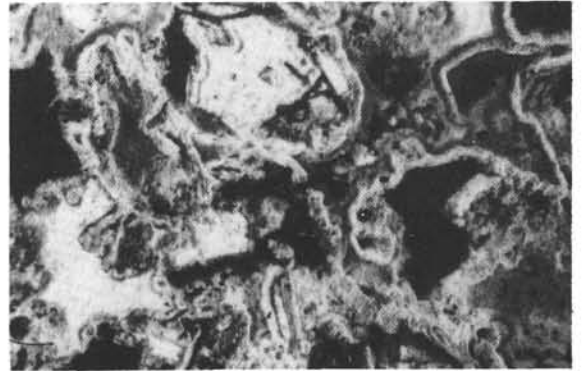
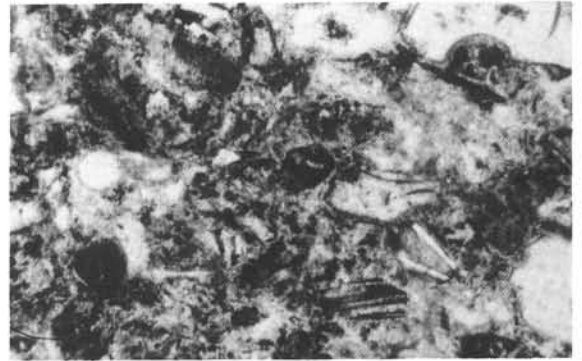
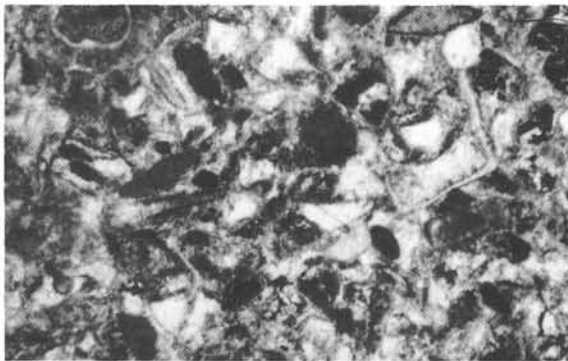


Figure 32. *Volcanogenic sediments from Site 216.*

REGIONAL SUMMARY AND CONCLUSIONS

The major geologic events in the northeastern Indian Ocean, as interpreted from the recovered core material on Leg 22, are summarized in Figure 33. These important events are discussed in turn below. Using the tectonic reconstructions of Sclater and Fisher (in press) as base maps, a series of facies distribution diagrams in time have been attempted in Figure 34.

Formation and Subsidence of Oceanic Crust

Deep Basin Sites (211, 212, 213, 215)

Three sites drilled in the Wharton Basin (211, 212, 213) and one in the Central Indian Basin (215) recovered tholeiitic basalts considered to be typical of Layer 2 rocks (Chapter 17 this volume). In every case, the subbottom depth at which these basalts were encountered was in close agreement with that predicted for the acoustic basement as deduced from seismic records (see site reports). When these sites are plotted on the basement age versus depth curve of Sclater et al., 1971, it can be seen (Figure 35) that all but Site 212 shows a fairly good fit. The reason for the excessive depth versus basement age at Site 212 is because the site was drilled close to a major fracture zone (see Chapters 3, 15, 41).

The sedimentation histories of Sites 211, 212, 213, and 215 were plotted on the Sclater, et al., 1971 subsidence curve for typical oceanic crust (Figure 36). Sites 211, 213, and 215 show the typical oceanic subsidence history of calcareous sediments overlying ridge crest basalts succeeded by deeper water brown clays. At Sites 213 and 215, where coring was continuous, it can be seen that the CCD was situated at a depth of 3600 meters (51 m.y.B.P.) and about 3300 meters (53 m.y.B.P.) respectively. At Site 211, during the Late Cretaceous the area was above the CCD, which was deeper than 3500 meters; however, the boundary between calcareous and noncalcareous sediments was not cored.

Site 212 did contain a very small amount of metamorphosed calcareous sediment (Plate 5a) with as yet unidentified fossils (Plate 5b) immediately above and within the basalt, and just above this, brown clays were recovered, but no age dates were obtained from either sediment. Also, it is uncertain whether or not the calcareous material was redeposited (see later).

Ninetyeast Ridge Sites (214, 216, 217)

Of three sites drilled on Ninetyeast Ridge, two (214, 216) penetrated basalt and all penetrated shallow-water calcareous sediments in the basal part of the stratigraphic column.

The basalts from Ninetyeast Ridge are often highly vesicular and amygdalar, do not show pillow structures, and were most probably extruded in very shallow water or subaerially.

The early sinking history of Ninetyeast Ridge, as deduced from the recovered cores in Sites 214, 216, and 217, is described in detail by Pimm, et al. (in preparation). In brief, all three sites show a shallow-water history rapidly deepening to oceanic depths. This sinking occurred in the Paleocene to earliest Eocene at 214, in the late Maastrichtian at 216, and late Campanian to early Maastrichtian at 217. The lithology of these shallow-water sediments at all three sites show many common features but also significant differences. To summarize, all sites show a micritic chalk sequence with abundant thick-shelled forms, a glauconitic interval, a microfossil component of benthonic foraminifera, a restricted diversity nannofossil assemblage, and sponge spicules. Site 214 has a lowermost interval of mostly subaerially deposited volcanoclastic sediments interbedded with lignite. In Site 216, basal volcanogenic material is reworked into marine sediments, but in Site 217, no volcanic material was recovered. Site 217 was the only hole which penetrated a dolomitized reef facies at the base of the drilled section.

Once the various portions of the Ninetyeast Ridge have subsided below shelf depths, they follow closely the subsidence curve for typical oceanic crust as shown by Pimm and Sclater (in press). In Table 7 an attempt is made to compare the thicknesses of pelagic calcareous oozes at the three sites drilled on Ninetyeast Ridge. Although absolute thicknesses cannot always be determined because of discontinuous coring in the younger sediments at Sites 216 and 217, the boundary limits (shown in the Table) between core depths are such that some valid comparisons can be made.

In general, Table 7 and the accumulation rate diagram (Figure 5) show that all three sites have had a similar history of oceanic sedimentation. Minor variations are apparent, particularly in the Paleogene sequences, and these are due to actual hiatuses in the sections or at least greatly attenuated intervals. The details for each site are given as footnotes to Table 7.

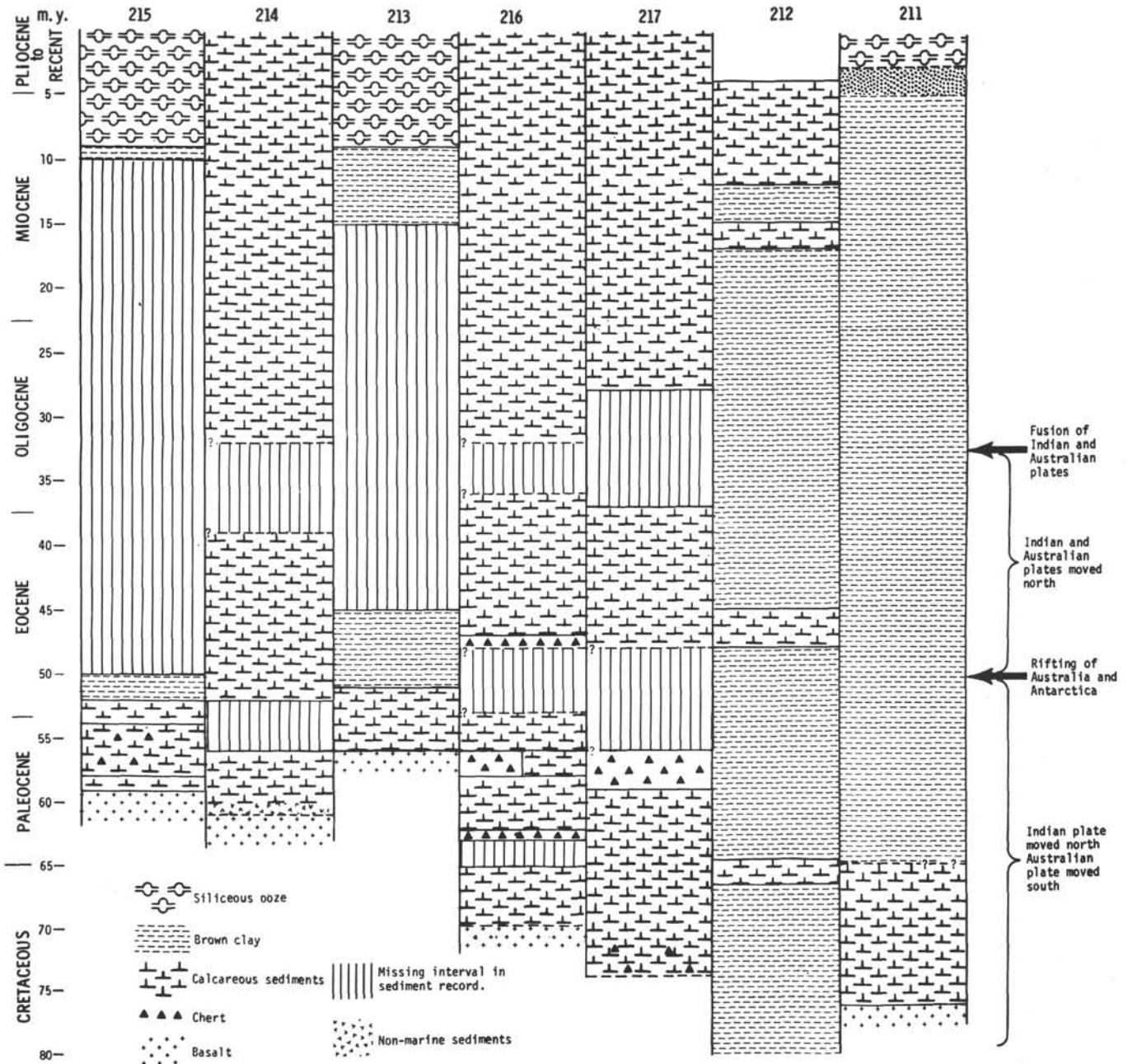


Figure 33. Major geologic events in northeastern Indian Ocean.

The thickness of Pliocene and younger sediments at Site 214 is significantly greater than at the other two sites. Also, the accumulation rate of Pliocene sediments at Site 214 is about twice the rate of Miocene sediments below. This is probably related to the much greater abundance of foraminifera in the Pliocene and Quaternary at Site 214, which was attributed (elsewhere in this chapter) to this site being in the zone of high productivity situated just south of the Equator in the Indian Ocean.

It should be borne in mind that there is a considerable (up to nearly 50%) admixture of clay material in the Pliocene and Quaternary sediments at Site 217 so that the much slower accumulation rates of pelagic calcareous ooze here compared with Site 214 would be even more marked if this were also taken into account.

Comparison of Sedimentation on Either Side of Ninetyeast Ridge (Sites 213, 215)

Sites 213 and 215 were drilled on the east and west sides of Ninetyeast Ridge, respectively. The tectonic setting of Ninetyeast Ridge, the pronounced linear feature separating the two basins in which Sites 213 and 215 were drilled, is described in detail by Sclater and Pimm (in preparation). Both drill sites were continuously cored to acoustic basement (just over 150 meters below bottom in both sites) so that the history of sedimentation at each site could be compared. Tectonic reconstructions of the region based on interpretations of the magnetic anomaly pattern (McKenzie and Sclater, 1971; Sclater and Fisher, in press; also Chapters 1 and 41, this volume) indicate that in the earliest Eocene and prior, (older than 53 m.y.-anomaly 21) Site

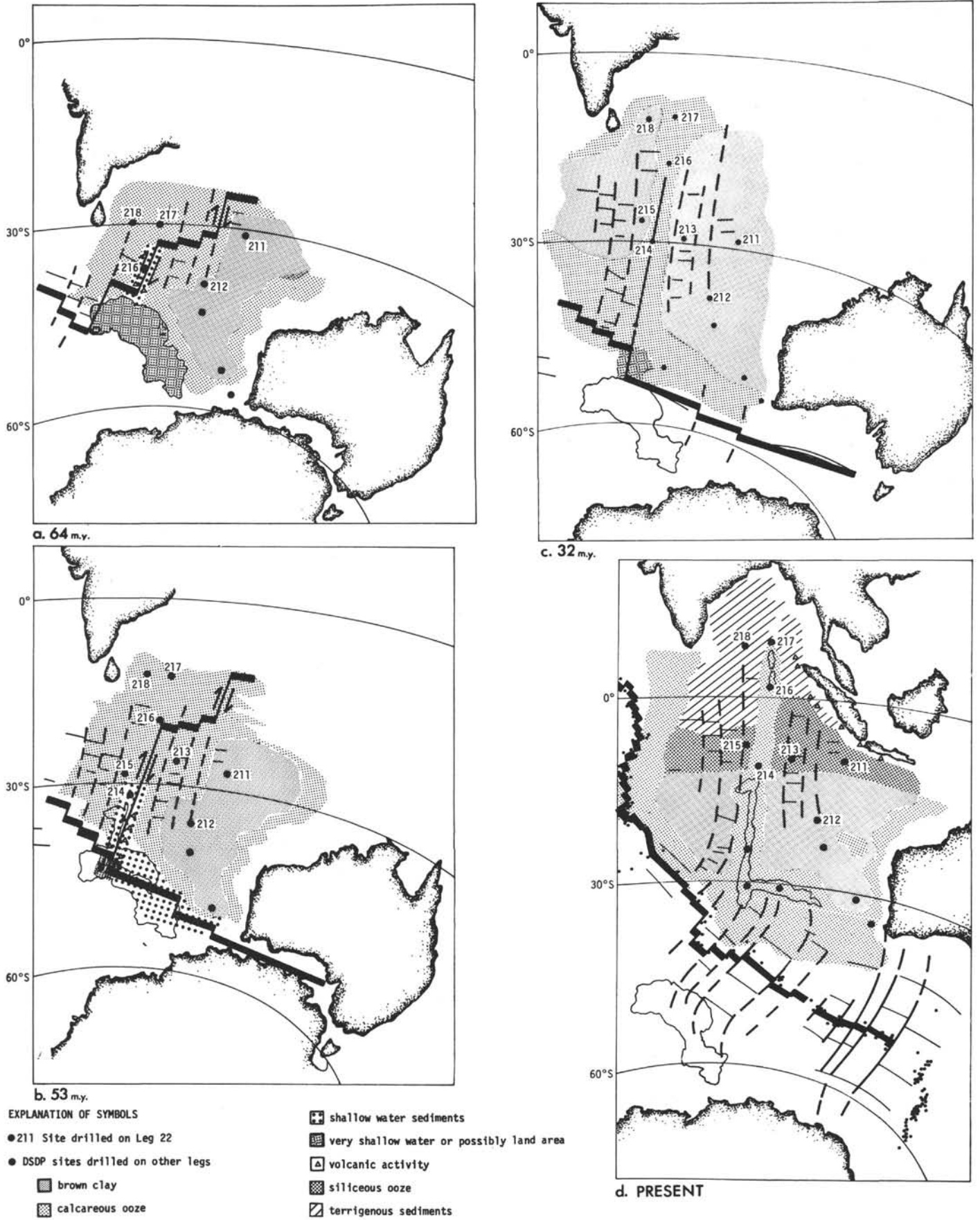


Figure 34. Distribution of major sedimentary facies with time.

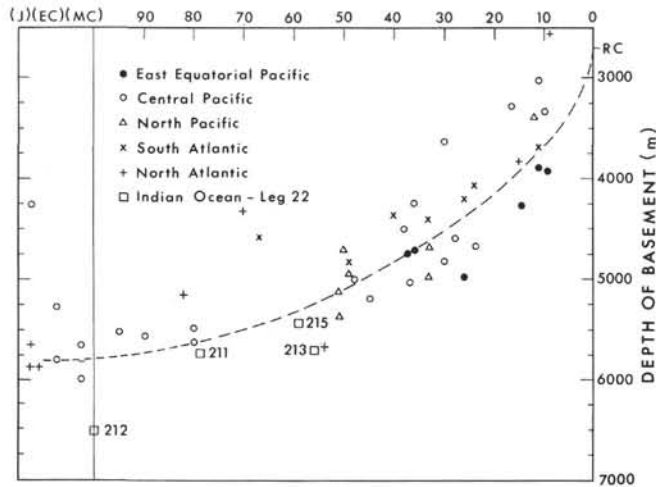


Figure 35. Basement age versus depth for Sites 211, 212, 213, and 215. Age based on fossils overlying basalt. Data from DSDP sites (after Berger 1972).

215 was located on the Indian plate and moving northwards away from the southeast branch of the Indian Ridge

spreading center. Site 213 is situated on oceanic crust generated from a former spreading center in the northern part of the Wharton Basin; the oceanic crust south of this center was part of the Australian plate, which had a motion in the opposite direction to the Indian plate prior to early Eocene times. During the early Eocene, the Indian and Australian plates moved north together and since the Oligocene have acted as one structural unit moving slowly northwards away from the Indian Ridge spreading center and its continuation southeastwards between Australia and Antarctica.

The sedimentary record at Sites 213 and 215 was carefully examined to see what evidence there was to support the tectonic history outlined above. In Paleocene times, the portion of Ninetyeast Ridge (area of Site 214) between the two sites was a very prominent feature—either emergent or covered by very shallow water. Evidence for this is seen in the cores recovered from Site 214. To the south of Site 213, the area of Broken Bridge probably formed a pronounced barrier; Site 255 showed a marked angular unconformity separating Cretaceous limestones from Eocene littoral sediments (Luyendyk, Davies et al., 1973). Therefore, it appears that the area of Site 213, indeed much of the Wharton Basin, was isolated by structural highs from the rest of the Indian Ocean in the early Tertiary (see Figure 34c).

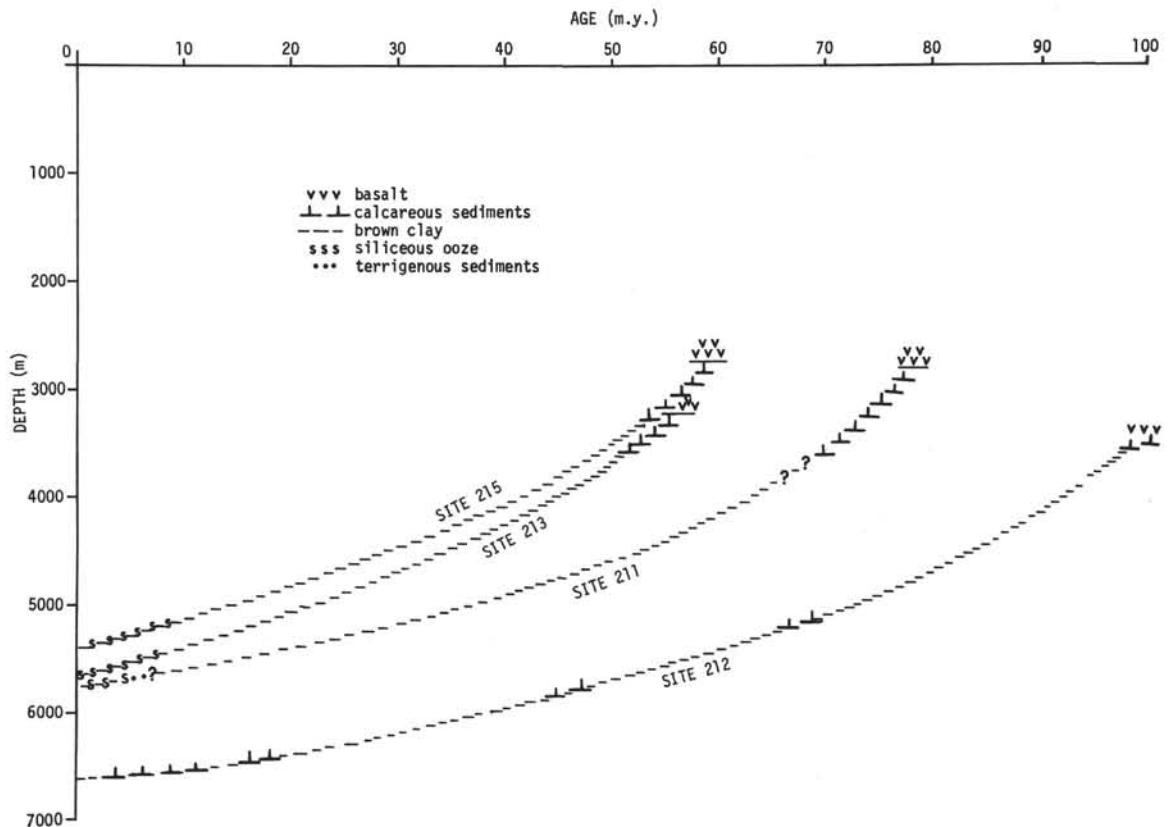


Figure 36. Subsidence history of Sites 211, 212, 213, and 215.

TABLE 7
Comparison of Thicknesses of Pelagic
Calcareous Oozes on Ninetyeast Ridge

Age	Site 217		Site 216		Site 214	
	Thickness (m)	Cumulative Subbottom Depth (m)	Thickness (m)	Cumulative Subbottom Depth (m)	Thickness (m)	Cumulative Subbottom Depth (m)
Quaternary	22	22		?	21	21
Pliocene	38±10	~60	54+	54+	64	85
Miocene	150±20	~210	105+(<28)	187	155	219
Oligocene	103±10 ^a	313	70 ^a	257	38 ^a	257
Eocene	47+<10 ^b	~360	34 ^c	291	76 ^d	333
Paleocene	60 ^b	420	41 ^e	332		

^aMost of early Oligocene missing.

^bMost of late Paleocene, early Eocene and part of middle Eocene represented by only 20 meters of core.

^cOnly core catcher sample of early Eocene present.

^dPart of late Eocene missing.

^eAbout 2 m.y. break at Tertiary/Cretaceous boundary.

In Figure 37, a detailed comparison of several parameters measured on cores from Sites 213 and 215 is presented. It can be seen that the overall sedimentation history for the two sites is remarkably similar, not only in the Neogene which might be expected, but also in the early Eocene and Paleocene where no striking differences are apparent.

The sequence of Paleocene to early Eocene calcareous oozes is thicker at Site 215, but this can be accounted for by the slightly older (about 3 m.y.) basal age here and possibly also the redeposition of shallow-water benthonic foraminifera (see Chapter 6). The accumulation rate at Site 215 for Paleocene sediments is 20 m/m.y.; yet, many of the calcareous components show signs of extensive dissolution. The accumulation rate is much lower in the calcareous sediments at Site 213 (Figure 5).

The only lithologic difference in the calcareous sequence at the two sites is the occurrence of a few chert nodules in Paleocene oozes at Site 215. This cherty interval in 215 occurs in foraminifera Zones P.4 and P.5, which are also present in Site 213, but no chert was seen here. At this time (~56 m.y.), the Wharton Basin was partially isolated from the Indian Ocean, directly to the west and south as described above. Also, Site 213 would have been situated more than 1000 km north of the latitude of Site 215 following reconstructions based on the magnetic anomaly pattern and the Leg 22 drilling results (Figure 34b).

The transition from a calcareous sequence to zeolitic brown clay is rather gradual in Site 213 (throughout Core 14) and occurs in the top part of the early Eocene (foram Zone P.7 and younger). In Site 215, the same boundary occurs within about 100 cm, in Core 9, Section 3 at a slightly older age (about foraminifera Zone P.6b to P.7). There is a marked decrease in porosity coinciding with the transition from clay to calcareous sediments at both sites.

Both Sites 213 and 215 show either a very condensed sequence or an inferred major hiatus in the middle Tertiary. In 213, about 12 meters of unfossiliferous clay separates middle Eocene from early middle Miocene (a time span of about 30 m.y.) and in 215 only 4 meters separates early Eocene from late Miocene (a time span of 40 m.y.) (Figures 5, 33, and 37). These inferred hiatuses are discussed later.

The pelagic brown clay sequence is about three times as thick in Site 213 as 215 (about 60 m against <20 m). This can only partly be accounted for by the inferred hiatus which is greater by about 10 m.y. in Site 215. Mineralogy of these clays is identical in both sites.

The area of Site 215 was reached by the distal end of terrigenous sediments forming the Bengal Fan in the late Miocene. A total of less than 7 meters of silty clay was deposited in two separate intervals (Figures 3 and 37; also, see section on Bengal Fan at end of this chapter).

Siliceous oozes dominate the top 60+ meters of sediment in both sites, although the relative proportions of early and late Pliocene are opposite in each.

Deposition of Calcareous Sediments Below the CCD at Site 212

Introduction

The most significant feature of the sedimentary column at Site 212 is the presence of several calcareous ooze and chalk units interbedded with pelagic brown clay at a site whose present water depth is 6243 meters. Sedimentary structures within the calcareous units (see earlier), the nature of the contacts between calcareous and clay units, and paleontological data indicate that possibly all the calcareous material has been redeposited below the carbonate compensation depth by submarine currents and not by grain by grain settling through the water column.

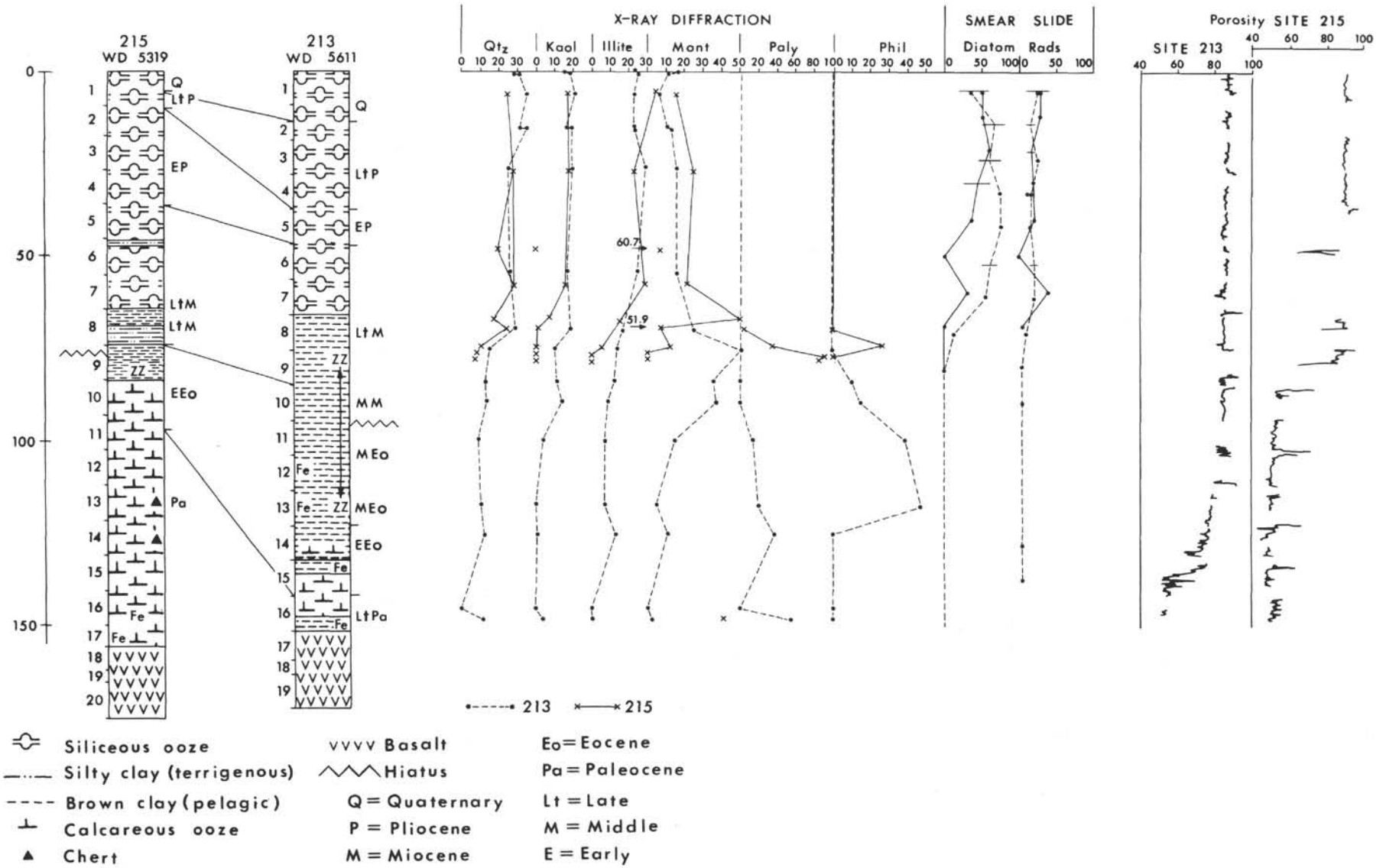


Figure 37. Comparison of sedimentary sequences at Sites 213 and 215.

On paleontologic and lithologic evidence, the stratigraphic section is divided into nine units (see Figure 3 and site report).

Any model proposed for the history of Site 212 has to satisfactorily explain the features of the cored succession listed below (and described in detail at several places in this chapter and in Chapter 3):

1) The alternation of calcareous and noncalcareous sediments.

2) The deposition of carbonate well below the postulated depth of the lysocline over the last 70 m.y. (Figure 38).

3) Calcareous Units 3, 5, and 7 have very restricted time ranges, each more or less confined to one nannofossil zone and showing no age gradation from top to bottom.

4) Calcareous Units 1 and 2 have wider time ranges and also contain mid-Tertiary contaminants.

5) The nature of the contacts between calcareous and noncalcareous sediments.

6) Textural grading, lamination, size sorting, and reworking of clay in parts of calcareous units.

7) Different states of foraminifera preservation and low diversity of some nannoplankton floras; presence of siliceous fossils in calcareous Unit 5.

8) The appearance of glauconite in some places.

9) Reduced zones at the top of clays overlain by thick calcareous units.

No attempt is made here to systematically account for all of these listed features in the model proposed or to try and unravel the exceedingly complex relationship between worldwide events of carbonate sedimentation and those seen in Site 212. The simplistic model explained below is merely one example of how such carbonate redeposition could have occurred at Site 212.

Sedimentation Model

The model proposed for the sedimentation history of Site 212 is one of reworking of the calcareous material in Units 1, 2, 3, 5, and 7 from above the lysocline into the deeper parts of the Wharton Basin. Site 212 is actually situated in the deepest part of the Wharton Basin. The calcareous material accumulated in a pronounced deep caused by a major fracture zone. The regional depth of the Wharton Basin is about 6000 meters and over most of its extent is only covered by acoustically transparent sediments less than 100 meters thick (Ewing et al., 1969; Carpenter and Ewing, in press, Veevers, Chapter 10 this volume). Piston cores (Ewing et al., 1969) in the Wharton Basin and DSDP Site 256 (Luyendyk and Davies, 1973), and also in Sites 211 and 213 (this volume), at the margins of the basin, show that noncalcareous sediments—brown clay and/or siliceous oozes—from most, or all, of this acoustic sediment cover. At Site 212, the depth to basalt (which is correlated with acoustic basement) is 6759 meters and the sediment cover is 516 meters thick. Seismic profiles of this area (Chapters 3, 15) show that the sediments are acoustically stratified and ponded within this deep depression.

The thickness of the noncalcareous portion of the section at Site 212 totals just under 100 meters, which is comparable to the deduced thickness from seismic profiles

of transparent sediments over much of the Wharton Basin. The time duration of brown clay in Units 4 and 6 is dated by the fossils in calcareous sediments above and below, despite themselves being devoid of fossils. The accumulation rate of these two clay intervals is similar (Figure 5). These two facts together with the homogeneity of the clays themselves (see earlier) all provide strong evidence that the brown clays of Site 212 are not redeposited like the calcareous units, but are the result of normal pelagic grain by grain settling, which prevailed over all of the Wharton Basin since the Upper Cretaceous.

The anomalously thick section at Site 212, then, is postulated as being entirely due to the presence of calcareous sediments which have been carried into the deepest part of the Wharton Basin and ponded there by submarine currents.

The questions that must be answered, then, are where did the calcareous material come from and what was the nature of the transporting current. It has been pointed out above that Site 212 is situated in the deep trough of a major fracture zone. Immediately west of the site (Sclater and Fisher, in press), the sea floor rises to a depth of only 4500 meters at the present time. If one accepts the age depth constancy curve of Sclater et al. (1971), then both Site 212 and the high sea floor to the west can be plotted on subsidence curves as in Figure 38. The limestone fragments occurring on top of, and within, the metabasalt of Unit 9 are recrystallized, but traces of fossils were still visible in thin section (Figure 2, Plate 5) though their age has yet to be determined. Recrystallization has converted the original texture of the calcareous material into a diffuse patchwork of calcite exhibiting undulatory extinction (Figure 1, Plate 5) or abundant small anhedral grains (Figure 2, Plate 5) and thereby destroyed the evidence for determining whether the calcite is in situ or has been redeposited. Nevertheless, the subsidence curve (Figure 38) shows that the area of Site 212 could have been shallow enough to be above the CCD at the time of Unit 9's formation.

By Late Cretaceous times, the area of Site 212 is considered to have been too deep for pelagic carbonates to settle through the water column on to the sea floor. However, the sea floor to the west could still have been above lows in the level of the CCD for the brief periods represented by Units 7 and 5 (Figure 38) and thereby been the most likely source area for the calcareous material redeposited at Site 212. These fluctuations in the CCD would account for the very limited time range of the calcareous material which was redeposited in the two units.

By middle Miocene times, the potential source area west of Site 212 for calcareous material to accumulate would itself have most probably been below the CCD (Figure 38). Consequently, the source of Units 1, 2, and 3 may have been different from that of 5 and 7. It should be noted here that all of the youngest three units contain an admixture of older mid-Tertiary contaminants (see site report).

Hiatuses

Figures 33 and 39 show the time spans of the hiatuses inferred from the recovered cores on Leg 22. It can be seen that there are major hiatuses in the sedimentary record at

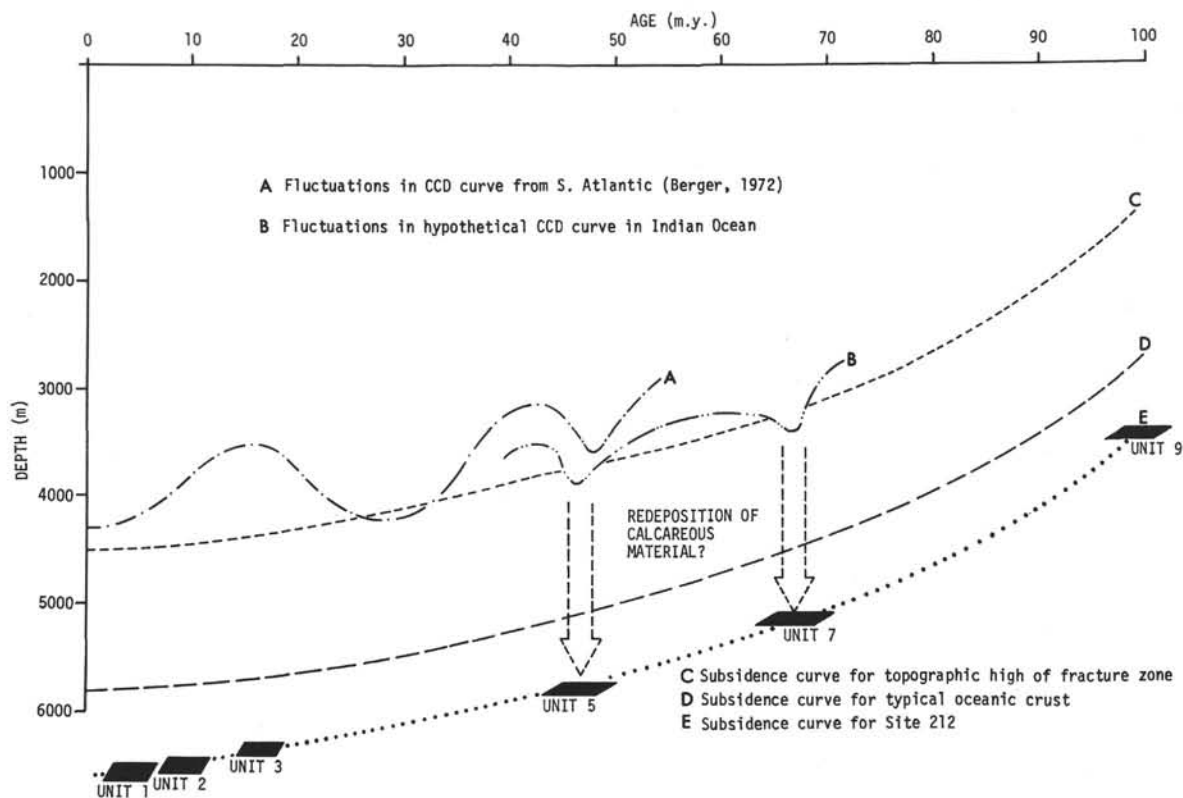


Figure 38. Subsidence curves for sea floor in vicinity of Site 212.

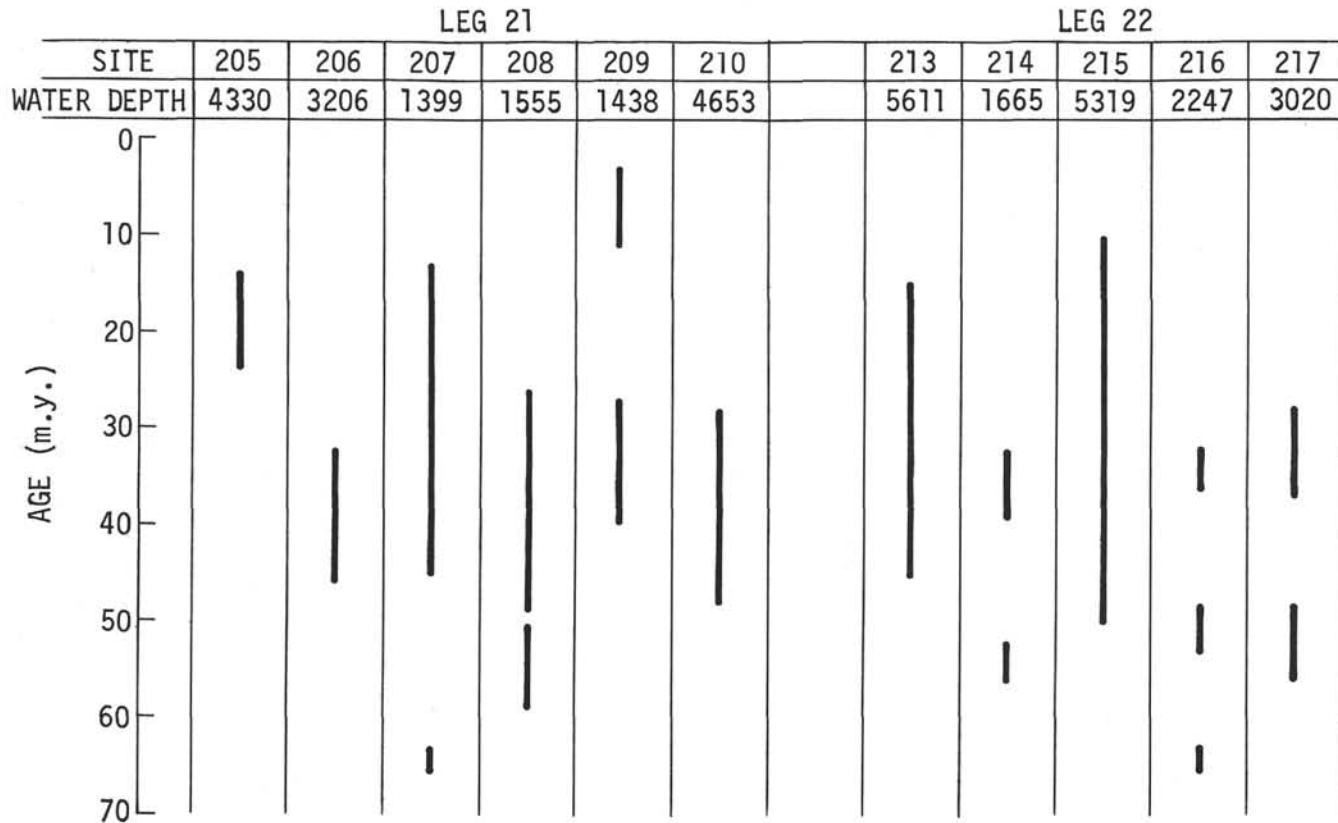


Figure 39. Duration of hiatuses penetrated on DSDP Legs 21 and 22.

Sites 213 and 215, centered close to 35 m.y.B.P. At the same time, small hiatuses are present in Sites 214, 216, and 217. Leg 21 of the DSDP revealed the occurrence of a regional unconformity centered in the early Oligocene (Kennet, et al., 1972). As in Leg 22 sites, the unconformity is present on both ridges and basins though, by contrast, the duration of the unconformity is not markedly greater in the deep-water sites of Leg 21 (Figure 39).

By plotting the hiatuses of Sites 213 and 215 on the subsidence curves (Figure 36), it can clearly be seen that they must be related to erosion or nondeposition caused by a deep-water (i.e., >4000 m) bottom current. Pimm and Sclater (in press) have discussed the importance of being able to use the subsidence history of a site to determine the depth range at which a particular hiatus was formed. The regional extent of the Oligocene unconformity in both the areas of Leg 21 in the Australian basins and Leg 22 in the Indian Ocean would suggest that in some unexplained way the vigorous deep-water circulation was directly responsible for erosion (or nondeposition caused by some other means) at deep- as well as shallow-water locations in the Oligocene. However, it was also demonstrated by Pimm and Sclater (in press) that some agent other than deep-water erosion was responsible for the hiatuses of Eocene and Paleocene age that only occur in shallow-water sites.

The establishment of this vigorous deep-water Oligocene circulation was clearly related to the separation of Australia and Antarctica in the Eocene (anomaly 22) and the subsequent subsidence of the sea floor between the two continents to allow development of the deep-water circum-polar current by Oligocene times (Pimm and Sclater, in press).

Distribution of Chert

Ninetyeast Ridge Sites (214, 216, 217)

The thickest development of chert in all of the Leg 22 drill sites was in 217, at the northern end of Ninetyeast Ridge (see Figures 3, 4, and 9). In 217, the cherts form a major part of the Campanian sequence between 555 to 664 meters. Upper Paleocene sediments at 217 between 353 and 403 meters also contain a few chert beds.

In Site 216, a few thin chert beds were recovered at 283 meters in the middle Eocene, from 310 to 320 meters in the late Paleocene, and at 330 meters in the early Paleocene.

Drilling at Site 214 did recover a few marine sediments of Paleocene age between about 360 and 390 meters, but no chert was present. The Paleocene sediments at Site 214 were deposited in a shallow-shelf environment, those at Site 216 and 217 were deposited in a deeper water, more oceanic, facies (see Pimm, et al., in prep). However, chert was found in a shallow-shelf facies in Campanian sediments at Site 217. No conclusions can be drawn that the absence of chert at Site 214 is due to the absence of siliceous fossils in shallow-water sediments of Paleocene age or that the latitude of Site 214 was not in a productivity zone for these fossils at that time. Site 215 situated in deep water to the west of Ninetyeast Ridge in almost the same latitude as Site 214 does contain Paleocene chert (see below). In any case, there does appear to be a trend of increasing chert

development to the north in Paleocene carbonate sediments on Ninetyeast Ridge.

Other Sites

Chert nodules were recovered from Paleocene (foram Zones P.4-P.5) calcareous oozes at Site 215 but not in similar sediments of the same age at Site 213 in the Wharton Basin. Sites 211 and 212, also situated in the Wharton Basin, did not penetrate calcareous sediments of late Paleocene age, but Site 259, drilled on Leg 27 in the Perth Abyssal Plain, did penetrate calcareous late Paleocene sediments, but no chert was recovered (Veevers, Heitzler, et al., 1973).

Chert was recovered from Sites 219, 220, and 221 (drilled on Leg 23) in calcareous sediments of middle Eocene to middle Paleocene, early Eocene, and middle Eocene age, respectively (Whitmarsh, Weser et al., 1972).

Therefore, it is possible that the absence of chert in the Wharton Basin (despite the very limited evidence of only two sites) in contrast to its presence in two sites in the northern parts of Ninetyeast Ridge and four sites in the Central Indian Basin, may be related to paleocirculation patterns in the early Tertiary. At that time, the southern part of Wharton Basin would have been almost totally isolated from the rest of the Indian Ocean by Ninetyeast Ridge to the west and Broken Ridge to the south (Figure 34).

Bengal and Nicobar Fans

Sites 218 and 211 penetrated thick sequences of terrigenous sediments which built the submarine features known as the Bengal and Nicobar fans, respectively. Two other sites (215, 217) also penetrated fine-grained terrigenous sediments believed to be from the same source as the material which built these fans.

A visual estimate, made on board ship, of the relative proportions of sand-silt-clay and pelagic contribution in each core of Site 218 was plotted on a depth scale (Figure 40). This diagram clearly indicates four major "pulses" of coarser terrigenous sedimentation. Using the rather poor biostratigraphic control available for Site 218 (Chapter 9), tentative correlations with the other sites are discussed below.

At Site 211, the 200-meter-thick terrigenous unit has been dated as early Pliocene (*Sphaeroidinella dehiscens* Zone; see Chapter 2) and, therefore, is partly equivalent to Pulse 2 of Site 218. As the minimum Pliocene sedimentation rate at Site 211 is almost double the maximum rate in Site 218 (see terrigenous sediments section), a large proportion of the sediment load carried into the head of the Bay of Bengal was transported down submarine channels to the east of Ninetyeast Ridge to build the Nicobar Fan. The presence of thick silty sand beds in the Pliocene at Site 211, a distance of about 3850 km from the head of the Bay of Bengal, attest to the tremendous energy of the transporting submarine currents at this time. The absence of terrigenous material (equivalent to Pulse 1 of Site 218) in Quaternary sediments at Site 211 could be related to one or more of the following causes:

1) Damming to the north by juxtaposition of the Ninetyeast Ridge against the Indonesian trench system.

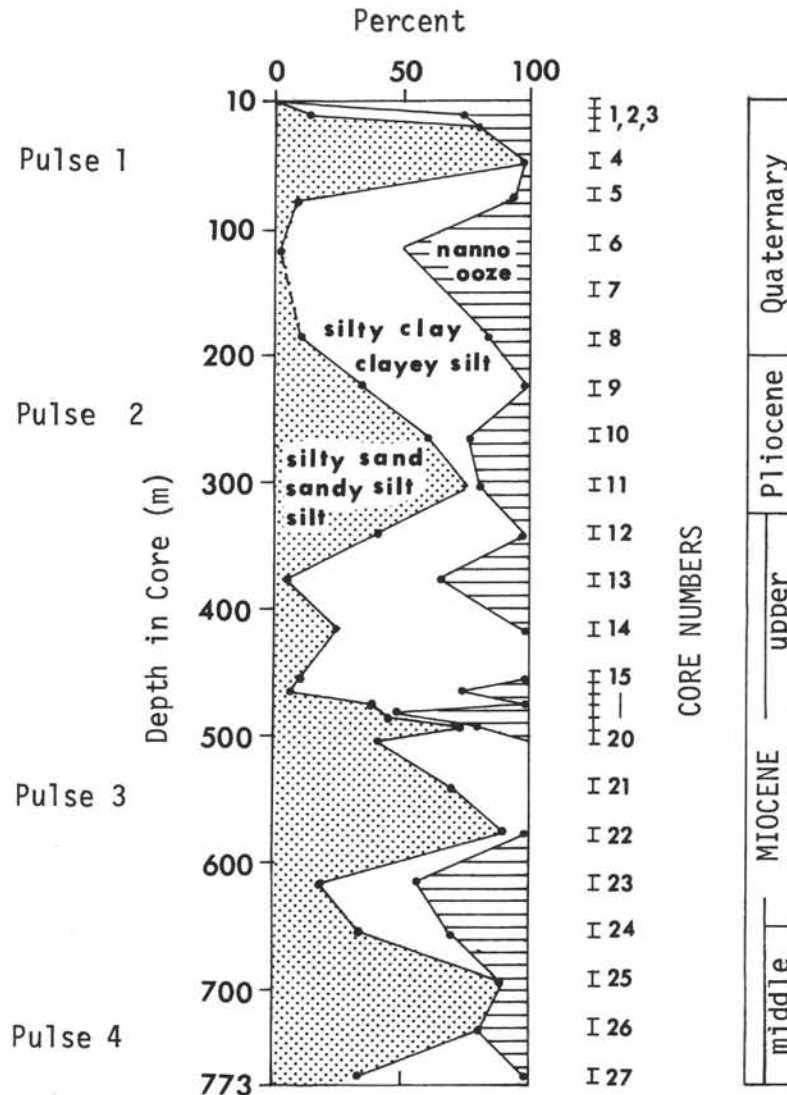


Figure 40. *Fluctuations in terrigenous sedimentation at Site 218.*

2) Damming caused by formation of the pre-trench rise associated with buckling of the Indian plate as it descends into the Sunda Trench.

3) Diversion of the main transporting currents down submarine channels in the Bengal Fan instead of the Nicobar Fan.

At the present time, some terrigenous material is still penetrating around the east side of Ninetyeast Ridge and is mainly being transported down the axis of the Indonesian Trench. No material is presently being added to the Nicobar Fan as submarine channels which traverse the feature are devoid of sediment. However, this must be a relatively recent development as these channels have not yet been filled with any sediment whatsoever (F. Zimmel, personal communication).

The two thin beds of fine-grained terrigenous sediment penetrated at Site 215 were dated as late Miocene (radiolarian zone *Ommatartus antepenultimus*). Therefore, Pulse 3, recognized in the Bengal Fan at Site 218, reached its maximum southerly extent (at Site 215) at this time; seismic profiles in the vicinity of Site 215 confirm that this

area is at the extreme distal end of the Bengal Fan. None of the other pulses were detected at Site 215.

At Site 217, clay-sized material, interpreted as being from the same source as the Bengal Fan sediments, occurs as a significant (up to 50%) admixture in pelagic calcareous ooze down to a depth of about 145 meters. These clays range in age from Quaternary to late Miocene i.e., the time span of Pulses 1 through 3 at Site 218.

ACKNOWLEDGMENTS

The author wishes to acknowledge the wealth of descriptive data contributed by his shipboard scientific colleagues which forms the basis for much of this synthesis. John Sclater and R. L. Fisher kindly made available tectonic reconstructions of this part of the Indian Ocean.

Many stimulating discussions on various aspects of this study were provided by J. Curray, R. Douglas, D. Moore, T. Vallier, J. Sclater and O. Weser. In addition Curray, Vallier and Weser reviewed the manuscript and offered several useful criticisms. A special thanks is given to Elaine Bruer who painstakingly typed and assisted in the accumulation of all the data.

This work was supported by the National Science Foundation.

REFERENCES

- Arrhenius, G., 1952. Sediment cores from the East Pacific: Swedish Deep-Sea Exped. (1947-1948) Rept., v. 5, pt. 1, 89 p.
- Berger, W. H., 1972. Deep sea carbonates: dissolution facies and age-depth constancy: *Nature*, v. 236, p. 392.
- Berggren, W. H., 1972. A Cenozoic time scale—some implications for regional geology and paleobiogeography: *Lethaia*, v. 5, p. 195-215.
- Bramlette, M. N., 1958. Significance of coccolithophorids in calcium-carbonate deposition: *Geol. Soc. Am. Bull.* v. 69, p. 121.
- Carpenter, G. and Ewing, J., in press. Crustal deformation in the Wharton Basin: *J. Geophys. Res.*
- Ewing, M., Eittreim, S., Truchan, M., and Ewing, J., 1969. Sediment distribution in the Indian Ocean: *Deep-Sea Res.*, v. 16, p. 231-248.
- Hayes, D. E., Pimm, A. C., et al., 1972. Initial Reports of the Deep Sea Drilling Project, Volume 14: Washington (U. S. Government Printing Office).
- Hays, J. D., Saito, T., Opdyke, N. D., Burckle, L. H., 1969. Pliocene-Pleistocene sediments of the equatorial Pacific: their paleomagnetic, biostratigraphic, and climatic record: *Geol. Soc. Am. Bull.*, v. 80, p. 1481-1514.
- Heirtzler, J. R., Dickson, G. O., Herron, E. M., Pitman, W. C., III, and LePichon, X., 1968. Marine magnetic anomalies, geomagnetic field reversals, and motions of the ocean floor and continents: *J. Geophys. Res.*, v. 73 (6), p. 2119.
- Kaneps, A. G., 1973. Carbonate chronology for Pliocene deep-sea sediments. In van Andel, Tj. H., Heath, G. R., et al., Initial Reports of the Deep Sea Drilling Project, Volume XVI: Washington (U. S. Government Printing Office), p. 873-882.
- Kennett, J. P., Burns, R. E., Andrews, J. E., Churkin, M., Jr., Davies, T. A., Dumitrica, P., Edwards, A. R., Galehouse, J. S., Packham, G. H., and van der Lingen, G. J., 1972. Australian-Antarctic continental drift, Palaeo-circulation changes and Oligocene deep-sea erosion: *Nature*, v. 239, p. 51-55.
- Luyendyk, B. P., Davies, T. A., Rodolfo, K. S., Kempe, D. R. C., McKelvey, B. C., Leidy, R. D., Horvath, G. J., Hyndman, R. D., Theirstein, H. R., Boltovskoy, E., and Doyle, P., 1973. Across the southern Indian Ocean aboard *Glomar Challenger*: *Geotimes*, v. 18, no. 3, p. 16.
- McKenzie, D. and Sclater, J. G., 1971. The evolution of the Indian Ocean since the Late Cretaceous: *Geophys. J. Roy. Astron. Soc.*, v. 25, p. 437-528.
- Parker, F. L. and Berger, W. H., 1971. Faunal and solution patterns of planktonic foraminifera in surface sediments of the South Pacific: *Deep-Sea Res.*, v. 18, p. 73-107.
- Pimm, A. C., McGowran, B., and Gartner, S., in preparation. Early sinking history of Ninetyeast Ridge.
- Pimm, A. C. and Sclater, J. G., in press. Early Tertiary discontinuities in the sediment record of deep sea drilling sites in the Northeastern Indian Ocean: *Nature*.
- Sclater, J. G., Anderson, R., and Bell, M. L., 1971. The elevation of ridges and the evolution of the central eastern Pacific: *J. Geophys. Res.*, v. 76, p. 7888.
- Sclater, J. G. and Fisher, R. L. in press. The evolution of the east central Indian Ocean with emphasis on tectonic setting of Ninetyeast Ridge: *Geol. Soc. Am. Bull.*
- Veevers, J. J., Heirtzler, J. R., Bolli, H. M., Carter, A. N., Cook, P. J., Krasheninnikov, V. A., McKnight, B. K., Proto-Decima, F., Renz, G. W., Robinson, P. T., Rocker, Jr., K., and Thayer, P. A., 1973. Deep Sea Drilling Project, Leg 27 in the eastern Indian Ocean; *Geotimes*, v. 18, no. 4, p. 16.
- Whitmarsh, R. B., Weser, O. E., Ali, S., Boudreaux, J. E., Fleischer, R. L., Jipa, D., Kidd, R. B., Mallik, T. K., Matter, A., Nigrini, C., Siddiquie, H. N., Stoffers, P., 1972. Deep Sea Drilling Project, Leg 23, in the Arabian Sea: *Geotimes*, v. 17, no. 7, p. 22.

APPENDIX A
Grain Size Analyses, Leg 22

Core, Section, Top of Interval (cm)	Sub- bottom Depth (m)	Sand (%)	Silt (%)	Clay (%)	Classification
Site 211					
1-1,70	0.7	0.3	36.3	63.3	Silty clay
1-2, 22	1.7	6.3	58.2	35.6	Clayey silt
1-6, 82	8.3	0.1	16.7	83.2	Clay
1-6, 145	8.9	0.3	23.6	76.2	Clay
4-1, 133	96.3	51.0	41.7	7.3	Silty sand
4-2, 36	96.9	51.3	41.3	7.5	Silty sand
4-2, 44	96.9	0.1	94.1	5.9	Silt
4-2, 80	97.3	5.2	15.3	79.4	Clay
4-2, 130	97.8	0.5	41.2	58.3	Silty clay
5-3, 102	137.0	13.9	65.6	20.5	Clayey silt
6-5, 10	186.6	37.8	46.0	16.3	Sandy silt
8-1, 130	257.8	47.8	36.7	15.5	Silty sand
9-2, 130	297.3	3.4	34.7	61.9	Silty clay
9-3, 130	298.8	31.7	42.6	25.7	Sand-silt-clay
Site 212					
2-4, 45	14.4	0.0	34.3	65.6	Silty clay
2-4, 51	14.5	0.0	31.5	68.5	Silty clay
Site 213					
3-1, 33	18.8	0.6	22.4	77.1	Clay
8-1, 130	67.3	0.3	15.5	84.2	Clay
8-3, 70	69.7	0.0	22.0	78.0	Clay
8-4, 138	71.9	1.1	28.7	70.2	Silty clay
8-6, 74	74.2	0.1	13.0	87.0	Clay
9-1, 138	76.9	0.0	9.5	90.5	Clay
9-3, 67	79.2	0.1	10.0	89.9	Clay
9-4, 115	81.2	0.0	11.5	88.5	Clay
9-6, 76	83.8	0.1	11.7	88.2	Clay
10-1, 138	86.4	0.1	11.4	88.6	Clay
10-3, 78	88.8	0.1	13.0	86.9	Clay
10-4, 137	90.9	0.0	11.8	88.1	Clay
10-6, 74	93.2	0.1	11.3	88.6	Clay
11-1, 136	95.9	0.0	32.7	67.3	Silty clay
11-3, 77	98.3	0.0	24.5	75.5	Clay
11-4, 133	100.3	0.0	19.0	81.0	Clay
11-6, 68	102.7	0.0	15.4	84.6	Clay
Site 214					
1-1, 64	0.6	52.0	26.8	21.2	Sand-silt-clay
1-4, 144	5.9	28.5	39.5	32.0	Sand-silt-clay
1-6, top	7.5	33.6	33.9	32.5	Sand-silt-clay
2-2, top	11.0	35.3	33.6	31.1	Sand-silt-clay
2-4, top	14.0	45.4	29.1	25.4	Sand-silt-clay
3-1, 23	19.2	37.5	30.2	32.2	Sand-silt-clay
3-3, 100	23.0	25.2	39.1	35.8	Sand-silt-clay
3-3, 111	23.1	40.5	29.6	29.9	Sand-silt-clay
3-6, 70	27.2	29.4	33.9	36.7	Sand-silt-clay
4-2, 133	31.3	22.8	35.9	41.3	Sand-silt-clay
4-3, 16	31.7	34.0	28.9	37.1	Sand-silt-clay
4-5, 32	34.8	32.7	31.5	35.8	Sand-silt-clay
5-3, 54	41.5	28.7	33.6	37.6	Sand-silt-clay
5-6, 58	46.1	40.1	26.3	33.6	Sand-silt-clay
6-1, 92	48.4	33.5	29.7	36.8	Sand-silt-clay
6-3, 62	51.1	41.5	26.6	31.8	Sand-silt-clay

APPENDIX A – Continued

Core, Section, Top of Interval (cm)	Sub- bottom Depth (m)	Sand (%)	Silt (%)	Clay (%)	Classification
Site 214 – Continued					
7-1, 107	58.1	24.3	29.4	46.3	Sand-silt-clay
7-3, 63	60.6	27.1	32.1	40.8	Sand-silt-clay
7-5, 123	64.2	24.5	32.5	43.1	Sand-silt-clay
8-3, 48	70.0	24.4	32.0	43.6	Sand-silt-clay
8-6, top	74.0	26.0	32.6	41.5	Sand-silt-clay
9-1, 123	77.2	6.6	66.4	26.9	Clayey silt
9-3, 114	80.1	9.9	56.6	33.4	Clayey silt
9-6, 112	84.6	13.4	55.4	31.2	Clayey silt
10-2, 107	88.1	13.4	57.8	28.8	Clayey silt
10-5, 116	92.7	13.0	55.7	31.3	Clayey silt
10-6, 66	93.7	13.8	53.1	33.1	Clayey silt
11-1, 135	96.3	10.1	53.9	36.0	Clayey silt
11-3, 86	98.9	22.2	44.1	33.7	Sand-silt-clay
11-3, 92	98.9	22.3	36.6	41.1	Sand-silt-clay
11-5, 135	102.3	16.7	37.4	45.9	Silty clay
12-5, 57	111.1	13.2	44.3	42.5	Clayey silt
13-3, 93	117.9	5.4	47.0	47.6	Silty clay
14-3, 86	127.4	3.0	51.7	45.3	Clayey silt
15-2, 113	135.6	9.5	52.2	38.3	Clayey silt
15-3, 132	137.3	10.1	47.6	42.3	Clayey silt
15-5, 113	140.1	9.2	52.8	38.0	Clayey silt
16-1, 68	143.7	9.3	57.8	32.9	Clayey silt
16-5, 42	149.4	7.8	57.9	34.3	Clayey silt
17-1, 122	153.7	3.0	55.4	41.6	Clayey silt
17-3, 93	156.4	4.1	61.1	34.8	Clayey silt
17-5, 112	159.6	4.5	60.7	34.8	Clayey silt
18-1, 122	163.2	5.3	60.1	34.6	Clayey silt
18-3, 112	166.1	13.0	56.9	30.1	Clayey silt
18-5, 80	168.8	15.0	53.0	32.0	Clayey silt
19-1, 112	172.6	5.8	62.3	31.9	Clayey silt
19-5, 82	178.3	8.7	61.5	29.8	Clayey silt
20-3, 82	184.8	10.8	54.5	34.7	Clayey silt
21-3, 105	194.6	8.8	60.0	31.2	Clayey silt
21-5, 52	197.0	1.3	64.1	34.6	Clayey silt
22-2, 105	202.6	0.6	71.9	27.5	Clayey silt
22-5, 32	206.3	0.9	69.1	30.0	Clayey silt
23-2, 90	211.9	0.8	68.0	31.3	Clayey silt
23-5, 90	216.4	0.3	69.3	30.4	Clayey silt
24-2, 90	221.4	0.1	66.8	33.1	Clayey silt
25-2, top	230.0	1.0	51.7	47.3	Clayey silt
26-1, top	238.0	1.3	53.6	45.1	Clayey silt
27-3, top	250.5	0.6	63.7	35.7	Clayey silt
28-2, top	258.5	0.1	66.3	33.5	Clayey silt
28-5, 77	263.8	0.3	67.6	32.1	Clayey silt
29-5, 80	273.3	0.4	53.9	45.7	Clayey silt
29-6, 124	275.2	0.5	69.7	29.8	Clayey silt
30-1, 94	276.9	0.4	75.9	23.7	Silt
31-3, 74	289.2	1.9	57.3	40.8	Clayey silt
32-3, 78	298.8	3.0	59.2	37.8	Clayey silt
33-3, 84	308.3	1.6	72.8	25.6	Clayey silt
34-5, 90	320.9	2.7	68.0	29.2	Clayey silt
35-3, 94	327.4	21.4	50.6	28.0	Sand-silt-clay
35-4, 112	329.1	40.9	39.9	19.1	Silty sand

APPENDIX A – Continued

Core, Section, Top of Interval (cm)	Sub- bottom Depth (m)	Sand (%)	Silt (%)	Clay (%)	Classification
Site 214 – Continued					
36-3, 50	336.5	30.6	27.7	41.7	Sand-silt-clay
37-2, 124	345.2	66.2	18.1	15.7	Silty sand
41-3, 100	384.5	8.8	24.8	66.4	Silty clay
41-3, 136	384.9	7.2	32.7	60.2	Silty clay
Site 215					
8-2, 40	66.4	0.0	9.1	90.8	Clay
8-3, 40	67.9	0.4	15.3	84.3	Clay
8-4, 40	69.4	0.0	33.3	66.7	Silty clay
8-5, 42	70.9	0.0	27.8	72.2	Silty clay
9-1, 51	74.5	0.2	22.4	77.4	Clay
9-2, 40	75.9	0.5	13.0	86.5	Clay
9-3, 45	77.4	0.1	13.0	87.0	Clay
10-2, 38	85.4	0.1	49.6	50.3	Silty clay
10-3, 78	87.3	0.6	54.5	44.9	Clayey silt
11-1, 40	93.4	1.0	47.0	52.1	Silty clay
11-2, 40	94.9	2.0	45.5	52.5	Silty clay
11-5, 40	99.4	2.0	48.0	50.0	Silty clay
Site 216					
2-1, 93	45.4	12.3	42.9	44.8	Silty clay
2-6, 113	53.1	14.4	37.2	48.4	Silty clay
3-2, 107	85.1	6.5	40.0	53.5	Silty clay
4-1, 79	121.3	3.6	58.5	37.9	Clayey silt
5-2, 105	161.1	1.0	52.7	46.3	Clayey silt
8-2, 112	189.6	1.8	57.3	41.0	Clayey silt
34-4, 66	439.2	22.5	49.4	28.2	Sand-silt-clay
34-4, 70	439.2	1.6	42.8	55.7	Silty clay

APPENDIX A – Continued

Core, Section, Top of Interval (cm)	Sub- bottom Depth (m)	Sand (%)	Silt (%)	Clay (%)	Classification
Site 217					
1-1, 36	0.4	8.1	33.7	58.2	Silty clay
2-3, 72	43.7	7.0	28.5	64.5	Silty clay
4-5, 60	122.6	1.8	27.6	70.6	Silty clay
8-3, 90	271.9	2.2	54.5	43.2	Clayey silt
Site 218					
2-1, 128	5.3	0.4	35.8	63.8	Silty clay
2-2, 67	6.2	0.0	41.5	58.5	Silty clay
2-3, 120	8.2	0.5	20.7	78.8	Clay
2-5, 55	10.6	40.7	47.5	11.8	Sandy silt
3-2, 136	16.4	39.2	49.2	11.6	Sandy silt
5-1, 103	71.0	0.1	35.0	65.0	Silty clay
5-2, 88	72.4	0.2	36.4	63.4	Silty clay
6-2, 88	110.4	5.3	42.2	52.5	Silty clay
8-2, 117	186.7	26.9	62.8	10.2	Sandy silt
10-1, 105	261.0	62.9	33.4	3.7	Silty sand
11-2, 100	300.5	9.5	62.1	28.4	Clayey silt
14-1, 89	412.9	34.3	52.5	13.2	Sandy silt
17-1, 135	470.4	0.0	12.4	87.6	Clay
17-3, 23	472.2	36.8	50.1	13.1	Sandy silt
19-1, 136	489.4	0.0	11.5	88.4	Clay
20-1, 36	497.9	0.0	24.1	75.9	Clay
21-1, 88	536.4	0.0	62.4	37.6	Clayey silt
22-2, 65	575.7	3.6	51.9	44.5	Clayey silt
23-1, 28	611.8	0.0	33.6	66.4	Silty clay
23-2, 78	613.8	0.1	17.8	82.1	Clay
24-2, 86	651.9	12.1	40.5	47.3	Silty clay
25-2, 93	689.9	0.1	63.8	36.1	Clayey silt
26-1, 116	726.7	0.0	20.8	79.2	Clay
27-1, 124	764.7	8.0	53.9	38.1	Clayey silt

APPENDIX B
Summary of Smear Slide and Visual Analysis

Core	Age ^a	Facies		Nannofossils		Foraminifera		Siliceous Fossils ^f		Volcanics	Sedimentary Structures	Other Features
		Dom. ^b	Sub. ^c	Abund.(%) ^d	Pres. ^e	Abund.(%) ^d	Pres. ^e	Abund. (%) ^d	Pres. (Rad) ^g			
Site 211												
1	Q	Silic.	Ash					65 D>R>Sp>Si	G	Thin ash, rhyol. glass	Color banding	
2	Q	Silic	Ash					80 D>R>Sp>Si	G,M	Pumice, consol ash fragments	Color banding	
3	Lt Pl	Silic & clay	Ash					35-90 D>R>Sp>Si	G,M	Thin ash, rhyol. glass	Color banding, mottling	
4	Pl	Terr	Silic clay			Tr	G	20 R>Sp>D	P,M	Ash mottles	Bedding, grading mottling	3% heavies
5	Pl	Silic/terr						60 R>D	M,P	Glass pumice	Bedding	1-2% heavies, 1% FeO
6	Pl	Silic/clay/terr	Terr					30-60 R>Sp	M	Tr glass	Bedding, grading	6% phillipsite
7	Pl	Terr				Tr	G	Tr			Bedding	2% heavies, fragments calc. siltstone
8	Pl	Terr	Clay			Tr	M				Bedding	2% heavies
9	Pl	Terr				Tr	M				Bedding, laminae	2% heavies
10	?	Clay				Tr						≤15% FeO in places
11	?	FeO/clay	Ash							Altered basaltic glass		Amorphous FeO dominant 10% pyrite in ash
12	Ma, Ca	Calc	Clay	50	P	R	M			Diabase sill	Laminations & bedding	FeO rich at contact Tr dolomite
13	Ca	Calc	Clay & ash	70	P	R	M			FeO rich ash laminae	Laminations & bedding, burrowing	Tr dolomite FeO rich clay layers
14	Ca	Calc	Clay	70-40	P	Tr	M			Basalt	Laminations & bedding	3-10% dolomite FeO rich clay layers
15	?									Basalt		
Site 212												
1	E Pl	Calc		80	G,F	5	P	Tr	P	1-2% glass shards		1-2% FeO
2	Pl Mi	Clay	Calc	0-90	G	0-3	P			Ash pockets, 75% glass	Bedding	1% z, 2-10% FeO
3	Mi	Calc		93	G	Tr	P	Tr	M		Faint lamination	
4	Mi	Calc	Clay	92	G	1	P					
5	Lt Mi	Calc		85	G	5	F			Tr glass	Faint laminations	
6	Lt Mi	Calc		85	G	Tr	F			Tr glass		
7	Lt Mi	Calc		85	G	2	F					
8	Lt Mi	Calc		88	G	2	F				Faint laminations	

APPENDIX B – Continued

Core	Age ^a	Facies		Nannofossils		Foraminifera		Siliceous Fossils ^f		Volcanics	Sedimentary Structures	Other Features
		Dom. ^b	Sub. ^c	Abund.(%) ^d	Pres. ^e	Abund. (%) ^d	Pres. ^e	Abund. (%) ^d	Pres. (Rad) ^g			
Site 212 – Continued												
9	Lt Mi	Calc		88	G	2	F			1% glass	Faint laminations	1% micronodules
10	M Mi	Calc	Clay	82	F,G	1	F				Bedding & mottles	0-2% FeO
11	M Mi	Calc	Clay	80	F	1	F				Mottling	1% FeO, Tr FeS
12	M Mi	Calc	Clay	82	F	2	F				Semi-lith	1% FeO
13	M Mi	Calc		20-30	F	30-40	F			<2% glass & feld.	Lamination & cross lamination, semi-lith.	
14	M Mi	Calc	Clay	80	F						Rare mottles, semi-lith.	
15	M Mi & ?	Clay	Calc	Tr	F	T	P				Bedding, lamination, graded, semi-lith.	Tr glauc., 10-15% FeO, Mn micronod., 10% z, one reduced zone
16	?	Clay									Semi-lith.	40% z, 14% FeO, 1% Mn micronod.
17	?	Clay									Semi-lith.	40% z, 14% FeO, 1% Mn micronod.
18	Lt M Eo	Calc		Tr	F						Bedding, lamination in chalk and ripples, semi-lith.	5-10% FeO, 2-50% z
19	Lt M Eo	Calc		80	F			Sp-1, R-Tr	M		Semi-lith.	Tr glauc.
20	Lt M Eo	Calc		Tr	F			Sp-1, R-Tr	M,G		Semi-lith.	
21	Lt M Eo	Calc	Silic	77	F			R-5, Sp-5, D-2	M,G,P		Laminations (pale green) semi-lith.	
22	Lt M Eo	Calc	Silic	80	F			R-5,Sp-5,D-Tr	M,G	<1 glass	Some clay inclusions, semi-lith.	Tr glauc. & volcanic
23	Lt M Eo	Calc	Clay	<80	F	0-2	F	R-1-2	G		Laminations, inclusions, contorted lamin.-sharp?	Tr glauc., 24% z in clay
24	Lt M Eo	Calc		Tr	F							
25		Calc		Tr	F	Tr		R-Tr,Sp-Tr			Mottles	Tr glauc.
26		Calc		70-80	F	Tr						Tr glauc.
27		Clay	Calc	<5						2% glass	Bedding & lamination	7% z, 5% FeO, reduced zones
28		Clay									Chemical banding	5% FeO, 4% z
29	Lt K	Clay	Calc	Tr	P	Tr	F			Tr glass	Bedding, chem banding & mottling	10-22% FeO, 12% z

APPENDIX B – Continued

Core	Age ^a	Facies		Nannofossils		Foraminifera		Siliceous Fossils ^f		Volcanics	Sedimentary Structures	Other Features
		Dom. ^b	Sub. ^c	Abund.(%) ^d	Pres. ^e	Abund.(%) ^d	Pres. ^e	Abund.(%) ^d	Pres.(Rad) ^g			
Site 212 – Continued												
30	Lt K	Calc	Volc	76	P	1	F			10% glass	Color banding & interlamination	4% Mn
31	Lt K	Calc		73	P	1	F				Color changes	
32	Lt K	Calc		71	P	1	F				Color mottles	
33	Lt K	Calc		73	P	Tr	F			1% glass		
34	Lt K	Calc		?73	P	Tr	F			3% glass	Lamination & mottles	
35	Lt K	Calc	Clay	54	P	8	F			Calc., 2% glass	Bedding, grading, color banding & mottles, frags. of bed below	One reduced zone, 30% FeO, 5% z
36	?	Clay				Tr	F			2% glass		40% z, 2% FeO
37	?	Clay									Color banded	60-70% z, 4% FeO
38	?	Clay										25% FeO, 17% z
39		Basalt										
Site 213												
1	Q	Silic ooze	Clay					R+D-55-80, Sp-5, Si-1	M	1-2% glass 1% feld., clear	Lamination of FeO Mn layers, color mottles	
2	Q, Lt Pl	Silic ooze	Volc					D-50-80, R-10-20, Sp&Si-3	M, G	10-25% glass	Ash-rich laminations, color mottles	
3	Lt Pl	Silic ooze						D-45-75, R-25, Sp&Si-5-10	G	2% glass, pumice frags.	Laminations of FeO Mn layers, color mottles	
4	Lt Pl	Silic ooze				Tr	P	D-75, R-16, Sp&Si-2	M, G	1% glass	Laminations of FeO Mn layers	
5	E Pl	Silic ooze	Volc			Tr	P	D-75, R-16, Sp&Si-5	G, P	Ash up to 25% in one place, 2% only basic	Mottles	
6	Lt Mi	Silic ooze				Tr	P	D-50-70, R-15-25, Sp&Si-4-9	G, M	2% glass, pumice	FeO Mn rich layers, mottles	
7	Lt Mi	Silic ooze	Clay					D-55, R-20, Sp&Si-3	G	3% glass, 1% feld., ash pocket & pumice	Mottles	

APPENDIX B – Continued

Core	Age ^a	Facies		Nannofossils		Foraminifera		Siliceous Fossils ^f		Volcanics	Sedimentary Structures	Other Features
		Dom. ^b	Sub. ^c	Abund.(%) ^d	Pres. ^e	Abund.(%) ^d	Pres. ^e	Abund.(%) ^d	Pres. (Rad) ^g			
Site 213 – Continued												
8	Lt Mi	Clay	Silic ooze					D-10, R-10, Sp-10, Si-1	G	1-2% glass, pumice, rhyol. ash pocket		Specks of Mn, 1% z
9	Lt Mi	Clay						R-1-3, Sp-1	M,P	1% glass	Mottles	3-25% z, 3-5% Mn/FeO
10	M Mi	Clay						R-3, Sp-1	M		Mottled, streaked	3% z, 5% Mn/FeO
11	?	Clay				Tr	P				Rare mottles	15-25% z, 3-6% MnO
12	?	Clay										20% z, 15% FeO, 10% MnO
13	?	Clay				Tr	M			Tr glass, basic		13-20% FeO, 3% z
14	E Eo	Clay	Calc	70	P,F	Tr	M	R-1			Bedding, burrow, mottles	15-30% FeO in clays
15	E Eo	Clay	Calc	84	F	1	P,M, E,G	R-1			Bedding, burrow, mottles	15-30% FeO in clays
16	Lt Pa	Calc	Clay	84	F	Tr	E				Bedding	FeO very high
17		Basalt										
18		Basalt										
19		Basalt										
Site 214												
1	Q	Calc		40-75	G	20-55	G	R-1, D-1, Sp-1, Si-1	M,G	2% glass in places	Laminations & mottles	
2	Q	Calc		50-70	G	15-45	G	R-1, D-2, Sp-2, Si-1	G,M	Tr glass	Bedding & laminae	
3	Q Pl	Calc		50(48)	F,G	45	G	Sp-Tr, R-Tr	G,M	Tr glass	Bedding & laminae	
4	Pl	Calc		50-65	F,G	30-45	G	R-Tr	M,G	Pumice Tr glass	Laminae, mottles (?drilling)	
5	Pl	Calc		55-60	F	35-40	G	R, Sp-Tr	M,G		Bedded, mottled	
6	Pl	Calc		50-55	P,F	40	G	Sp, R-Tr	G,M		Laminae, vague?	
7	Pl	Calc		55	G	40	G	R, D, Sp-Tr	G,M		Laminae, vague?	
8	Pl	Calc		50	G	45	G	R-Tr	G,M		Laminae, vague?	
9	Pl	Calc		50-65	G	30-45	G	R-Tr	G		Laminae, vague?	
10	Lt Mi	Calc		50	G,F	45	G	R-Tr	G		Color bands, harder layers, mottles	
11	Lt Mi	Calc		40-55	G	40-55	F	R-Tr	G,M		Color bands, harder layers	

APPENDIX B – Continued

Core	Age ^a	Facies		Nannofossils		Foraminifera		Siliceous Fossils ^f		Volcanics	Sedimentary Structures	Other Features
		Dom. ^b	Sub. ^c	Abund.(%) ^d	Pres. ^e	Abund.(%) ^d	Pres. ^e	Abund.(%) ^d	Pres.(Rad) ^g			
Site 214 – Continued												
12	Lt Mi	Calc		55	F,G	40	F	R-Tr	G,M		Rare bands, harder layers	
13	Lt Mi	Calc		55	F	40	F	R-Tr	G		Rare bands, mottles	
14	Lt Mi	Calc		55	F	40	F	R-Tr	G		Mottles	
15	Lt Mi	Calc		70-55	F	25-40	F	R,Sp-Tr	G	Pumice	Vague mottles	
16	Lt Mi	Calc		50	F	45	F	R-Tr	G,M		Indurated layers	
17	M Mi	Calc		50	F,P	45	F	R-Tr	G,M			
18	M Mi	Calc		80	F	15	F	R-Tr	M,P			
19	M Mi	Calc		75	P	20	F	R-Tr	M			
20	M Mi	Calc		82	P	15	P	R-Tr	M			
21	M Mi	Calc		82	P	15	P					
22	E Mi	Calc		82	P	15	P				Few color bands, mottles & burrows	
23	E Mi	Calc		82	P	15	P				Few color bands, mottles & burrows	
24	Lt G ₁	Calc		92	F	5	P				Few mottles	
25	Lt Ol	Calc		87	F	10	P				Few mottles	
26	M Ol			89	F	8	P				Few mottles	
27	E Ol	Calc		95	F	2	P				Few mottles	
28	Lt Eo	Calc	Ash	95	F	2	P			Ash pockets, 50% basic glass, 30% FeO, 5% feld.	Few laminae & color bands, ash mottles (drilling?)	
29	M Eo	Calc		95	F	2	F,P				Few laminae	
30	M Eo	Calc		95	F	2	F,P				Few laminae	
31	M Eo	Calc		87-92	F	5-10	F				Few laminae	
32	M Eo			79-84	F	3	F,P					
33	E Eo	Calc		92-94	F	3-5	F					
34	E Eo	Calc		77-87	P	10-20	F					
35	E Eo	Calc		80-85	P	5-13	F,P				Bedding? varying induration-chalk	1-3% glauc.
36	Lt Pa	Calc (shallow water from here down)		<2	P	Very variable mostly fragments. ~10-40(?) in places. Preserv. -P					Bedded	Mostly indeterminate calcite, large shells common, glauconite usually <5% pyrite common in lower part

APPENDIX B – Continued

Core	Age ^a	Facies		Nannofossils		Foraminifera		Siliceous Fossils ^f		Volcanics	Sedimentary Structures	Other Features
		Dom. ^b	Sub. ^c	Abund.(%) ^d	Pres. ^e	Abund.(%) ^d	Pres. ^e	Abund.(%) ^d	Pres.(Rad) ^g			
<i>Site 214 – Continued</i>												
37	Pa	Calc		Tr	P			Sp-2,D-Tr				
38	Pa	Calc		2	P			Sp-3,D-3		1% feld., 1% glass		
39	Pa	Calc		1	P			Sp-5,D-1		1% feld., 1% glass		
40	Pa	Calc	Volc	Tr	P			R,D,Sp-few		Volc. rock frags., feld. phenos.	Laminae (shells), lime cement vary- ing, induration	
41	Pa	Calc	Volc	2	P	1	P					
42	?	Lignite	Volc							Volc. clay aggregates	Bedding	Abundant z
43	?	Volc	Lignite							Feldspar & volc clay	Bedding	10% pyrite
44	?	Volc	Lignite							Feldspar & volc clay	Bedding	5-15% pyrite
45	?	Volc	Lignite							Volc clay	Bedding	
46	?	Volc	Lignite							Feldspar, volc clay, lava frag- ments	Bedding	Pyrite, FeO, and chlorite present
47	?	Volc	Lignite									Similar to Core 46
48		Basalt								Basalt		
49		Basalt								Basalt		
50		Basalt								Basalt		
51		Basalt	Volc							Basalt, brown glass	Bedding	
52		Volc	Lignite			Tr	P			Volc clay, feldspar, basalt fragments, brown glass		Chlorite, FeO
53		Basalt	Volc							Basalt, volc. clay		
54		Basalt										

APPENDIX B – Continued

Core	Age ^a	Facies		Nannofossils		Foraminifera		Siliceous Fossils ^f		Volcanics	Sedimentary Structures	Other Features
		Dom. ^b	Sub. ^c	Abund.(%) ^d	Pres. ^e	Abund.(%) ^d	Pres. ^e	Abund.(%) ^d	Pres.(Rad) ^g			
Site 215												
1	Q/ Lt Pl	Silic				Tr	P	R-25,D-50,Sp-10,Si-2	G		Color banding & mottles	Mn-rich layers, some FeO
2	E Pl	Silic				Tr		R-25,D-50,Sp-10, Si-2	G,M		Color banding & mottles	Mn-rich layers, some FeO
3	E Pl	Silic				Tr	F	D-60, R-10-20, Sp-2-5, Si-2	G,M		Color banding & mottles	Mn-rich layers, some FeO
4	E Pl	Silic				Tr	F	D-25-60,R-15-20, Sp-5-10	G	3% glass	Color banding & mottles	Mn-rich layers, some FeO
5	Lt Mi	Silic	Clay					D-35,R-20, Sp-2,Si-1	G		Patchy colors	1% z
6	Lt Mi	Clay	Terr					R-20	G,M	Tr glass	Bedding	Indeterminate CaCO ₃
7	Lt Mi	Silic	Clay			Tr	F	D-30,R-40,Sp-1,Si-1	G,P	Tr glass		
8	Lt Mi	Terr	Clay					R-5,Sp-3,Si-Tr	M,P	5% glass	Bedding	
9	E Eo	Clay	Calc	70	F	Tr	P				Transitional bedding, mottles?	10% z, 10% FeO-Mn
10	E Eo	Calc		80-85	F,P,G		1	F,G				Some authigenic carbonate
11	E Pa	Calc		92	F,P	3	G	R-Tr				Some authigenic carbonate
12	Pa	Calc		79	F,P	1	P					
13	Pa	Calc	Chert	85	G,F	Tr	M				Burrows in chert	
14	Pa	Calc	Chert	95?	F	Tr	P				Color mottles	
15	Pa	Calc		92?	F	Tr	P				Color streaking	
16	Pa	Calc	Clay	87-90	F	Tr	P,M					FeO in clay rich layers
17	Pa	Calc	Basalt	Tr	G,F	Tr	F,P				One indurated limestone bed	FeO in clay rich layers
18		Basalt										
19		Basalt										
20		Basalt										
Hole 216												
1	Q	Calc	Ash	30-70	G	25-55	G	R-1,D-1,Sp,Si-Tr	P	Ash beds, 90-95% glass, 3-7% feldspar	Bedding, few mottles	
2	Pl	Calc	Ash	55-60	F	30	M		M	Ash bed, 70% glass	Bedding, vague mottles	
3	Lt Mi	Calc		80-90	P	5	P		M	10% glass	Bedding	

APPENDIX B – Continued

Core	Age ^a	Facies		Nannofossils		Foraminifera		Siliceous Fossils ^f		Volcanics	Sedimentary Structures	Other Features
		Dom. ^b	Sub. ^c	Abund.(%) ^d	Pres. ^e	Abund.(%) ^d	Pres. ^e	Abund.(%) ^d	Pres.(Rad) ^g			
Hole 216 – Continued												
4	M Mi	Calc		85-88	P	7-10	P		G,M	Tr glass	Rare mottles	
5	E Mi	Calc		80	P	15	P		G,P,M			
6	E Mi to Lt Ol	Calc		85-90	P	5	P		G,M		Chalk starts here	
7	E Mi to Lt Ol	Calc		85	P	5	M,P	R,Sp,Si-Tr	G,M			
8	Lt Ol	Calc		85	P	5	P	R,Sp-Tr	G,M			
9	Lt Ol			94	P	Tr	P	Tr	G,M			
10	Lt Ol	Calc		93		Tr	P	R,Sp-Tr	G,M			
11	Ol	Calc			F		F	R-Tr	M			
12	Ol	Calc		92		Tr	P	R-Tr	G			
13	Ol	Calc		92		Tr	P	R,Sp-Tr	G			
14	Ol	Calc		92	F	Tr	P	R,Sp-Tr	G			
15	?Ol Lt Eo	Calc		93	F	Tr	P	R,Sp-Tr	G			
16	M Eo	Calc		Tr	P		P	Tr	G	Pumice		
17	M Eo	Calc		86	P		P	Tr	G			
18	M Eo E Eo	Calc	Chert		P		P		M		Bedding	
19	Pa			?	P	Tr	P					
20	Pa	Calc		97	P		F					Mn Micronodules
21	Pa	Calc	Chert	93		1	F				Laminae & bedding	Mn Micronodules
22	M Pa	Calc		93	P		F					
23	E Pa/ L Ma	Calc	Chert	<5-90 (inc. micarb.)	P	2	F,P		P	Tr glass	Bedding, burrows	Tr glauc., 5% z & authigenic carbonate in places
24	L Ma	Calc		40-87 (inc. micarb.)	P	3-25	P				Bedding, laminae burrows	5% glauc., but 50% in one bed
25	L Ma	Volc clay	Calc, ash	1	F	2-5	P			40% glass in pockets with 25% volc. clay	burrows & mottles	2% glauc.
26	Ma	Volc clay	Calc		F	5	P			20% glass in places	burrows &	10-15% glauc., shells
27	Ma	Volc clay	Calc		P		P			20% glass in places	burrows & mottles	glauc.

APPENDIX B – Continued

Core	Age ^a	Facies		Nannofossils		Foraminifera		Siliceous Fossils ^f		Volcanics	Sedimentary Structures	Other Features
		Dom. ^b	Sub. ^c	Abund.(%) ^d	Pres. ^e	Abund.(%) ^d	Pres. ^e	Abund.(%) ^d	Pres.(Rad) ^g			
Hole 216 – Continued												
28	Ma	Volc clay	Calc	10	P	5	P			20% glass	Burrows & mottles	5% glauc., chlorite abundant, shells
29	Ma	Volc clay	Calc	5		5	P			20% glass also vitric tuff bed	Bedding, burrows & mottles	5% glauc.
30	Ma	Volc clay	Calc, ash	5-20	P	1	P	D-1,R-2,Sp-2	M	50-90+% basic glass in ash beds, 5-10% glass, 5% feld. elsewhere	Bedding, burrows & mottles	
31	Ma	Calc/volc clay	ash	5	P	Tr-3	P	Sp-1,R-Tr	M	20-30% glass, Tr-2% feld.	Bedding, burrows & mottles	Shells
32	Ma	Volc/clay/calc		Tr	P	Tr	P	Sp-1, D-5		5-10% glass, Tr-feld.	Bedding, burrows & mottles	Shells
33	Ma	Volc clay	Calc	Tr	P	2	P	D-1		15-25% glass		Heavies common, chlorite
34	Ma	Volc clay	Calc	Tr	P	1	P	Sp-Tr		10-40% glass		Chlorite abundant in places
35	Ma	Volc clay	Calc	Tr	P	Tr	P	Sp-1				Shells, 2% glauc., chlorite
36	Ma	Calc	Volc	Tr	P	Tr	P			Tr-40% glass	Burrows, mottles	Shells, FeO, analcite, calcite vein
37		Basalt										
38		Basalt										
Hole 216A												
1	Lt Mi	Calc		68	F	10	F	R-1	G,M		Color banding	
2	Lt Mi	Calc		65	P	15	P	F-Tr,Sp-Tr	G,M		Color mottles	
3	M Mi	Calc		85	P	3	P	R-1,Sp-1	G	In clay rich zone 2% glass	Bedding	
4	M Mi	Calc		93	P	2	P	R-Tr	M,P	Tr glass		
5	M Mi	Calc		60	P	15	P	R-Tr	G,M	Tr glass	Color mottles	
6	M Mi	Calc		80	P	3	P	R-2	M,G	5% glass		
Hole 217												
1	Q	Calc	Terr	41	G	15	F	R-2,D-1,Sp-1,Si-1	E	Tr glass	Color banding & mottles	
2	E Pl	Calc	Terr	20-45	G	10-15	P	R-Tr	P	≥10% rhyol glass in places	Color banding & mottles	

APPENDIX B – Continued

Core	Age ^a	Facies		Nannofossils		Foraminifera		Siliceous Fossils ^f		Volcanics	Sedimentary Structures	Other Features
		Dom. ^b	Sub. ^c	Abund.(%) ^d	Pres. ^e	Abund.(%) ^d	Pres. ^e	Abund.(%) ^d	Pres.(Rad) ^g			
Hole 217 – Continued												
3	Lt Mi	Calc	Terr	64	G	2	F	R-Tr	G,E	Tr glass	Color banding, bioturbation	Mn
4	Lt Mi	Calc	Terr	55-60	G,P	3-5	P	R-3-5,D-1-3,Sp-2	G		Mottles (burrow?)	Pyrit. burrow cast
5	M Mi	Calc		77	G	2	P	<1% total	M			
6	Lt Oligo	Calc	Volc	75-85	F,P	2-7	F	R-1,Sp-Tr	G,M	30% glass	Slight-mod. bioturbation mottle	
7	Oligo	Calc		84	F	3	M	R-1-3,Sp-Tr	G,M		Faint laminae, mod.—slight bioturbation	
8	Oligo	Calc		85	F	3	P	R-2,Sp-Tr	G	Rarely 5% glass	Mottles	
9	M Oligo	Calc		89-93 (?)	F	Tr-3	P	R-Tr-3	G	Tr glass	Streaking, bioturbation	
10	M Eo	Calc		75-85	P		P	R-5,Sp-Tr	G	Tr glass	Laminae, mottling	
11	No recovery											
12	Pa	Calc	Chert	87	F	3	F	Tr	P		Mottles	
13	M Pa	Calc	Chert	80	F	10	F				Bedding, bioturbation	
14	M Pa	Calc		90-95	F	5-10	F				Color alternations, bioturbation	
15	Pa	Calc	Chert	60-65	F	5-10	F,P				Laminae, bioturbation	
16	Pa	Calc		75	F	12-15	F				Bioturbation	
17	Lt Ma	Calc		85	F	5	F,P				Color bands, mottles, bioturbation	
18	Lt Ma	Calc		89	P	1	P				Variiegated colors bioturbated	
19	Lt Ma	Calc		90	F	Tr	F			Tr glass, feld.	Variiegated colors	
20	Lt Ma	Calc		90	G	Tr	F					
21	M Ma	Calc		85	F	5	F				Color bands, bioturbated	
22	M Ma	Calc		80	P	1	F				Bedding ? color bands, bioturbated	
23	M Ma	Calc		<10	P	2	F				Ft. bedding, mottling	Indeterminate calcite dominant, few shells
24	E Ma	Calc		<10	F	Tr	F				Mottles & bioturbated	Indeterminate calcite dominant, few shells

APPENDIX B – Continued

Core	Age ^a	Facies		Nannofossils		Foraminifera		Siliceous Fossils ^f		Volcanics	Sedimentary Structures	Other Features
		Dom. ^b	Sub. ^c	Abund.(%) ^d	Pres. ^e	Abund.(%) ^d	Pres. ^e	Abund.(%) ^d	Pres.(Rad) ^g			
Hole 217 – Continued												
25	E Ma Lt Ca	Calc		<5	P	3	P				Mottles & bioturbated	Indeterminate calcite dominant, few shells
26	E Ma Lt Ca	Calc		<5	F	1-3	P				Good burrows, bioturbated	Indeterminate calcite dominant, shells abundant
27	E Ma Lt Ca	Calc		<5	F	1-5	P				Mottles bioturbated	Indeterminate calcite dominant, shells abundant
28	E Ma Lt Ca	Calc		<5	F	1-5	P				Laminae, mottles, bioturbated	Indeterminate calcite dominant, shells abundant
29	Ca	Calc		<5	P	3	P				Laminae, mottles, bioturbated	Indeterminate calcite dominant, shells abundant
30	Ca	Calc	Chert, silic 1st	Tr	P	0-3					Laminae, mottles bioturbated	Indeterminate calcite dominant, shells abundant
31	Ca	Calc	Chert	Tr	P		P				Laminae, mottles & bioturbated	Indeterminate calcite dominant, few shells
32	Ca	Calc	Chert	1-5	P	7	P			Tr	Laminae, mottles	Indeterminate calcite dominant, few shells
33	Ca	Calc		?	P	2	P				Laminae, slumps also mottles	Indeterminate calcite dominant, few shells, glauconite fragments
34	Ca	Calc	Chert	?	P	3	P			Tr	Laminae, slight bioturbation	
35	Ca	Calc	Chert, ash							10% devit. glass		
36	Ca	Calc	Chert	?		Tr	P				Bedding	
37	Ca	Dolo	Chert	?							Bedding	30-75% dolomite, 10-50% indeterminate calcite
Hole 217A												
1	Q	Calc	Terr	40		10	P	R&D-2-10	M			Some Mn, 40-50% clay
2	Q	Calc	Terr	50		15	P	R&Sp-Tr	P			Some Mn, 30-40% clay
3	Q/ Lt Pl	Calc	Terr	50		15	P		P	Tr glass		30% clay
4	Lt Pl	Calc	Terr	50		15	P		P			Some Mn, 30% clay
12	Ca	Dolo	Chert, calc	Tr	P							3% pyrite, shells
13	Ca	Dolo	Chert, calc	Tr	P							Shells
14	Ca	Dolo	Chert, calc	Tr	P		P					

APPENDIX B – Continued

Core	Age ^a	Facies		Nannofossils		Foraminifera		Siliceous Fossils ^f		Volcanics	Sedimentary Structures	Other Features
		Dom. ^b	Sub. ^c	Abund.(%) ^d	Pres. ^e	Abund.(%) ^d	Pres. ^e	Abund.(%) ^d	Pres.(Rad) ^g			
Hole 217A – Continued												
15	Ca	Dolo	Chert									Shells
16	Ca	Dolo	Chert									3% pyrite
17	Ca	Dolo	Chert, clay									
Hole 218												
1	Q	Calc	Terr	65	G	3-7	F	1-5	P			Burrowing
2	Q	Terr	Calc	40-70		10	P	0-23	G,P			Bedding, laminae, grading
3	Q	Terr				Tr	P					Bedding
4	Q	Terr				Tr	P					Bedding, grading, laminae
5	Q	Terr	Calc	70	F	Tr	P	11	In calc			Bedding, laminae, grading, mottles
6	Q	Terr	Calc	70	F	Tr	P	3	In calc			Bedding
7	Q	Terr				Tr	P	Tr				CC sample
8	Q	Terr	Calc	57	F	3	P	2	In calc	Ash bed: 60% acid glass		Bedding
9	?	Terr				Tr	P					Bedding, laminae
10	E Pl	Terr	Calc			Tr	P					Bedding, laminae, grading
11	E Pl	Terr	Calc	70?	F	7	P					Bedding, grading, laminae
12	Lt Mi	Terr		Tr	F	Tr	P					Bedding, grading
13	Lt Mi	Terr	Calc	40-70	F	Tr	P					Bedding, grading, laminae, burrowing
14	Lt Mi	Terr		Tr	F	Tr	P					Bedding, grading, laminae
15	Lt Mi	Terr		Tr	F	Tr	F					Bedding, laminae, grading
16	Lt Mi	Terr	Calc	84?	F	1	F					Bedding, laminae, burrowing, grading
17	Lt Mi	Terr					F					Bedding, laminae

APPENDIX B – Continued

Core	Age ^a	Facies		Nannofossils		Foraminifera		Siliceous Fossils ^f		Volcanics	Sedimentary Structures	Other Features
		Dom. ^b	Sub. ^c	Abund.(%) ^d	Pres. ^e	Abund.(%) ^d	Pres. ^e	Abund.(%) ^d	Pres.(Rad) ^g			
Hole 218 – Continued												
18	Lt Mi	Calc	Terr	80	F	1	F				Bedding, laminae, burrowing	n.d.
19	Lt Mi	Terr	Calc		F		F				Bedding, laminae, burrowing	2% heavies
20	Lt Mi	Terr									Bedding, laminae, burrowing	8% heavies
21	Lt Mi	Terr		Tr	F	Tr	F				Bedding, laminae	2% heavies
22	Lt Mi	Terr									Bedding, laminae	n.d.
23	Lt Mi	Terr	Calc	85	F	Tr	F				Bedding, laminae, grading, burrowing	5% heavies
24	Lt Mi	Terr	Calc	85	F		F				Bedding, laminae, grading, burrowing	n.d.
25	M Mi	Terr	Calc	75	F	Tr	F				Bedding, laminae, grading	n.d.
26	M Mi	Terr				T Tr	F				Bedding, laminae grading	n.d.
27	M Mi	Terr				Tr	G				Bedding, laminae, grading	6% heavies

Note: Calcareous fossil percentages refer to calcareous facies only.

^aQ = Quaternary, Pl = Pliocene, Mi = Miocene, Ol = Oligocene, Eo = Eocene, Pa = Paleocene, Ma = Maastrichtian, Lt = Late, M = Middle, E = Early

^bDominant

^cSubordinate

^dAbundance (Total)

^ePreservation: G = Good, M = Moderate, F = Fair, P = Poor

^fD = Diatoms, R = Radiolaria, Sp = Sponge Spicules, Si = Silicoflagellates

^gPreservation (Radiolaria only)

APPENDIX C
Carbon Carbonate Analyses, Leg 22

Core, Section, Top of Interval (cm)	Subbottom Depth (m)	Total Carbon (%)	Organic Carbon (%)	CaCO ₃ (%)
Site 211				
1-6, 8	7.58	0.3	0.2	1
12-2, 124	411.74	1.5	0.0	12
12-2, 145	411.95	8.1	0.0	67
Site 212				
1-2, top	0.05	10.4	0.0	87
1-2, top	1.50	10.5	0.0	87
1-3, top	3.00	10.5	0.0	87
1-4, top	4.51	10.4	0.0	86
1-5, top	6.00	9.6	0.0	80
1-6, top	7.50	10.3	0.0	85
2-1, 4	9.54	9.0	0.0	75
2-4, 46	14.46	8.9	0.1	73
2-4, 53	14.53	10.7	0.0	89
3-1, 123	42.23	11.2	0.0	93
3-1, 14	41.14	11.2	0.0	93
5-1, 34	60.34	10.9	0.0	91
7-1, 19	107.69	10.5	0.0	87
8-1, 5	126.55	10.8	0.0	90
8-1, 11	128.11	10.8	0.0	90
8-3, 9	129.59	10.9	0.0	91
9-1, 99	136.99	10.8	0.0	90
10-1, 2	164.52	10.0	0.0	83
10-2, 2	166.02	10.0	0.0	83
10-3, 2	167.52	10.0	0.0	83
10-4, 2	169.02	10.0	0.0	83
10-5, 2	170.52	10.1	0.0	83
10-6, 2	172.02	10.0	0.0	83
11-1, 14	193.14	10.0	0.0	83
11-4, 14	197.64	10.1	0.0	84
12-5, 138	228.88	10.1	0.0	84
13-2, 59	252.09	10.4	0.0	87
13-4, 146	255.96	9.1	0.0	75
15-3, 109	273.09	10.4	0.0	86
15-1, 56	288.56	10.3	0.0	86
18-3, 34	319.84	9.5	0.0	79
19-2, 141	328.91	9.6	0.0	80
20-1, 122	336.72	9.6	0.0	80
21-3, 44	348.44	9.6	0.0	79
21-3, 139	349.39	9.3	0.0	77
22-2, 140	357.40	9.6	0.0	80
23-1, 83	364.83	9.6	0.0	80
26-2, 91	394.91	9.9	0.0	82
27-6, 82	410.32	0.4	0.1	3
29-1, 144	422.44	7.3	0.0	61
30-2, 4	432.04	9.3	0.0	77
30-3, 85	434.35	9.2	0.0	77

APPENDIX C – Continued

Core, Section, Top of Interval (cm)	Subbottom Depth (m)	Total Carbon (%)	Organic Carbon (%)	CaCO ₃ (%)
Site 212 – Continued				
31-1, 101	441.01	9.2	0.0	76
31-5, 121	447.21	9.1	0.1	75
32-6, 44	457.44	9.1	0.1	75
33-2, 67	461.17	9.1	0.1	75
35-3, 82	481.82	8.9	0.1	73
35-4, 82	483.32	8.8	0.2	72
Site 213				
14-6, 91	131.41	8.9	0.1	74
15-5, 101	139.51	10.5	0.0	87
16-2, 110	144.60	11.4	0.0	95
16-4, 135	147.85	2.8	0.2	21
Site 214				
1-1, 67	0.67	11.1	0.1	92
1-4, 142	5.92	11.3	0.0	94
1-6, top	7.50	11.1	0.1	92
2-2, top	11.00	10.8	0.1	89
2-4, top	14.00	11.3	0.0	94
3-1, 26	19.26	11.3	0.1	93
3-3, 104	23.04	11.2	0.0	93
3-3, 109	23.09	11.2	0.1	93
3-6, 72	27.22	11.2	0.0	93
4-2, 130	31.30	11.3	0.0	94
4-3, 13	31.63	11.2	0.0	93
4-4, 64	33.64	11.3	0.0	94
4-5, 30	34.80	11.3	0.0	94
5-3, 67	41.67	11.4	0.0	94
5-6, 61	46.11	11.3	0.0	94
6-1, 91	48.41	11.4	0.0	94
6-3, 60	51.10	11.3	0.0	94
7-1, 105	58.05	11.4	0.0	95
7-3, 60	60.60	11.3	0.0	94
7-5, 120	64.20	11.3	0.0	94
8-3, 47	69.97	11.4	0.0	95
8-6, top	74.00	11.4	0.0	95
9-1, 120	77.20	11.5	0.0	95
9-3, 113	80.13	11.4	0.0	95
9-6, 110	84.60	11.4	0.0	95
10-2, 111	88.11	11.5	0.0	96
10-5, 113	92.63	11.4	0.0	94
10-6, 70	93.70	11.4	0.0	95
11-1, 133	96.33	11.6	0.0	96
11-3, 57	98.57	11.4	0.0	95
11-5, 139	102.39	11.5	0.0	95
12-5, 55	111.05	11.6	0.0	96
13-3, 92	117.92	11.5	0.0	95
14-3, 91	127.41	11.5	0.0	96

APPENDIX C – Continued

Core, Section, Top of Interval (cm)	Subbottom Depth (m)	Total Carbon (%)	Organic Carbon (%)	CaCO ₃ (%)
Site 214 – Continued				
15-2, 110	135.60	11.5	0.0	96
15-3, 129	137.29	11.5	0.0	96
15-5, 110	140.10	11.5	0.0	96
16-1, 70	143.70	11.4	0.0	94
16-5, 44	149.44	11.4	0.0	95
17-1, 120	153.70	11.6	0.0	96
17-3, 90	156.40	11.6	0.0	96
17-5, 110	159.60	11.6	0.0	96
18-1, 121	163.21	11.6	0.0	97
18-3, 110	166.10	11.6	0.0	96
18-5, 82	168.82	11.5	0.0	96
19-1, 110	172.60	11.6	0.0	96
19-5, 80	178.30	11.5	0.0	95
20-3, 80	184.80	11.6	0.0	97
21-3, 103	194.53	11.6	0.0	97
21-5, 51	197.01	11.7	0.0	98
22-2, 103	202.53	11.6	0.0	96
22-5, 30	206.30	11.6	0.0	97
23-2, 93	211.93	11.6	0.0	96
23-5, 93	216.43	11.7	0.0	97
23-6, 80	217.80	11.7	0.0	97
24-1, top	219.00	11.6	0.0	97
24-2, 92	221.42	11.7	0.0	97
24-3, top	222.00	5.9	0.0	49
24-5, top	225.00	11.7	0.0	97
24-6, top	226.50	11.5	0.0	96
25-2, top	230.00	11.7	0.0	97
26-1, top	238.00	11.6	0.0	96
26-2, top	239.50	11.6	0.0	96
26-5, top	244.00	11.7	0.0	97
26-6, fop	245.50	11.6	0.0	97
27-1, top	247.50	11.5	0.0	96
27-2, top	249.00	11.6	0.0	96
27-3, top	250.50	11.6	0.0	97
27-6, top	255.00	11.6	0.0	97
28-2, top	258.50	11.5	0.0	96
28-5, 81	263.81	11.6	0.0	97
29-3, top	269.50	11.5	0.0	96
29-5, 82	273.32	11.7	0.0	97
29-6, 121	275.21	11.6	0.0	96
30-1, 90	276.90	11.7	0.0	97
30-5, 90	282.90	11.5	0.0	96
31-3, 60	289.10	11.6	0.0	97
31-3, 67	289.17	11.7	0.0	97
31-6, 90	293.90	11.4	0.0	95
32-3, 81	298.81	11.4	0.0	95
33-3, 82	308.32	11.5	0.0	96
34-5, 88	320.88	11.7	0.0	98
34-6, 90	322.40	11.7	0.0	97
35-3, 74	327.24	11.2	0.0	93
35-3, 97	327.47	11.0	0.0	91
35-4, 115	329.15	10.0	0.1	83
40-1, 110	372.10	2.1	0.1	16
41-3, 97	384.47	1.3	0.3	8
41-3, 133	384.83	0.9	0.4	4

APPENDIX C – Continued

Core, Section, Top of Interval (cm)	Subbottom Depth (m)	Total Carbon (%)	Organic Carbon (%)	CaCO ₃ (%)
Site 215				
10-2, 127	86.27	11.1	0.0	92
10-3, 137	87.87	11.3	0.0	94
11-2, 47	94.97	11.5	0.0	96
11-4, 16	97.66	11.3	0.0	94
12-3, 16	105.66	11.4	0.0	95
12-6, 76	110.76	11.6	0.0	96
13-3, 44	115.44	11.0	0.0	91
14-2, 80	123.80	11.5	0.0	95
14-6, 55	129.55	11.6	0.0	96
14-6, 62	129.62	11.7	0.0	97
15-3, 81	134.81	11.3	0.0	94
15-5, 87	137.87	11.2	0.0	93
16-2, 67	142.67	11.1	0.0	92
16-5, 90	147.40	11.4	0.0	94
16-5, 130	147.80	10.7	0.0	89
Hole 216				
1-4, 130	5.80	10.6	0.1	88
1-6, 122	8.72	0.0	0.0	0
1-6, 130	8.80	10.5	0.1	87
2-1, 90	45.40	10.9	0.1	90
2-3, 90	48.40	10.0	0.0	83
2-6, 110	53.10	10.2	0.1	85
3-2, 110	85.10	11.0	0.1	91
4-1, 81	121.31	10.9	0.0	91
4-5, 71	127.21	0.6	0.0	4
5-2, 40	160.40	11.2	0.0	93
5-2, 102	161.02	11.1	0.0	92
5-6, 103	167.03	11.0	0.0	92
6-3, 37	171.37	10.7	0.0	89
8-1, 123	188.23	10.9	0.0	90
8-2, 110	189.60	11.0	0.0	91
9-2, 76	198.76	11.2	0.0	94
10-1, 62	206.62	11.2	0.0	93
12-1, 124	226.24	11.0	0.0	92
15-1, 123	254.73	11.2	0.0	93
16-2, 125	265.75	10.4	0.0	86
17-2, 111	275.11	10.5	0.0	87
20-1, 184	302.84	11.7	0.0	97
23-3, 120	333.70	10.9	0.0	91
24-5, 91	345.91	7.4	0.1	61
25-4, 94	353.94	3.1	0.1	25
25-4, top	353.00	3.0	0.1	24
32-3, 1	418.01	4.6	0.2	37
33-1, 45	424.95	2.8	0.2	21
33-1, 95	425.45	1.0	0.2	7
34-1, 50	434.50	3.0	0.2	23
34-3, 75	437.75	2.6	0.1	21
34-4, 65	439.15	3.6	0.1	29
34-4, 69	439.19	0.2	0.1	1

APPENDIX C – Continued

Core, Section, Top of Interval (cm)	Subbottom Depth (m)	Total Carbon (%)	Organic Carbon (%)	CaCO ₃ (%)
Hole 216 – Continued				
35-2, 88	445.88	1.5	0.1	12
35-3, 100	447.50	3.2	0.1	26
36-1, 100	454.00	3.3	0.1	27
36-3, 2	456.02	6.5	0.1	53
36-3, 12	456.12	4.8	0.1	40
Hole 216A				
1-3, 117	105.67	10.8	0.0	89
1-6, 119	110.19	11.1	0.0	93
2-2, 110	113.60	11.0	0.0	92
2-4, 120	116.70	11.4	0.0	95
2-6, 100	119.50	9.8	0.0	81
3-1, top	120.50	10.4	0.0	86
3-3, 120	124.70	10.6	0.0	88
4-2, 116	132.66	11.3	0.0	94
4-4, 96	135.46	11.2	0.0	93
4-6, 30	137.80	11.2	0.0	93
5-3, 85	143.35	11.2	0.0	93
6-1, 120	150.20	10.9	0.0	91
6-3, 120	153.20	10.6	0.0	88
6-5, 120	156.20	11.0	0.0	91
Hole 217				
1-1, 42	0.42	6.7	0.4	52
1-3, 22	3.22	6.7	0.3	53
2-3, 74	43.74	7.9	0.1	65
2-4, 5	44.55	8.1	0.2	66
3-1, 50	70.50	8.6	0.1	71
4-5, 64	122.64	7.2	0.2	59
6-2, top	184.00	9.2	0.0	76
6-5, 2	188.52	10.4	0.1	86
6-6, 55	190.55	10.3	0.0	86
7-2, 48	231.98	10.5	0.0	87
7-4, 2	234.52	10.5	0.1	87
7-4, 66	235.16	10.4	0.0	86
7-6, 80	238.30	10.7	0.0	89
8-3, 89	271.89	10.6	0.0	88
8-5, 2	274.02	10.3	0.1	85
9-5, 95	312.95	10.2	0.0	85
9-3, 52	309.52	9.0	0.0	74
10-2, 31	345.81	9.4	0.0	78
10-4, 1	348.51	8.7	0.1	72
14-3, 32	395.82	11.5	0.0	96
15-1, 110	403.10	9.3	0.0	77
15-2, 5	403.55	6.4	0.0	53
16-1, 95	412.45	10.5	0.0	87
16-4, 1	416.01	10.0	0.1	83
16-4, 73	416.73	10.1	0.0	84
17-1, 105	422.05	11.0	0.0	91
18-2, 3	432.03	10.4	0.1	86
19-3, 1	443.01	10.3	0.1	86
21-3, 112	463.12	10.0	0.0	83

APPENDIX C – Continued

Core, Section, Top of Interval (cm)	Subbottom Depth (m)	Total Carbon (%)	Organic Carbon (%)	CaCO ₃ (%)
Hole 217 – Continued				
22-1, 1	468.51	9.6	0.0	79
22-1, 56	469.06	9.7	0.0	81
23-1, 47	478.47	9.4	0.0	78
23-2, 1	479.51	10.6	0.0	88
23-1, 102	479.02	9.9	0.0	82
24-1, 9	487.59	10.4	0.0	86
25-3, 63	500.63	10.6	0.0	88
26-2, 1	508.01	10.4	0.0	87
26-3, 64	510.14	10.5	0.0	87
27-2, 1	517.51	9.5	0.1	78
27-2, 92	518.42	10.6	0.0	88
28-2, 38	527.38	10.4	0.0	86
29-1, 1	535.01	10.6	0.0	88
30-3, 1	547.01	10.6	0.1	88
31-2, 1	555.01	10.4	0.1	86
31-2, 130	556.30	5.0	0.1	41
33-2, 1	574.01	9.3	0.2	76
33-2, 24	574.24	5.6	0.1	46
34-1, 51	582.51	8.2	0.1	68
36-1, 123	602.23	8.2	0.1	67
Hole 217A				
1-1, 99	0.99	5.9	0.2	47
1-1, 123	1.23	5.9	0.4	46
1-1, 133	1.33	6.4	0.2	52
1-1, 142	1.42	6.2	0.2	50
1-1, 149	1.49	6.7	0.3	53
1-2, 10	1.60	6.8	0.3	54
1-2, 27	1.77	6.3	0.2	51
1-2, 43	1.93	7.8	0.3	62
1-2, 60	2.10	7.7	0.4	61
1-2, 79	2.29	7.1	0.2	58
1-2, 99	2.49	8.6	0.2	70
1-2, 149	2.99	6.6	0.1	54
1-3, 21	3.21	6.6	0.3	53
1-3, 51	3.51	6.9	0.1	56
1-3, 77	3.77	5.9	0.4	46
1-3, 106	4.06	6.1	0.2	49
1-3, 120	4.20	5.6	0.2	45
1-3, 138	4.38	0.6	0.1	4
1-4, 5	4.55	7.5	0.1	61
1-4, 36	4.86	6.8	0.4	53
1-4, 42	4.92	7.6	0.1	62
1-4, 63	5.13	7.5	0.1	62
1-4, 110	5.60	7.7	0.2	63
2-1, 97	10.47	7.2	0.3	57
2-1, 105	10.55	8.0	0.2	65
2-1, 128	10.78	8.8	0.1	73
2-1, 143	10.93	7.8	0.1	64
2-2, 2	11.02	7.3	0.2	59
2-2, 13	11.13	6.9	0.3	55
2-2, 28	11.28	7.9	0.1	65
2-2, 86	11.86	7.3	0.2	59
2-2, 125	12.25	8.2	0.1	67
2-3, 15	12.65	8.2	0.2	67
2-3, 56	13.06	7.6	0.1	63
2-3, 134	13.84	8.0	0.1	66

APPENDIX C - Continued

Core, Section, Top of Interval (cm)	Subbottom Depth (m)	Total Carbon (%)	Organic Carbon (%)	CaCO ₃ (%)
Hole 217A - Continued				
2-4, 45	14.45	8.0	0.1	66
2-4, 64	14.64	7.7	0.2	62
2-4, 123	15.23	8.2	0.1	68
2-4, 143	15.43	7.7	0.3	62
2-5, 24	15.74	8.7	0.1	72
2-5, 59	16.09	7.2	0.3	58
2-5, 90	16.40	8.4	0.2	69
2-5, 118	16.68	7.8	0.2	63
2-5, 136	16.86	8.2	0.1	67
3-1, 77	19.77	8.1	0.2	66
3-1, 144	20.44	8.4	0.2	69
3-2, 38	20.88	8.4	0.2	69
3-2, 120	21.70	8.3	0.1	68
3-3, 75	22.75	8.0	0.1	66
3-3, 84	22.84	7.7	0.3	62
3-3, 95	22.95	7.8	0.1	64
3-4, 7	23.57	7.8	0.2	64
3-4, 41	23.91	8.0	0.3	64
3-4, 61	24.11	8.0	0.1	65
3-4, 70	24.20	7.4	0.3	59
3-4, 97	24.47	7.5	0.3	60
3-4, 109	24.59	7.4	0.2	60
3-4, 127	24.77	8.2	0.1	67
4-2, 70	30.70	6.7	0.3	53
4-2, 14	30.14	7.9	0.2	64
4-2, 97	30.97	6.5	0.4	50
4-2, 106	31.06	7.7	0.1	63
4-2, 113	31.13	7.6	0.2	61
4-2, 130	31.30	8.4	0.2	68
4-3, 17	31.67	8.5	0.2	69
4-4, 13	33.13	7.6	0.2	62
4-4, 60	33.60	8.4	0.2	68
4-4, 94	33.94	7.4	0.2	60
Site 218				
2-1, 100	5.00	5.4	1.2	35
2-1, 128	5.28	1.6	0.4	10
2-2, 67	6.17	1.0	0.5	4
2-2, 137	6.87	6.4	0.6	49
203, 120	8.20	1.1	0.6	4
2-5, 35	10.55	0.6	0.2	3
2-6, 3	11.53	0.9	0.5	3
3-2, 4	15.04	0.9	0.5	4
3-2, 136	16.36	0.7	0.3	4
4-1, 120	42.70	3.3	0.4	24
4-2, 15	43.15	1.0	0.4	5
4-2, 100	44.00	0.9	0.4	5

APPENDIX C - Continued

Core, Section, Top of Interval (cm)	Subbottom Depth (m)	Total Carbon (%)	Organic Carbon (%)	CaCO ₃ (%)
Site 218 - Continued				
5-1, 103	71.03	1.0	0.6	3
5-2, 5	71.55	0.9	0.4	4
5-2, 88	72.38	1.2	0.6	5
6-2, 14	109.64	5.4	0.9	37
6-2, 88	110.38	5.2	0.8	36
6-2, 120	110.70	4.2	0.3	33
8-2, 117	186.67	4.7	0.2	38
8-2, 112	186.62	0.6	0.1	3
8-3, 4	187.04	2.4	0.5	16
10-1, 105	261.05	0.7	0.1	5
11-2, 19	299.69	0.9	0.4	4
11-2, 100	300.50	0.8	0.3	4
13-2, 1	375.51	2.9	0.2	22
13-2, 110	376.60	2.8	0.3	21
15-1, 95	450.95	1.3	0.3	8
16-1, 14	459.64	1.1	0.4	6
16-2, 4	461.04	1.4	0.3	9
16-2, 113	462.13	6.3	0.2	50
17-1, 136	470.36	1.4	0.5	8
17-3, 2	472.02	0.8	0.2	5
17-3, 23	472.23	0.9	0.2	5
18-1, 64	479.14	9.1	0.3	73
19-1, 107	489.07	1.3	0.5	7
19-1, 136	489.36	1.4	0.5	7
19-2, 27	489.77	8.4	0.2	68
20-1, 36	497.86	1.4	0.5	8
21-1, 88	536.38	1.6	0.4	10
21-2, 3	537.03	1.4	0.3	9
22-2, 10	575.10	1.4	0.3	10
22-2, 65	575.65	1.6	0.3	11
23-1, 24	611.74	1.2	0.4	7
23-2, 4	613.04	1.8	0.2	13
23-2, 78	613.78	4.0	0.2	32
24-2, 3	651.03	1.9	0.2	14
24-2, 37	651.37	4.3	0.2	34
24-2, 84	651.84	1.0	0.2	6
25-2, 1	689.01	1.5	0.2	11
25-2, 97	689.97	1.5	0.3	10
26-1, 118	726.68	1.8	0.4	12
26-2, 2	727.02	1.5	0.4	10
27-2, 1	765.01	0.9	0.3	5
27-1, 126	764.76	1.7	0.3	11

PLATE 1

Structures in Sediment Cores from Site 212.

- Figure 1 Core 2, Section 4, 39 to 79 cm.
Calcareous nannoplankton ooze interbedded with brown clay. Note sharp lower and gradational upper contact of calcareous ooze.
- Figure 2 Core 13, Section 2, 0 to 76 cm.
Strongly laminated foraminifera-nannoplankton ooze.
- Figure 3 Core 13, Section 2, 76 to 150 cm.
Strongly laminated and cross laminated (86 to 91 cm) foraminifera-nannoplankton ooze.
- Figure 4 Core 23, Section 5, 76 to 150 cm.
Interbed of grayish-olive-green nannoplankton-bearing zeolite-rich claystone in nannoplankton chalk; note sharp upper and gradational lower contact. The chalk contains abundant pale yellowish-brown laminations which range from regular to wavy to recumbent folds; some cross laminations also present. Some green claystone fragments present in the darker laminations.
- Figure 5 Core 27, Section 6, 26 to 100 cm.
Zeolite iron oxide-bearing brown clay with pale olive bleached zones rimmed by hematite rich dark reddish-brown clay. Bleached zones contain more ash and zeolite than surrounding clay.

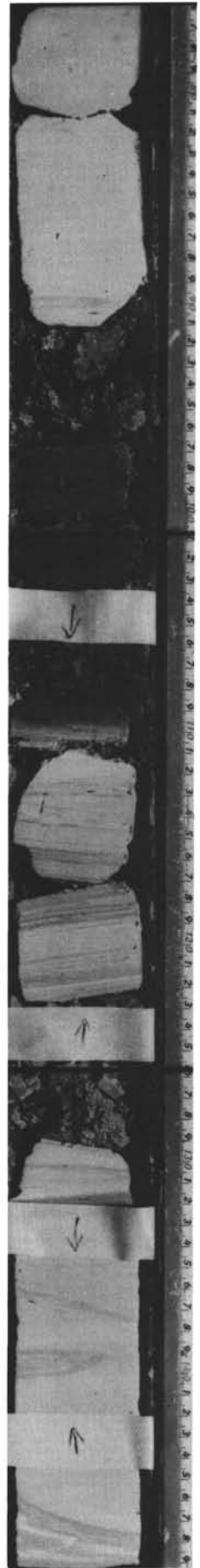
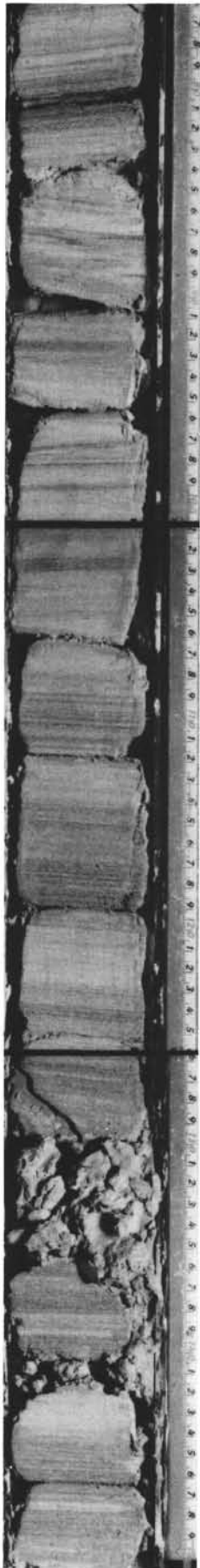
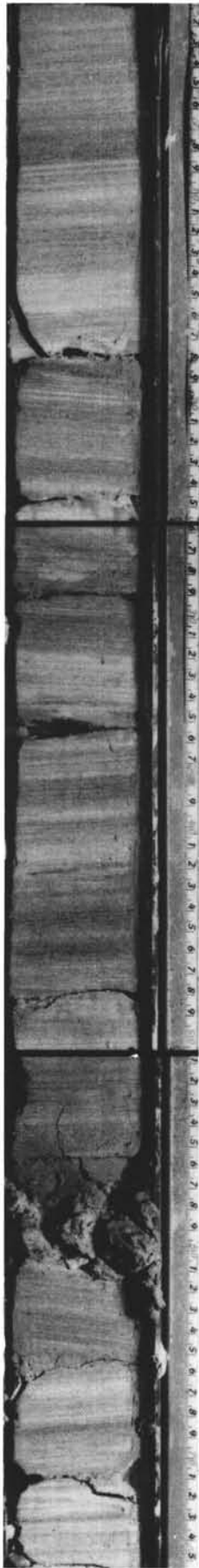


PLATE 2

Sedimentary Structures at Site 218 (also see Figure 40)

- Figure 1 Core 3-2, 29 to 101 cm.
Graded silty sand to sandy silt bed passing up into silty clay. Within center of Pulse 1.
- Figure 2 Core 5-1, 30 to 100 cm.
Silty sand to sandy silt beds, thicker ones are graded, interbedded with silty clay. Beginning of Pulse 1.
- Figure 3 Core 11-1, 130 to 150 cm.
Silty sand to sandy silt bed overlain by silty clay. From center of Pulse 2.
- Figure 4 Core 10-1, 56 to 126 cm.
Silty sand bed, slightly graded, with sharp lower and upper contact. Grain-size analysis at 105 cm (about 1/3 way down bed) gave 63% sand, 33% silt, and 4% clay. Note also silt laminations. From center of Pulse 2.
- Figure 5 Core 8-3, 43 to 118 cm.
Sandy silt and clayey silt laminations within silty clay to clay which in places (near top) contains admixture of nanoplankton ooze. From end of Pulse 2.



PLATE 3

Sedimentary Structures at Stie 218 from Interval
between Pulses 2 and 3 (Figure 40)

- Figure 1 Core 16-2, 31 to 105 cm.
Thin beds of sandy silt, silty clay and nannoplankton
chalk. Note presence of darker mottles, burrows, and
worm tubes in pale colored chalks.
- Figure 2 Core 13-1, 66 to 126 cm.
Bioturbated and fairly indurated nannoplankton
chalk interbedded with calcareous clay.
- Figure 3 Core 18-1, 37 to 104 cm.
Interbedded clay and bioturbated nannoplankton
chalk. Note burrow mottles of darker clay worked
from above into chalk below. Well-developed worm
tubes also present. In places chalk shows minor
folding. Few clay laminae present in clayey chalk.
- Figure 4 Core 19-2, 26 to 100 cm.
Strongly bioturbated nannoplankton chalk overlying
laminated silty clay.

PLATE 4

Sedimentary Structures at Site 218 (see Figure 40)

- Figure 1 Core 22-2, 40-111 cm.
Regularly spaced laminae of darker clay-rich very fine grained silt, multiple laminae of paler clean silt and few thin sandy silt beds in predominantly clayey silt sequence. Grain-size analysis at 65 cm give 4% sand, 52% silt, and 44% clay. From Pulse 3.
- Figure 2 Core 23-2, 77 to 150 cm.
Strongly bioturbated chalk from interval between Pulses 3 and 4.
- Figure 3 Core 24-1, 89 to 150 cm.
Graded sandy silt bed overlying clayey silt-silty clay. Abundant clean silt laminae and beds at top of photograph. From near top of Pulse 4.
- Figure 4 Core 24-2, 53 to 125 cm.
Sandy-clayey silt bed grading up into silty clay near top (grain size at 86 cm 12% sand, 41% silt, 47% clay). Note regularly spaced darker clay-rich silt laminae superimposed on this graded bed. Some clean silt laminae and bioturbated calcareous clays also present. From near top of Pulse 4.
- Figure 5 Core 26-2, 77 to 150 cm.
Mostly clayey silt and silty clay, partly graded and laminated, with few thin sandier beds. Note darker laminae regularly spaced throughout core. From Pulse 4.
- Figure 6 Core 27-1, 79 to 150 cm.
Mostly clayey silt and silty clay with several regularly spaced darker laminae. Grain size analysis at 124 cm gave 8% sand, 54% silt, and 38% clay. From base of Pulse 4.

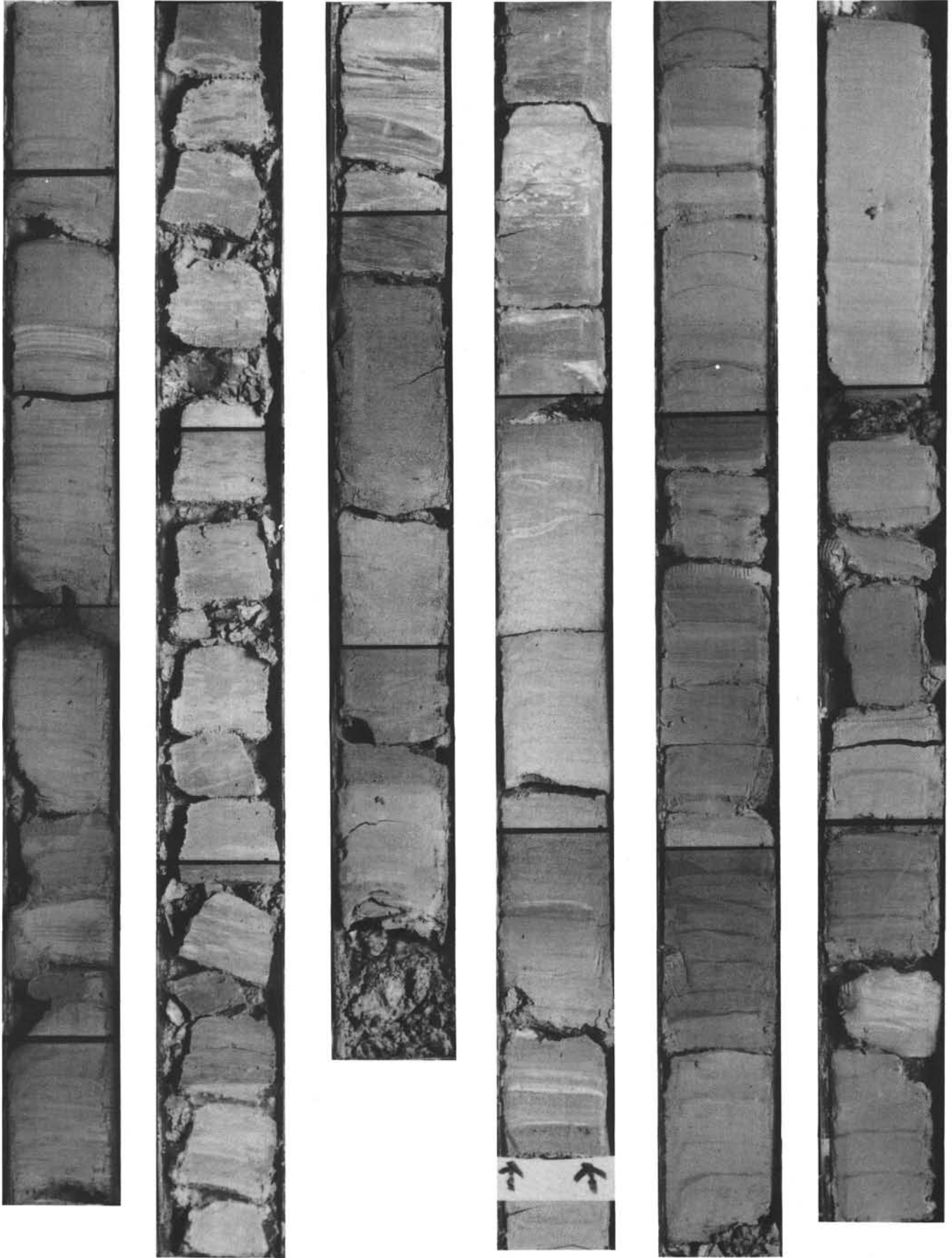


PLATE 5

- Figure 1 Site 212, Core 39, Section 1, 78 cm; Crossed nicols; magnification 90X.
Metamorphosed limestone trapped between pillows of basalt. Photomicrograph shows plagioclase crystal in a matrix of calcite showing undulatory extinction.
- Figure 2 Core 39, Section 1, 78 cm; magnification 90X.
Unidentified microfossil from metamorphosed limestone within basaltic basement at Site 212 in deepest part of the Wharton Basin. Age of closest datable sediment 32 meters above this is Maastrichtian.

